Laboratory and Field Testing of Precast, Three Sided Arch Culverts

by

Richard L. Meadows

A thesis submitted to the Graduate Faculty of
Auburn University
in partial fulfillment of the
requirements for the Degree of
Master of Science

Auburn, Alabama
August 4, 2012

Approved by

Justin D. Marshall, Chair, Assistant Professor of Civil Engineering
J. Brian Anderson, Associate Professor of Civil Engineering
Robert W. Barnes, James J. Mallett Associate Professor of Civil Engineering

Abstract

The use of precast, three-sided arch culverts has become fairly popular for new short-span bridges and bridge replacements due to their rapid construction time, aesthetic appeal, and minimal impact to the waterway, but little research has been performed into the strength of these structures. It has been thought that, due to arching action, large lateral earth pressures can be developed in the backfill behind the legs, and that these pressures allow the bridge to achieve strengths much larger than possible without the confinement of the backfill soil. The research detailed in this thesis sought verify the behavior of this bridge system through field testing of an existing bridge, as well as two ultimate load tests on individual bridge units.

It was concluded that the test bridges were too stiff to cause enough lateral deflection to activate passive earth pressures in the backfill, and the earth pressures had a minimal effect. Furthermore, it was found that non-ductile shear failures can occur in certain bridge designs, and the ductility of the steel used for reinforcement was not sufficient to allow flexural hinges to form.

Acknowledgements

I would first like to thank my committee members for their support during this project. I would like to thank Dr. Anderson for his insight and assistance, especially during the field testing, and for his help throughout the project. I would particularly like to thank Dr. Barnes for his guidance and insight during the laboratory load testing portion of the project. Finally, I would like to thank Dr. Marshall, my major professor, for his constant help, guidance, and organization throughout the entire project. I would further like to thank the faculty at Auburn University; it has truly been a pleasure to learn from so many outstanding professors during my total of six years here.

I would like to also thank all those who assisted in the research, both during the field and laboratory testing portions of the project. I would especially like to thank my partner in research, Jared Jensen. I appreciate his attitude and willingness to help throughout the project, but more importantly, I appreciate his friendship.

I also want to thank my entire family, especially my mother, whose constant support and encouragement have helped me get to this point.

Finally, I would like to express my appreciation for my wife, Rachel. Without her support and love during these past two years, I would not nearly be the man I am today. I want to thank her for her love and her presence in my life. I know we are both very excited to see where this next chapter in life takes us together.

Table of Contents

List of Tables

List of Figures

Chapter 1 Introduction

1.1 Overview

The use of precast, three-sided arch culverts has begun to become fairly popular for new bridges and bridge replacements, due to their rapid construction time, aesthetic appeal, and minimal impact to the waterway. However, little research has been performed into the strength of these structures. Many have speculated that, due to arching action, large lateral earth pressures can be developed in the backfill behind the legs, and that these pressures allow the bridge to achieve strengths much larger than possible without the confinement of the backfill soil. The research detailed in this thesis sought to verify this behavior through field testing of an existing bridge, as well as two ultimate load tests on bridge units.

1.2 Motivation

Foley Arch, a division of Foley Products, was seeking to have their arch culvert product tested in order to confirm that the arch meets strength design requirements.

1.3 Research Objectives

- Verify the effectiveness of the Foley Arch culvert system at both service load levels and at ultimate strength levels.
- Contribute additional research on the strength and effectiveness of precast, three-sided arch concrete culvert systems.

1.4 Testing Overview

- Test a newly constructed bridge for design load/service load behavior.
- Test a shorter span bridge unit for ultimate load capacities.
- Test a longer span bridge unit for ultimate load capacities.

1.5 Thesis Organization

This thesis is divided into six chapters. Chapter 1 is an introduction to the research project, providing the motivation, objectives, and overview of research performed. Chapter 2 provides background on precast, three-sided arch culverts, as well as a literature review of previous testing. Chapter 3 details the testing, results, and analysis of a 42 ft span bridge constructed in Cabarrus County, NC. Chapter 4 details the testing, results, and analysis of an

individual 20 ft span bridge unit tested in the Structures Research Laboratory in Auburn, AL. Chapter 5 details the testing, results, and analysis of an individual 36 ft span bridge unit tested in the Structures Research Laboratory in Auburn, AL. Finally, Chapter 6 summarizes the project and provides conclusions based on the testing.

Chapter 2 Background and Literature Review

2.1 Background and Description of Bridge System

2.1.1 Overall System Description

The precast, three-sided arch culvert system consists of a number of precast arch units bearing onto a keyed strip footing foundation, with precast wingwalls and headwalls used to prevent soil runoff. Backfill soil is placed and compacted behind and above the bridge system, up to the desirable grade. An asphalt or concrete pavement can then be placed over the roadway. An image of a typical precast, three-sided arch culvert system can be seen in Figure 2-1. An image of an installed three-sided arch culvert bridge can be seen in Figure 2-2. Units are placed in a keyed strip footing in order to prevent lateral movement of the legs and to ensure that each unit is aligned properly. Units are generally not tied together, and therefore behave independently of each other, but can be tied together if necessary.

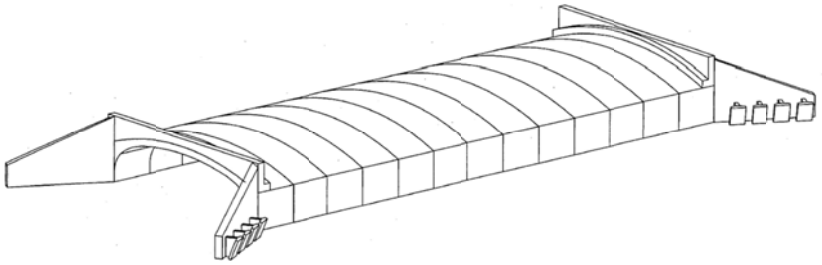

Figure 2-1 Typical Three-sided Arch Culvert System (FoleyArch 2010)

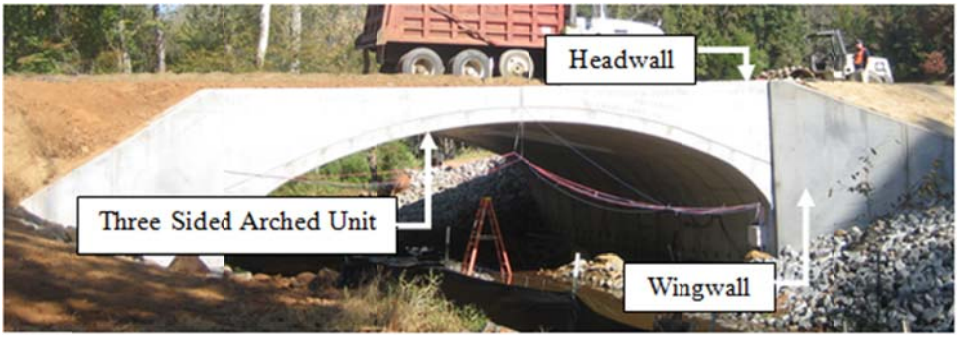

Figure 2-2 Installed Three-sided Arch Culvert System

2.1.2 Unit Description

The three-sided arch culvert consists of a circular arch with a large radius that frames into two legs, which bear on the foundation. The corners of these culverts have an increased thickness

to account for the higher strength demands and allow the load path to better transition into vertical loads in the legs. The arch shape converts a portion of the vertical load into axial forces in the concrete, therefore allowing these culverts to have thinner sections along their span compared to typical box culverts. Units have a uniform thickness along the arch and a uniform thickness in the legs, with geometry dictating the thickness in the corners. A sketch of a typical three-sided arch culvert unit can be seen in Figure 2-3.

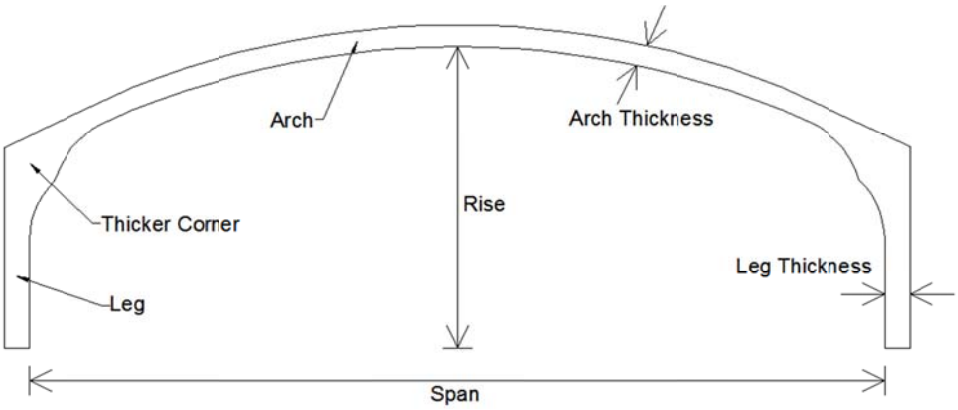

Figure 2-3 Typical Three-sided Arch Culvert Unit

Individual units are highly adjustable. Span length, rise, thicknesses, and unit widths can all be manipulated in order to provide a custom solution in a variety of applications.

2.1.3 Production and Shipping

Reinforcement of these units generally consists of mats of deformed welded wire fabric, such as that seen in Figure 2-4. These mats of reinforcement can be used in single or double layers, and the wires have a small enough diameter that they can be easily bowed to fit the curved arch section without kinking, as seen in Figure 2-5.

Figure 2-4 Deformed Welded Wire Fabric

Figure 2-5 Steel Mat Bowing to Fit Arch Radius

Reinforcement layout generally consists of at least one layer of steel near both the inner and outer surfaces of the bridge. No shear reinforcement is provided. Steel layers rise along the length of the legs, where they are then bent to conform to the corner. This mat of steel then extends into the arch a distance before it is splices with a different layer of steel that spans the arch of the unit. In particularly large corners, an additional layer of steel is bowed to fit the large, curved section of the corners.

Due to the thin sections in which concrete is cast, these units are cast on their sides, using highly flowable concrete that requires minimal vibration. An image of the casting process can be seen in Figure 2-6.

Figure 2-6 Casting of Bridge Unit

Units are shipped via truck, with one unit per trailer, due to the geometry of the arch units. With the exception of shorter span, low-rise units, units are also shipped on their side. At the site, units are lifted, rotated in midair, and set in place by a crane using pick points. An image of the shipping orientation of an individual bridge unit can be seen in Figure 2-7, and an image of the rotating process can be seen in Figure 2-8.

Figure 2-7 Arch Culvert Unit Being Shipped

Figure 2-8 Arch Culvert Unit Being Rotated

2.1.4 System Advantages

The three-sided arch culvert system has many advantages over typical exposed deck bridges as well as similar buried box culverts. Arch culverts are aesthetically pleasing, and cause a minimal impact to the waterway, since they are bottomless. The backfill cover above the structure helps distribute live loads evenly, making the buried culvert less susceptible to damage from concentrated loads. Compared to exposed bridges, the buried arch culverts have much lower maintenance costs. Due to the arch shape, these units provide a more efficient resistance to loading than typical box culverts. Arch units use the backfill soil to provide a lateral pressure on the legs, helping the arch resist deflection due to the vertical loads above it. The arch shape also allows thinner sections to be used, due to the conversion of vertical load into axial force in the arch. The axial force developed in the arch also helps to reduce both the amount of cracking and the crack sizes.

2.2 Previous Research

The following section details previous research and testing of three-sided arch culverts. Research is listed in reverse chronological order.

2.2.1 Zoghi and Farhey (2006)

Researchers field tested a 36 ft span bridge, composed of seven units, each six feet wide and nine feet tall. After testing, CANDE, a finite element analysis program specifically used for buried structures, was used to create a model that fit the recorded data from the field test. Since this thesis is focused primarily on testing, the results from finite element modeling are not discussed.

The middle unit was the most highly instrumented, and also the designated test unit. Instrumentation consisted of earth pressure cells at top and bottom of the legs on both sides and dial gages measuring deflections at seven locations. Dial gages were placed at the top and bottom of both legs to measure horizontal deflections, and at midspan and quarter span to measure vertical deflections. Backfill up to three feet of cover was placed and compacted over the bridge. A hydraulic jack capable of 200 kips of load was placed over a roughly four foot by four foot area over midspan of the middle unit. Load was applied in 20 kip increments, with readings being taken at each increment.

In addition, vertical deflections in adjacent units were measured. However, it was found that those units had negligible deflections, which is expected since the units are not tied together in any way (Zoghi and Farhey 2006).

Test results show that the unit was very stiff, having a minimal response to the load. Even after applying the full 200 kips of load, only 1.5 in of vertical deflection was measured. After removing the load, no significant damage to the concrete was found and the steel did not yield. Virtually no horizontal displacement at the bottom of the legs was measured, and it was concluded that a pin support condition at the bridge foundation is reasonable. Maximum measured deflections at the top of the legs were around 0.25 in. Researchers did conclude that arching action helps develop passive earth pressures which aid in bridge strength, saying "an extreme overload capacity can be developed by mobilizing the passive earth pressures along the side walls without concern for local failures" (Zoghi and Farhey 2006). However, the effects of lateral earth pressure are not significant until higher loads are reached. Measured data shows "the contribution of earth pressure is relatively small under normal operating loads" (Zoghi and Farhey 2006). Earth pressures greater than 6.25 ksf were measured at the top of the legs, and pressures of 1.00 ksf were measured at the bottom of the legs. However, ultimate load capacity of the bridge could not be surpassed with the equipment used (Zoghi and Farhey 2006).

2.2.2 McGrath and Mastroianni (2002)

Researchers field tested two 28 ft span bridges, both 6.5 ft tall, but each with slightly different designs. One bridge had two layers of steel, one near both the inner and outer surface, while the other bridge only had a single layer of steel near the inner surface. After testing, CANDE was used to model the bridges in 2-D, while ABAQUS, a general purpose finite element analysis program, was used to model the bridges in 3-D. Since this thesis is focused primarily on testing, the results from finite element modeling are not discussed.

The field test measurements included arch deflections, earth pressures, concrete strains, and reinforcing bar strains. Two types of loading were used for the field testing procedure,

tandem-axle load conditions and HS-20 load conditions. Tandem-axle loading was performed at three feet, two feet, and one foot of cover using two tandem-axle trucks with 71 kips on each pair of axles. The HS-20 loading condition was performed using a hydraulic jack, at one foot of cover. The HS-20 loading condition was calculated to be 87 kips in the jack; however, the hydraulic jack was used to provide much higher load as well.

Both bridges carried the maximum load that the equipment being used could apply. In both bridges, the test was terminated due to bearing failure of the soil under the load plates. The single layer of steel design resisted a load of 236 kips, while the double layer of steel design resisted a load of 296 kips prior to failure of the cover soil. Even at these high loads, no failure or yielding of the reinforcement occurred. Cores were cut from the tested structure and it was determined that the reinforcement at the crown of the structure had not yielded at the maximum load applied during the test (McGrath and Mastroianni 2002).

2.2.3 McGrath, Selig and Beach (1996)

Researchers field tested a 36 ft span bridge, composed of ten units, each 5.25 ft wide and 11 ft tall. After testing, CANDE was used to create a model that fit the tested bridge. Since this thesis is focused primarily on testing, the results from modeling are not discussed.

The seventh, eighth, and ninth units were instrumented with soil stress cells and tape extensometers to measure lateral earth pressures and bridge deflections, respectively. Soil stress cells were placed at the top and midheight of both legs. Tape extensometers measuring lateral deflections were placed at the top and midheight of both legs, also, while tape extensometers measuring vertical deflections were placed at quarter span and midspan. At one foot of cover over the bridge, a live load test was performed by driving a three axle truck over the bridge and stopping at specific locations, taking measurements at each location. The load on the truck was meant to represent an HS-25+30% AASHTO truck load. One side of the truck axle was centered over the seventh unit, with the other side extending over the eighth unit. After load test, two additional feet of cover were added to the bridge and pavement was placed, bringing the bridge to the design backfill cover of three feet. Additional measurements were taken after the backfill process was completed and at six, 12, 18, and 24 months after construction completion.

Researchers found that the live load test had very little impact on the bridge. The maximum vertical deflection was 0.1 in due to live load, while the maximum soil pressures were 0.50 ksf in the middle cells and 0.17 ksf in the top cells. Both deflections and soil pressure were more significantly affected by the addition of the final two feet of cover, but the measured values were still very small (McGrath, Selig and Beach 1996).

2.2.4 Beach (1988)

Researchers field tested a 19 ft span bridge, composed of three units, each eight feet wide and seven feet tall. Unlike other tests, however, they were able to achieve the ultimate failure of the bridge. After testing, CANDE was used to model the bridge. Since this thesis is focused primarily on testing, the results from modeling are not discussed.

The middle unit was instrumented with deflection gages at six locations. Horizontal deflections were measured at the bottom of both legs and top on one leg. Vertical deflections were measured at midspan and quarter spans. Connection plates between the units are normally installed, but were not for this test because they wanted the units to behave independently (Beach 1988). Backfill was placed up to one foot of cover over the units. A 200 kip capacity actuator was used to apply load on a beam that spread the load evenly across the width of the middle unit.

Load was applied in increments of 6.2 kips, and the ultimate load was achieved at 133.5 kips. At ultimate load, the bridge continued deflecting without resisting additional load. A midspan deflection of about 2.75 in was measured prior to unit failure, which also occurred at midspan. At failure of the culvert, three distinct hinges formed at the corner haunches and at midspan. At all three locations the tension steel yielded and ruptured, while the concrete never crushed in compression. The culvert still held the 133.5 kip load even after this failure, supposedly due to the backfill pressure supporting the legs. Researchers also noted that the legs behaved as pin supported (Beach 1988).

The researchers conclude “because of the relatively high stiffness of the culvert, the predominant effect in this test was the structural behavior of the precast unit” (Beach 1988). They also speculate that the soil-structure interaction would have more effect on longer spans and higher fills.

2.3 Research Summary and Contribution

Previous research concludes that the effects of backfill are significant, but only at very high load levels. This conclusion could not be verified, however, because the majority of previous research did not achieve ultimate loading and failure of the structures. The only research that did achieve failure found that the structure was too stiff to cause significant lateral earth pressures (Beach 1988). Research also did not detail internal forces, such as moments and axial forces, felt by the structure, presenting only measured deflections and earth pressures.

This thesis contributes to the body of work by presenting research on the internal forces and lateral earth pressures measured in a field test. It also contributes by testing two separate units through ultimate load and failure. Even though ultimate load testing took place in a

laboratory setting, conclusions about the effects of backfill soil on ultimate strength can be made based on measured displacements of the units laterally.

Chapter 3 Field Test – 42 ft Span

3.1 Introduction

A 42 ft span bridge constructed in Cabarrus County, NC was used for a field test of the Foley precast arch culvert bridge system. The bridge consisted of 13 units placed next to each other, spanning over Wiley Branch Creek on Cabarrus Station Road. Each unit was 42 ft long clear span, four feet wide, and has a 14ft inside clear height at midspan. An image of unit overall dimensions taken from the design drawings can be seen in Figure 3-1. An image of the reinforcement layout in half of a unit can be seen in Figure 3-2, with the specified reinforcement areas detailed in Table 3-1. The reinforcement layouts in the two halves of each unit were mirrors of each other. Though the exact reinforcement details are not shown here, calculations later on are based on gross concrete properties, and therefore not dependent on reinforcement. Note that transverse steel runs parallel to the roadway, meaning that it is the primary flexural resistance steel. This is the nomenclature used by Foley Arch, and will continue to be used throughout this thesis. Backfill was placed and compacted along the sides and top of the bridge up to a total of approximately two feet of cover over the midspan prior to live load testing. Wingwalls and headwalls are used to retain the backfill soil. The bridge units were grouted into a keyed strip-footing foundation to prevent lateral movement of the bottom of the bridge. An image of the bridge structure prior to placement of backfill can be seen in Figure 3-3.

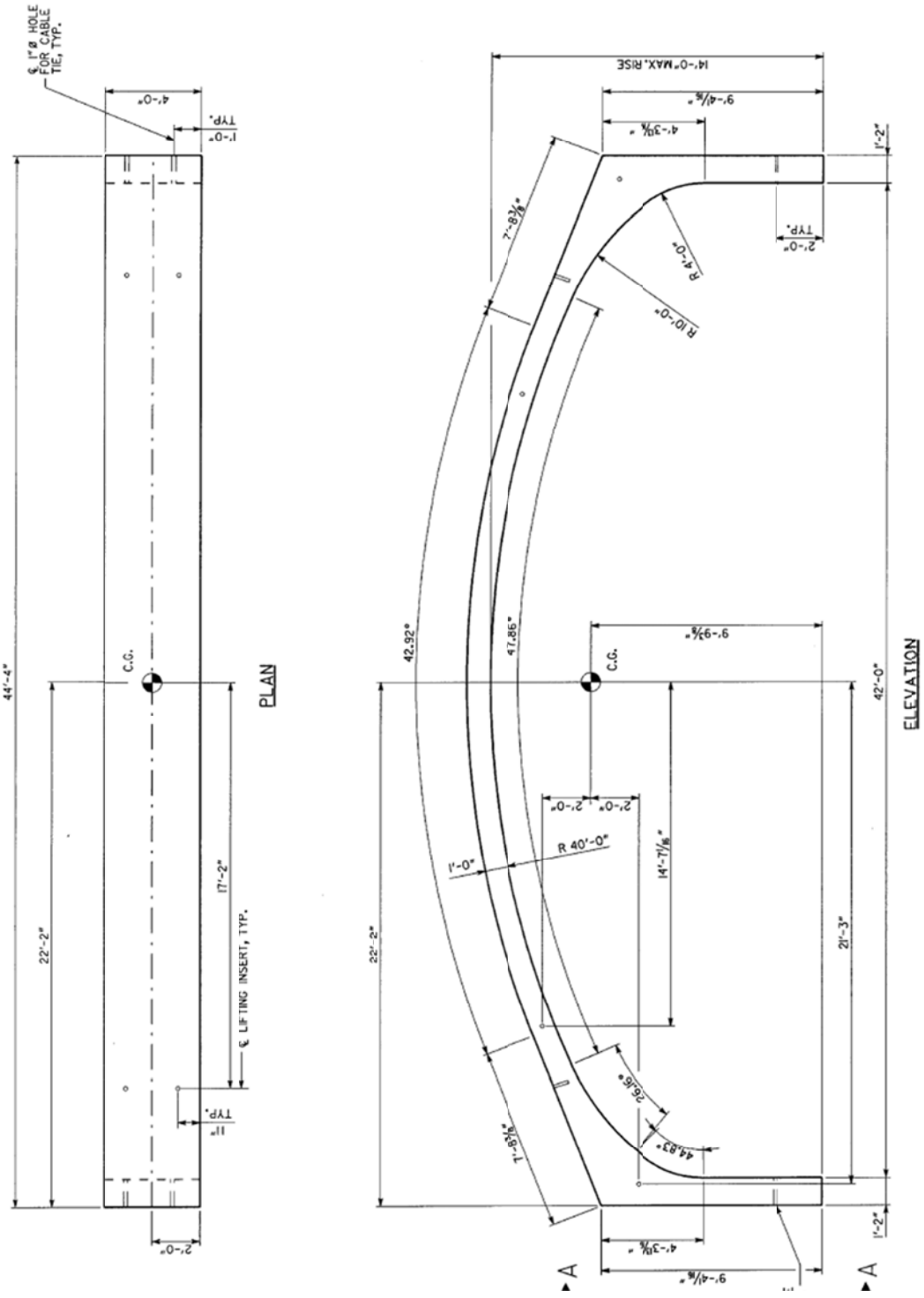

Figure 3-1 42 ft Bridge Unit Overall Dimensions (FoleyArch 2010)

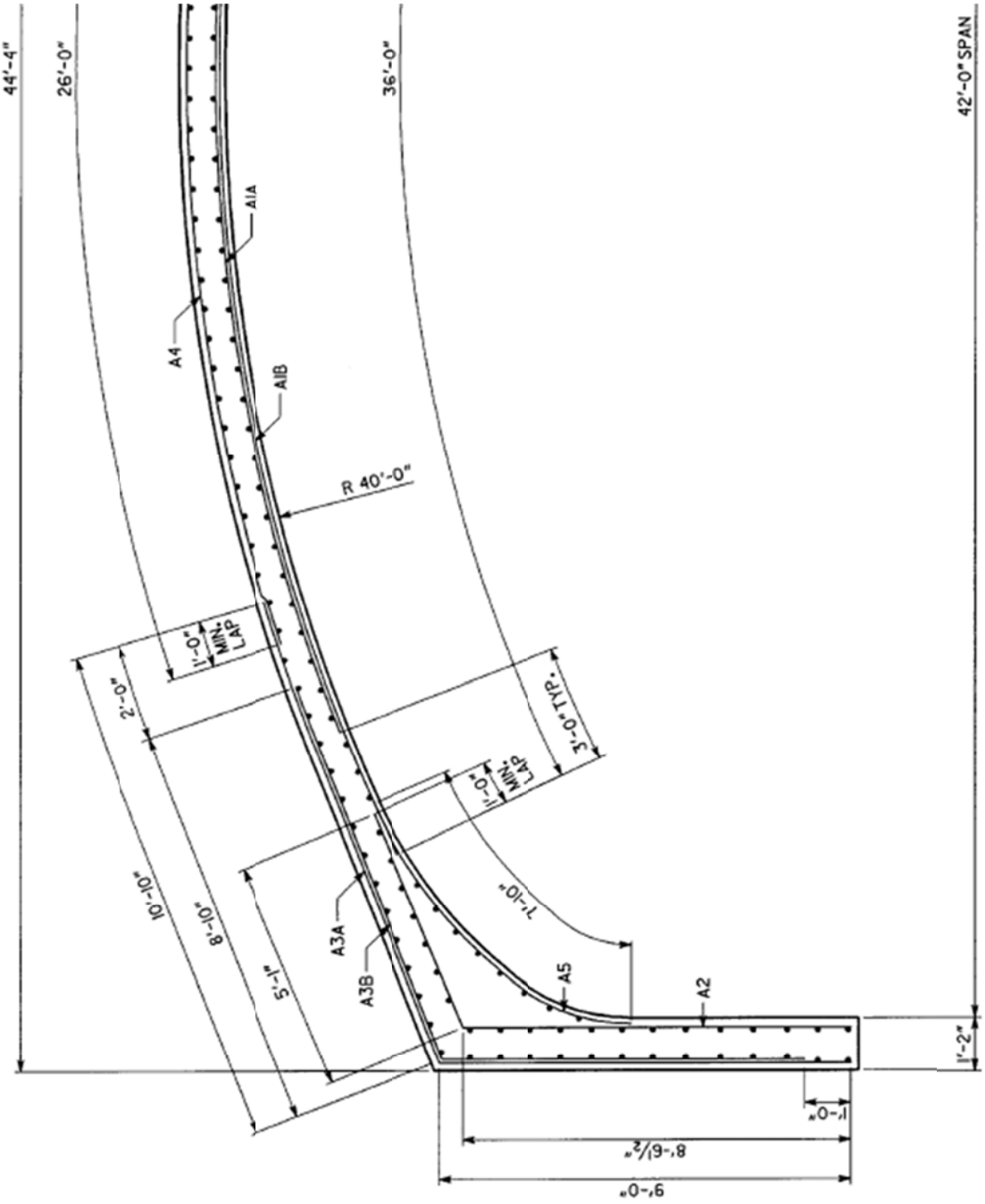

Figure 3-2 42 ft Bridge Unit Reinforcement Layout (FoleyArch 2010)

Table 3-1 42 ft Bridge Unit Reinforcement Details (FoleyArch 2010)

Designation	Length (ft)	Transverse Area Required (in2/ft)	Longitudinal Area Required (in2/ft)
A1A	30'-0"	0.79	0.31
A1B	36'-0"	0.79	0.31
A2	13'-8"	0.31	-
A3A	19'-10"	0.6	0.15
A3B	16'-10"	0.31	-
A4	26'-0"	0.31	0.31
A5	7'-10"	0.31	0.15
Design based on uncoated reinforcing meeting ASTM A-615, Grade 60, fy = 60,000psi			
Minimum Yield Strength for welded wire fabric shall be 65,000 psi			

Figure 3-3 42 ft Bridge Structure

This chapter details how the 42 ft bridge was tested, as well as the results of that testing. It contains sections on the instrumentation, setup, and procedure used for testing. It also contains analysis and results from testing, followed by discussion of those results.

3.2 Instrumentation

This section contains a detailed description of the instrumentation used on the 42 ft span bridge. It also contains details about the different types of instruments used, including how each was installed.

3.2.1 Instrumentation Layout

In order to measure moments and axial forces within the bridge units, five vibrating wire strain gages were placed along the inside centerline of three identical bridge units, with one highly-instrumented unit also having corresponding vibrating wire strain gages on the outside surface. The strain gage layout and gage numbering scheme can be seen in Figure 3-4. On the first two units, one gage is placed on each of the legs at the point where the thickness begins to increase near the corner, one gage is placed on the arch where the thickness begins to increase

near the corner, and one gage is placed directly at midspan. On the highly-instrumented unit, the inner gage layout is the same with the exception that one of the gages placed at the beginning of the standard arch curvature had to be offset from the centerline by one foot due to the presence of rebar chairs at the location where holes were to be drilled. The gages on the outer layer on this unit were placed at the same cross-sections and on the centerline in order to find the strains at the same points on opposite sides of the cross section. The only exception to this was at the aforementioned offset location, in which two gages, one at the corresponding offset and one on the centerline, were used on the outside of the unit.

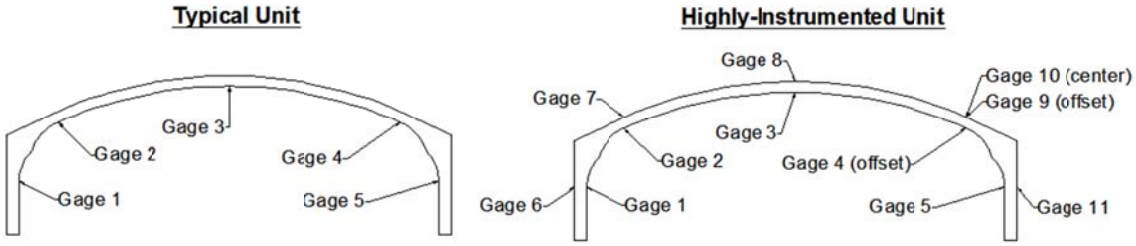

Figure 3-4 Field Test Strain Gage Layout

In addition, two earth pressure cells (EPCs) were placed on each exterior leg of the highly-instrumented unit, one near the bottom and one near the top. The exact layout of each EPC, numbered 38 through 41, can be seen in Figure 3-5. The reason the EPC 39 is not as low as EPC 41 is due to the presence of some backfill on that side when the pressure cells were installed.

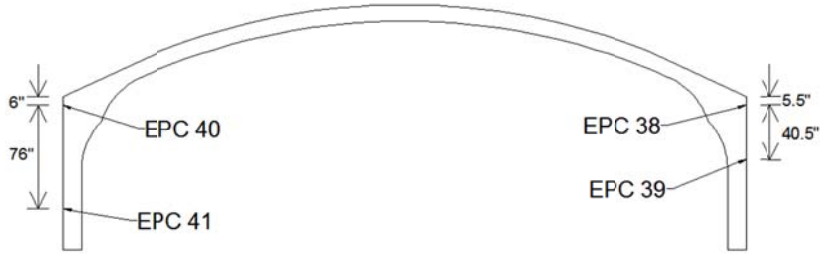

Figure 3-5 Earth Pressure Cell Layout

Before load testing, two displacement potentiometers were installed in order to measure live load displacements. These were placed on the inside of the highly-instrumented unit at the midspan and at the point on the northeastern leg where curvature begins.

The three instrumented units were placed next to each other in order to better determine how a vehicle load is spread through the backfill to the actual bridge units. The highly-instrumented unit was placed furthest to the outside in order to maximize the effect of the live load in that unit. This occurs because, when the live load is directly above it, there is less width

of the bridge for the live load to be distributed over. The specific layout of the three gaged units in the 13 unit bridge can be seen in Figure 3-6.

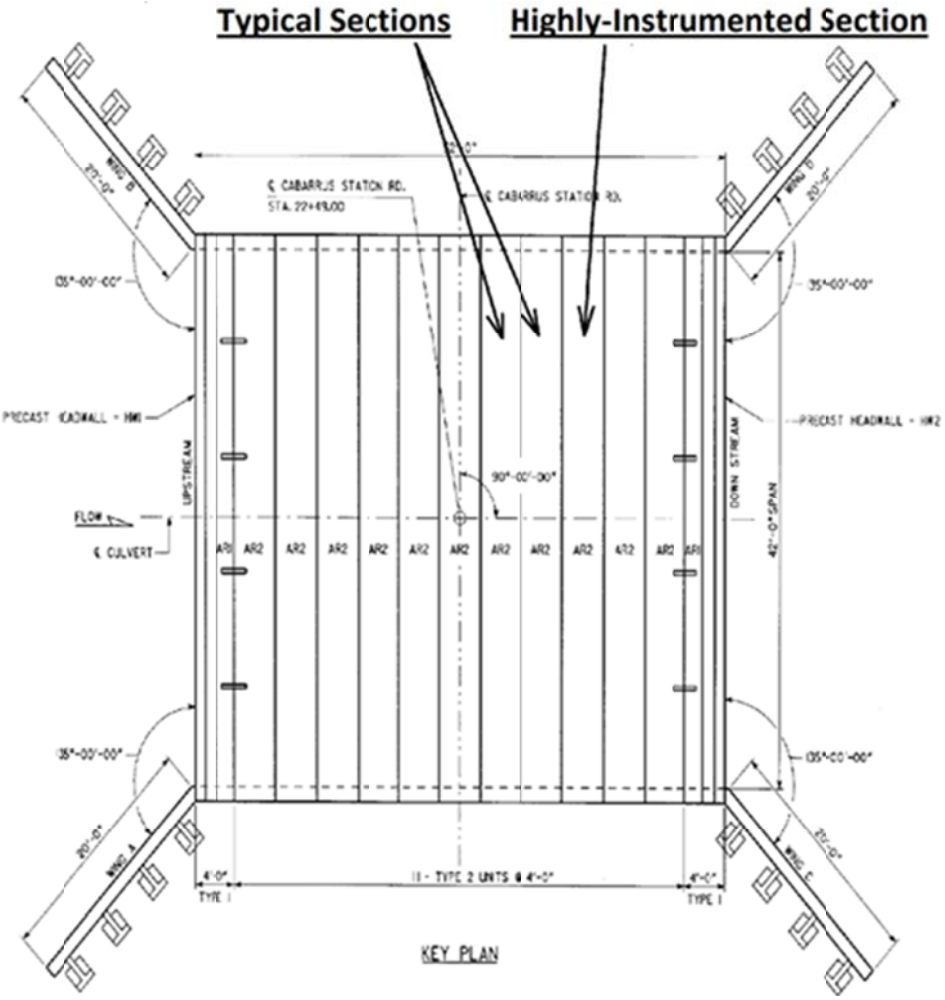

Figure 3-6 Bridge Unit Layout

3.2.2 Vibrating Wire Strain Gages

Model 4000 vibrating wire strain gages from Geokon were installed to measure strains on the surface of the concrete cross section. A vibrating wire strain gage consists of a protected metal wire that is held tight and "plucked" by a plucker unit like a guitar string, and the frequency of vibration recorded. As the wire is stretched, the frequency of vibration changes, and this frequency is then used to calculate the strain in the wire. The strain gage is attached to the surface of the structure by brackets, which can be attached in multiple ways. The gages on these units are installed using a method laid out by Bridge Diagnostics Inc. using screw-on mounts. Prior to shipping, the brackets were attached to the bridge units by pre-drilling a hole in the concrete surface and fixing the brackets with Tapcon masonry screws. Where necessary, Loctite construction adhesive was used in and around the predrilled hole to prevent the bracket from

becoming loose. A spacer bar and welding jig were used to ensure that the brackets lined up properly and did not rotate or move during installation. After shipping and placement of the bridge units, the vibrating wire strain gages and plucker units were slid into place and fixed with the mounting screws that came with the brackets. A fully installed strain gage can be seen in Figure 3-7.

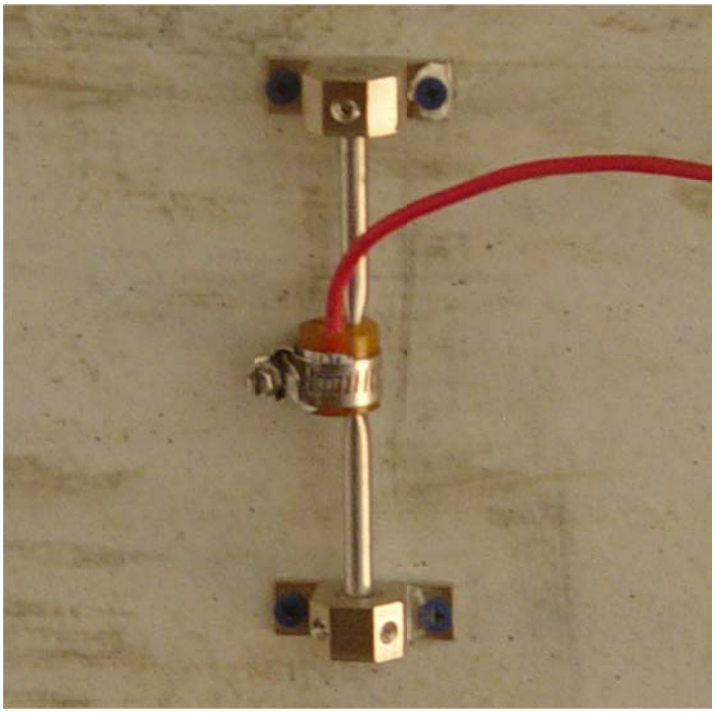

Figure 3-7 Vibrating Wire Strain Gage

To protect the strain gages on top of the bridge from damage, a half-cylinder piece of PVC was attached over the gages with construction adhesive as a cover, with the ends of the cover sealed with duct tape. An image of the protective cover can be seen in Figure 3-8. Strain gages underneath the bridge were left exposed.

Figure 3-8 Strain Gage Protective Cover

3.2.3 Earth Pressure Cells

Model 4810 Vibrating Wire earth pressure cells from Geokon were installed to measure soil backfill pressures on the sides of the bridge. The earth pressure cells were installed using the method recommended by Geokon for installation on existing structures. Mortar is placed on the structure at the pressure cell location, and the pressure cell is pressed in place so that the excess mortar extrudes out the edges of the pressure cell. The pressure cell is then attached to the structure by predrilling holes and using Tapcon screws through the mounting lugs on the pressure cell. An installed earth pressure cell can be seen in Figure 3-9.

Figure 3-9 Earth Pressure Cell

3.2.4 Displacement String Pots

Two PT8/PT8000 Series displacement potentiometers, or "string pots," from Celesco were installed to measure the vertical displacement at midspan and the horizontal displacement of the legs. The string pots were attached to the bridge by first attaching each string pot to a small piece of one inch by four inch board with screws, then attaching the board to the concrete surface using Loctite 410 instant adhesive with Loctite 7452 accelerator. The string pot wires were then anchored to ground using posts and dead weight to prevent the wires from retracting. A high strength, no yield wire was used to bridge the gap between the end of the string pot wire and the anchor locations. An installed string pot can be seen in Figure 3-10.

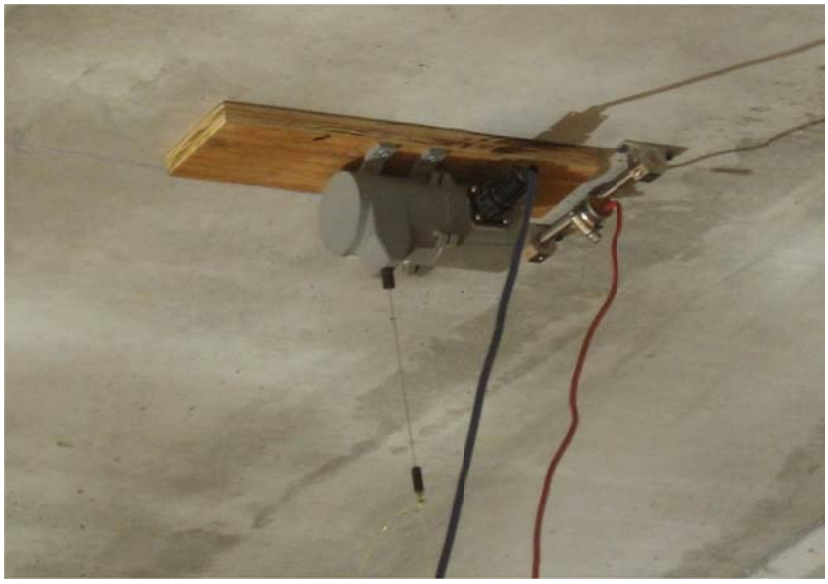

Figure 3-10 String Pot

3.3 Testing Setup and Equipment

This section contains some details on testing setup outside of instrumentation. It includes details on the soil used during the backfill process, the truck load used during live load testing, and the data acquisition system.

3.3.1 Backfill Soil

Construction documents specify the use of either AASHTO classification A-1-a, A-1-b, or A-3 soils to be used for engineering backfill. A table showing the backfill options can be seen in Table 3-2. The backfill soil used appeared to be a residual silty sand, SM, with an estimated unit weight of 110 to 115 pcf.

Table 3-2 Acceptable Engineering Backfill (FoleyArch 2010)

AASHTO CLASSIFICATION OF SOILS AND SOIL AGGREGATE MIXTURES

TYPICAL USCS MATERIALS	AASHTO GROUP	AASHTO SUBGROUP	PERCENT PASSING US SIEVE NO.			CHARACTER OF FRACTION PASSING NO. 40 SIEVE		SOIL DESCRIPTION
			#10	#40	#200	LIQUID LIMIT	PLASTICITY INDEX	
GW, GP, SP	A-1	A-1-a	50 MAX.	30 MAX.	15 MAX.	-	6 MAX.	LARGELY GRAVEL BUT CAN INCLUDE SAND AND FINES
GM, SW, SP, SM		A-1-b	-	50 MAX.	25 MAX.	-	6 MAX.	GRAVELLY SAND OR GRADED SAND, MAY INCLUDE FINES
SP, SM, SW	A-3	-	-	51 MIN.	10 MAX.	-	NON-PLASTIC	FINE SANDS

3.3.2 Truck Live Load

In addition to measurements taken during the backfill process, a load test was conducted after backfill using a full Mack CL700 three-axle dump truck. The truck had a gross vehicle weight of 56,820 lbs, measured when the truck received its load offsite. The total length of the

truck, which can be seen in Figure 3-11, was 20.5ft from front axle to rear axle. The total width of the truck was seven feet measured across the rear axle.

3.3.3 Data Acquisition

A CR1000 datalogger from Campbell Scientific was used to record data from the strain gages, earth pressure cells, and string pots. During the backfill process, data was recorded once every 30 minutes over 11 days. During the live load test, data was recorded once every 45 seconds.

3.4 Testing Procedure

This section consists of the procedure used during testing. For this test, two sets of data were recorded. The first set is recorded during the backfill process to measure construction loads on the bridge. The second set is recorded during a live load test on the bridge after the backfill process was completed.

3.4.1 Data Acquisition During Backfill Process

On September 7, 2010, after the bridge units had been placed and grouted into the footings, the strain gages and earth pressure cells were installed. Data was taken with these instruments over the next 12 days. During this time, backfill was placed around the legs and over the top of the bridge using standard construction practices up to a total cover of two feet. This data was recorded to see if the stresses on the structure during construction were more critical than those experienced during regular use.

3.4.2 Live Load Test

On September 19, 2010, a live load test using a full dump truck was performed. The strategy was to have the truck drive over the bridge, stopping at set intervals long enough for the data acquisition system to take several measurements, and then proceeding along the bridge. At each stop, the location of either the front axle or the centerline of the two rear axles was measured using a 100ft measuring tape that spanned the bridge. The truck made a total of three passes over the bridge, two heading toward the northeastern side and one heading toward the southwestern side. For the first and third run, traveling toward the northeastern side, the truck was aligned along the roadway such that the outside wheels ran over the highly-instrumented unit. For the second run, traveling toward the southwestern side, the truck was aligned such that the outside wheels were four feet over from the highly-instrumented unit. An image of the live load testing can be seen in Figure 3-11.

Figure 3-11 Live Load Testing

3.5 Analysis, Results, and Discussion of Testing

This section contains the measured data as well as calculated results from the 42 ft bridge test. For analysis purposes, the bridge units were divided into five instrumented cross sections based on the strain gage layout. Two cross sections are on the legs, two are near the corners, and one is at midspan. An image of this cross section layout is in Figure 3-12.

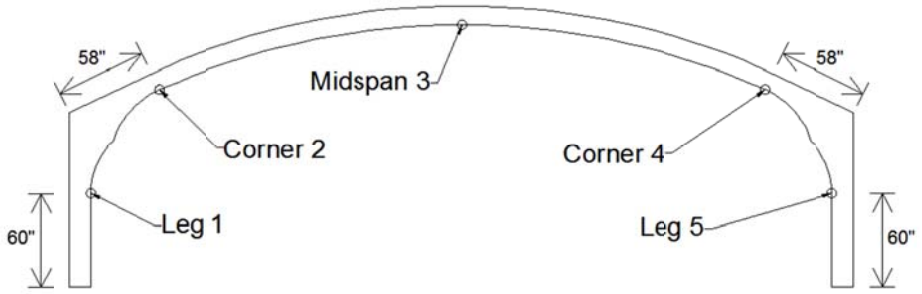

Figure 3-12 Cross Section Layout

3.5.1 Concrete Material Properties

Cylinder tests of the concrete in the bridge revealed the highly instrumented unit to have a compressive strength, f'c, of 8,670 psi. The other typical units had compressive strengths of 6,150 psi and 6,940 psi. These tests were performed by Foley Products prior to shipping of the units, in order to confirm adequate strength gain as part of their quality control.

3.5.2 Strains

A graph of the strains measured in the highly-instrumented unit during the backfill operation as well as the live load test can be seen below in Figure 3-13 and Figure 3-14,

respectively. Data was taken every 30 minutes for 11 days during the backfill operation, and every 45 seconds for roughly four hours during the live load test. Strains measured in the other units were lower in magnitude. The cycles in the strains measured during the backfill operation represent the contraction and expansion of the concrete due to temperature effects while directly exposed to sunlight. It is worth noting that the backfill operation reached the top of the bridge around October 15th, thus shielding the bridge from direct sunlight exposure and lessening the temperature effects. It is of note to point out that the strains did not go above the theoretical concrete cracking strain of 131 με, either during the backfill operation or during live load testing. This led to the assumption of uncracked, linear elastic behavior used for the calculation of moments and axial forces.

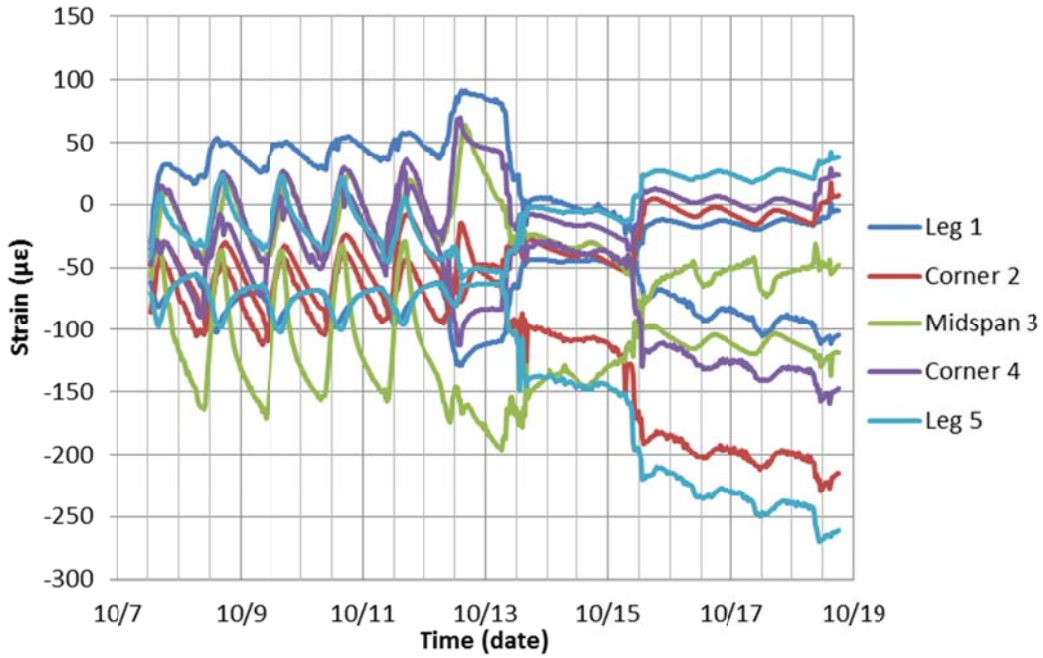

Figure 3-13 Strain in Highly-Instrumented Unit During Backfill Operation

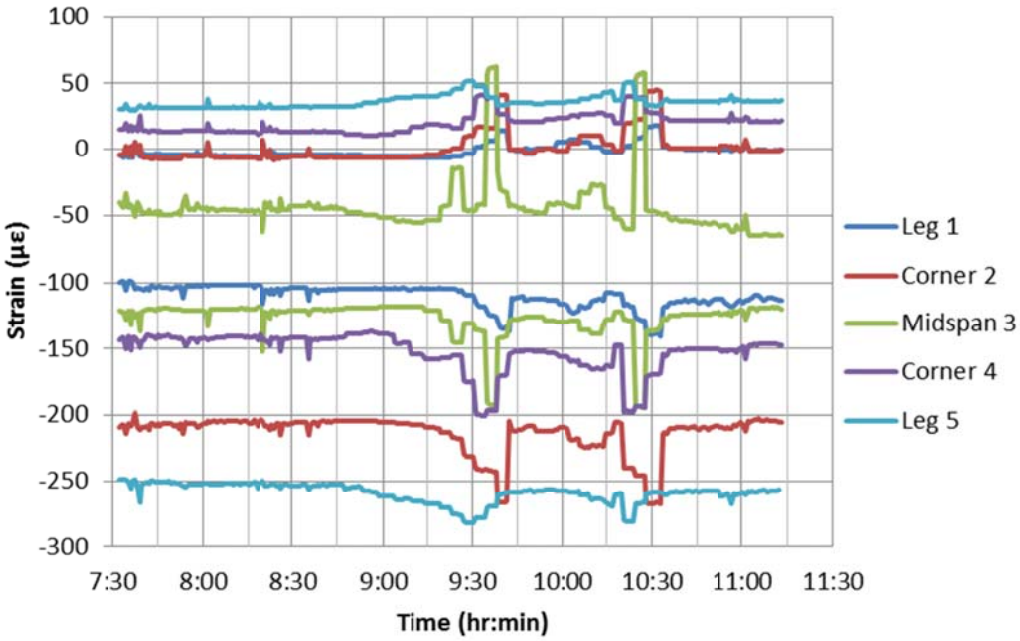

Figure 3-14 Strains in Highly-Instrumented Unit During Live Load Test

3.5.3 Moment and Axial Force Calculations from Strain

Calculations of moment and axial force in the cross sections were done assuming a linear elastic, homogeneous, rectangular cross section. Using the strains from the two strain gages on either side of the cross section, as well as the distance from the center of the strain gage to the concrete surface, a linear strain profile was established. The strain profile was then converted into a stress profile using the modulus of elasticity of the concrete. The average of the two stresses on the top and bottom of the cross section was used as the axial stress. The axial stress was then multiplied by the area of the cross section to determine the axial force. The difference between the average stress and one of the extreme fiber stresses was used as the bending stress. The bending stress was then multiplied by the moment of inertia and divided by half of the section thickness to determine the moment. This is based on the linear elastic behavior stress = My/I.

Due to the use of gross concrete section properties for moment and axial force calculations, the exact reinforcement layout is not necessary in these approximate calculations.

3.5.4 Moments and Axial Forces

The magnitude of moments measured in the bridge units was as expected. Larger, positive moments were measured at midspan, while smaller, negative moments were measured at the corners and legs. Moments were calculated on a per foot width of bridge, as was done in the design for the bridge. The maximum moment developed by the truck load was 10.5 kip-ft/ft at

midspan when the rear axles were centered over midspan. This compares favorably to the factored ultimate midspan moment strength of 38 kip-ft/ft. As for the cross sections, their maximum moments occurred when the rear axles were centered seven to ten feet away from midspan. The maximum moment due to the truck load was -6.5 kip-ft/ft for the corner gages and -5 kip-ft/ft for the leg gages. Figure 3-15 shows the development of moment versus time in the highly-instrumented unit, where the effect of the truck load was most pronounced. Figure 3-16, Figure 3-17, and Figure 3-18 show the development of moment versus the position of the centerline between the two rear axles for each of the three test runs. This graph provides a better illustration of the effect of the truck load as it passes over the bridge.

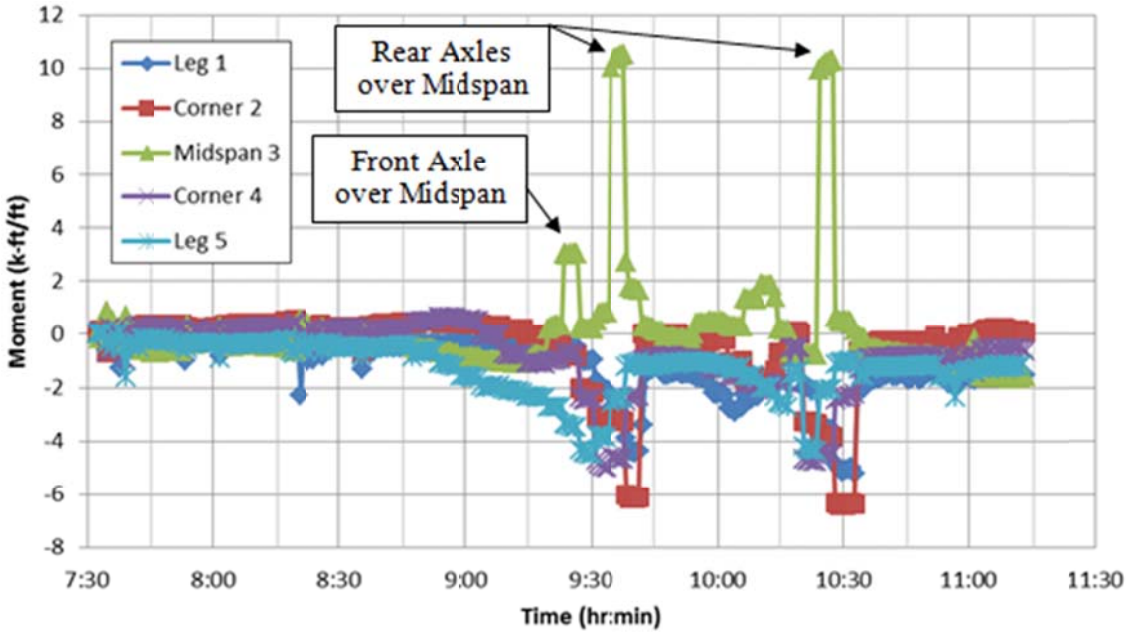

Figure 3-15 Moments due to Live Load Only Versus Time

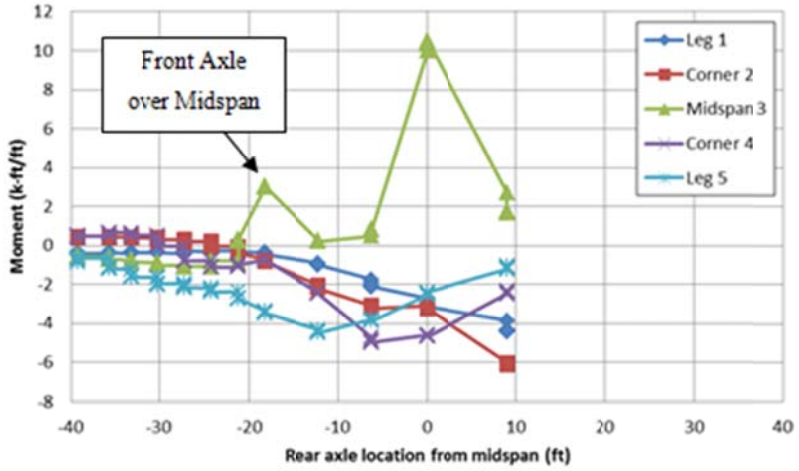

Figure 3-16 Live Load Moment vs. Rear Axle Location - Run 1

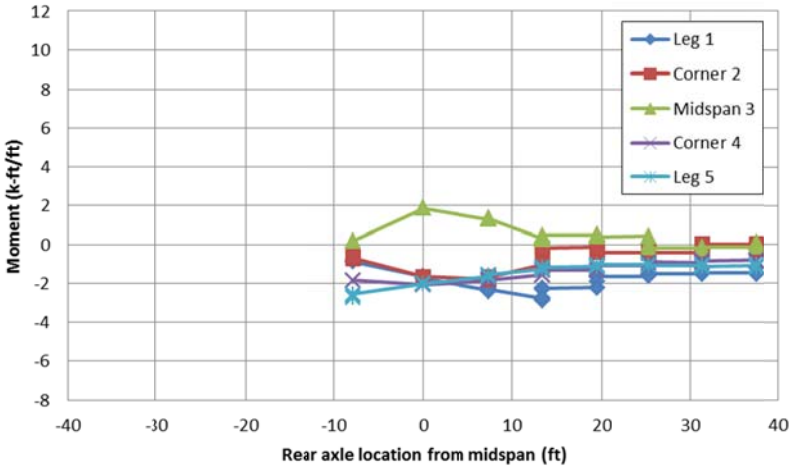

Figure 3-17 Live Load Moment vs. Rear Axle Location - Run 2

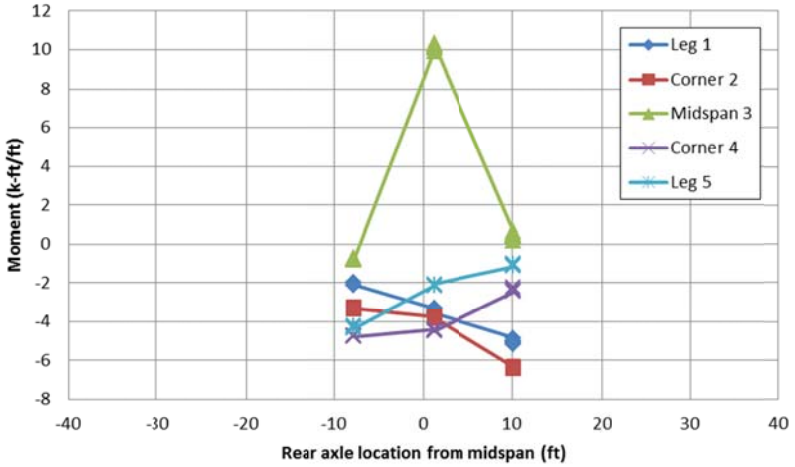

Figure 3-18 Live Load Moment vs. Rear Axle Location - Run 3

Moment diagrams show that for all measured cross sections, the maximum moment occurred when the centerline of the two real axles was over or near midspan. However, negative moments in cross sections one and two were larger when the truck was on that side of the bridge than in cross sections four and five. The opposite was true when the truck was on the other side of the bridge.

Axial forces in the cross sections were found to be negligible, and are therefore not presented in this report. The maximum compressive force felt in the bridge translates to only $0.08f'_cA_g$. However, it is worth noting that the presence of backfill around and above the bridge put all cross sections into a net compression, which helps prevent the concrete from cracking.

3.5.5 Lateral Earth Pressures

Lateral earth pressures on the external walls developed as anticipated when the truck load was applied to the bridge. As the truck load thrust the arch outward, larger lateral earth pressures were measured at the top of the wall, while very small pressures were measured at the bottom of the wall, indicating a "pinned" support condition, as opposed to a "roller" support condition. Figure 3-19 shows how the earth pressures developed versus time during the live load test in each EPC. Figure 3-20, Figure 3-21, and Figure 3-22 show the development of earth pressures versus the position of the centerline between the two rear axles for each of the three test runs. This graph provides a better illustration of the effect of the truck load as it passes over the bridge.

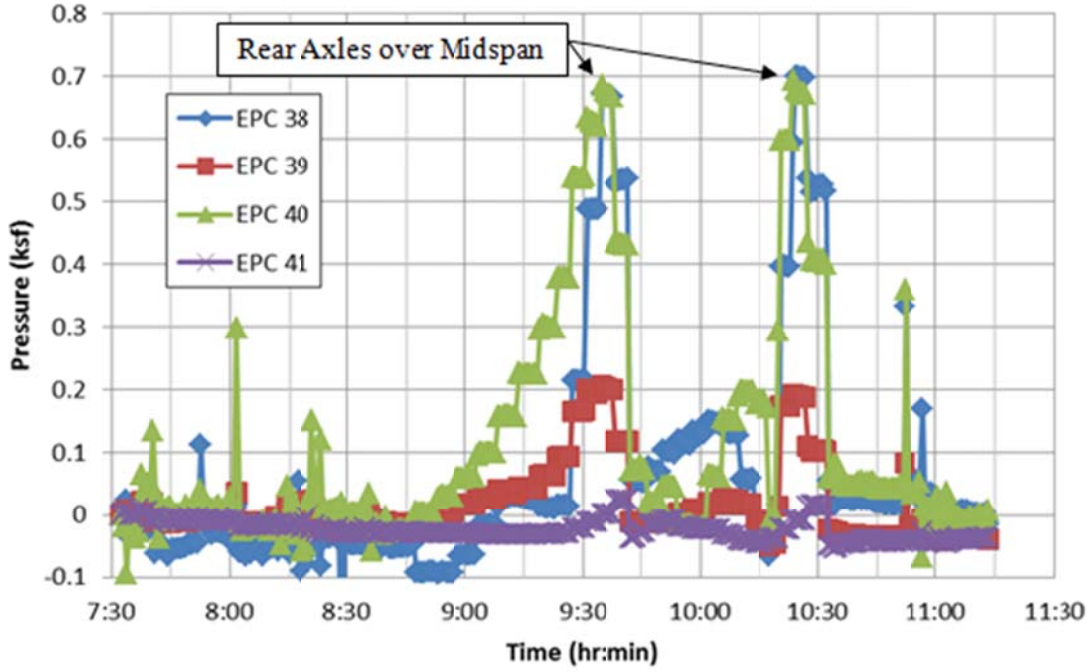

Figure 3-19 Lateral Earth Pressure due to Live Load Only Versus Time

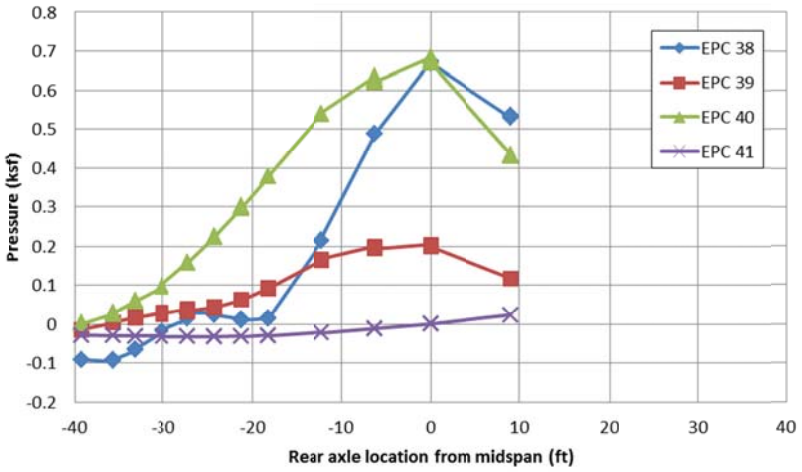

Figure 3-20 Live Load Lateral Earth Pressure vs. Rear Axle Location - Run 1

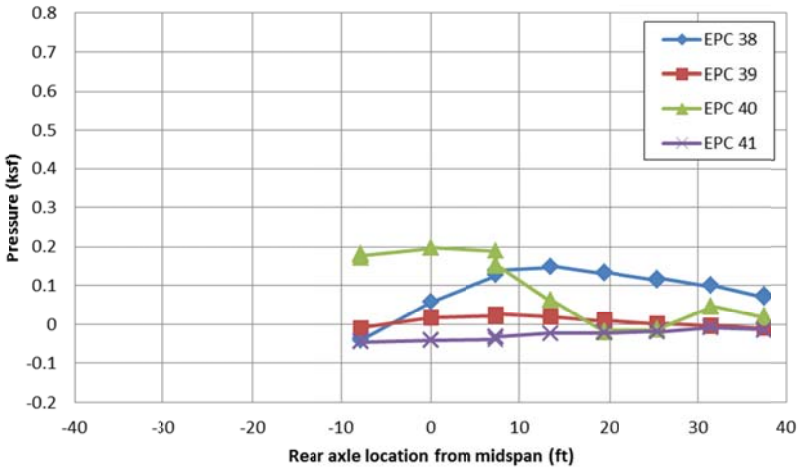

Figure 3-21 Live Load Lateral Earth Pressure vs. Rear Axle Location - Run 2

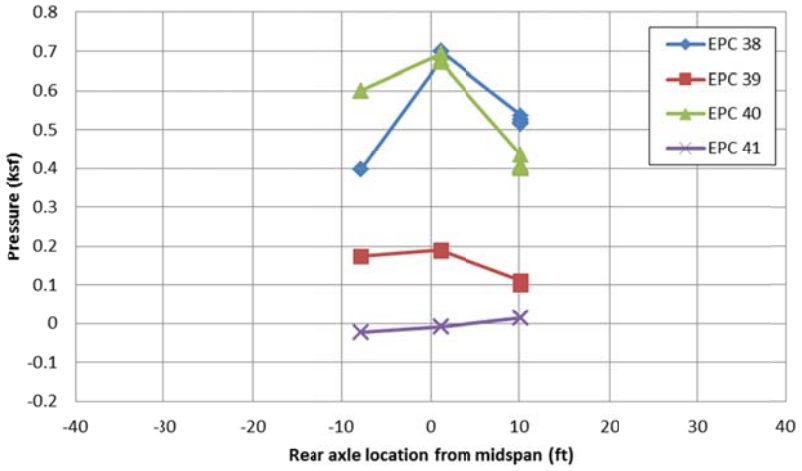

Figure 3-22 Live Load Lateral Earth Pressure vs. Rear Axle Location - Run 3

Lateral earth pressures that developed during the live load testing indicate that the largest pressures are felt at the top of the wall, with very small or even no lateral earth pressure developing near the bottom of the wall. This means that the grouted bottom of the bridge behaved as a pin, with backfill acting as a distributed spring resistance to the lateral displacement of the bridge. The largest measured earth pressures also occurred when the centerline of the two rear axles was over midspan, which is the expected time when there would be the most thrust. The development of the thrust as the truck moved along the bridge is also interesting. When the truck was on the left side of the bridge, earth pressures on the right side of the bridge were higher, due to the live load basically pushing the entire bridge laterally. The thrust on the two sides of the bridge evens out as the truck is over midspan. As the truck continues over the right side of the bridge, thrust is then higher in the left side. This was due to the off-centered truck load causing sway of the bridge frame. It is important to note that the thrusts caused by sway are small compared to the thrusts caused by the weight of the truck bending the arch and pushing it outward.

3.5.6 Displacement String Pots

It was discovered afterwards that the changing temperature in the field caused the string pot wire and no yield wire to expand, which affected the raw data. While this effect could be accounted for in the string pot wire itself, there was no way to account for the effect on the no yield wire used to bridge the gap between the string pot and the anchor points, as the exact properties of the wire were not known. Therefore, displacement string pot results are not available for this test.

3.5.7 Bridge Behavior

The bridge performed as expected. The backfill soil around and above the arch bridge caused compression in each cross section, which helped prevent cracking of the bridge. No cracking was found in any of the bridge units.

3.6 Chapter Summary

The 42 ft bridge behaved exceptionally well and was very stiff. Measurements taken during the backfill operation indicate that no cracking was caused during construction, and that the presence of backfill creates a net compression in the bridge. Under a live load test using a truck weighing 56,820lbs, the bridge showed no signs of cracking. Measured moment magnitudes were within reason, and relatively small lateral earth pressures were recorded. Pinned support behavior at the keyed footings was verified by the negligible buildup of lateral earth pressures near the bottom of the bridge.

Chapter 4 Laboratory Test – 20 ft Span

4.1 Introduction

A 20 ft span bridge unit was used for a laboratory test of the Foley Arch precast arch culvert bridge system. The single unit of a multi-unit bridge was designed for ten feet of backfill plus live load. The unit has a 20 ft clear span, an inside clear height of eight feet at midspan, and is four feet wide. An image of the overall dimensions and the reinforcement layout in the unit can be seen in Figure 4-1, with the exact reinforcement used detailed in Table 4-1. Note that transverse steel runs parallel to the roadway, meaning that it is the primary flexural resistance steel.

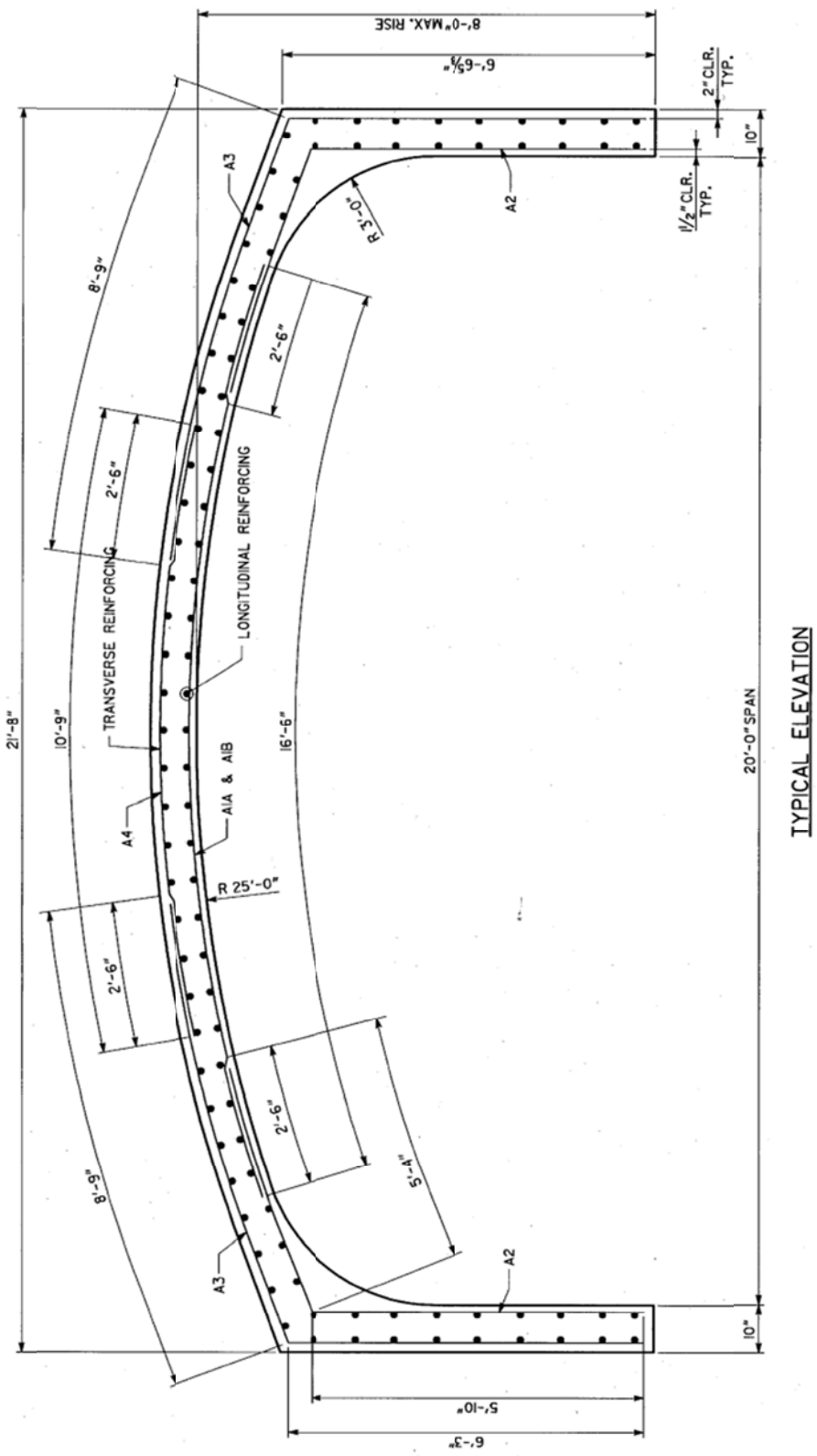

Figure 4-1 20 ft Bridge Unit Reinforcement Layout (FoleyArch 2010)

Table 4-1 20 ft Bridge Unit Reinforcement Details (FoleyArch 2010)

Designation:	Mesh Size	Length (ft)	Transverse Area Supplied (in2/ft)	Longitudinal Area Supplied (in2/ft)
A1A	D16.7xD8 2x4.75	16'-6"	1.002	0.202
A1B	D16.7xD8 2x4.75	14'-0"	1.002	0.202
A2	D10.5xD8 4x7	11'-2"	0.315	0.137
A3	D10.5xD8 2x7	15'-0"	0.63	0.137
A4	D10.5xD8 4x4	10'-9"	0.315	0.24
Design based on uncoated reinforcing meeting ASTM A-615, Grade 60, fy = 60,000psi				
Minimum Yield Strength for welded wire fabric shall be 65,000 psi				

The bridge unit was cast on March 2, 2011 at the Foley plant in Winder, GA, and shipped to the Structures Research Laboratory at Auburn University on June 1, 2011. Due to the unit geometry, it was able to be shipped standing up. The unit was light enough that it was able to be picked up using the laboratory crane alone. Three load tests were performed on the bridge between August 3 and August 10, 2011. At ultimate load conditions, the unit held more than 182 kips before failing.

This chapter details how the 20 ft unit was tested, as well as the results of that testing. It contains sections on the instrumentation, setup, and procedure used for testing. It also contains analysis and results from testing, followed by discussion of those results.

4.2 Instrumentation

This section contains a detailed description of the instrumentation used on the 20 ft span bridge unit. It also contains details about the different types of instruments used, including how each was installed.

4.2.1 Instrumentation Layout

The 20 ft clear span bridge unit was initially instrumented with 15 sister bar strain gages, ten concrete surface strain gages, three displacement potentiometers, or wirepots, and four load cells. Two additional wirepots were added later.

Strain gages were placed at five cross section locations on the bridge: at midspan, at the corners where the section began to increase in thickness, and on the legs where the section began to increase in thickness. The layout of the instrumented cross sections can be seen in Figure 4-2. Three sister bar gages were placed at each location and tied to the reinforcing cage. These sister bar gages were tied on the side of the cross section that would be the expected tension side, meaning the inner side of the bridge at midspan, and the outer side of the bridge at the corners and legs. Two concrete surface strain gages were placed at each cross section, at third points

along the width, on the concrete surface expected to be in compression, meaning the outer side at midspan, and the inner side at the corners and legs.

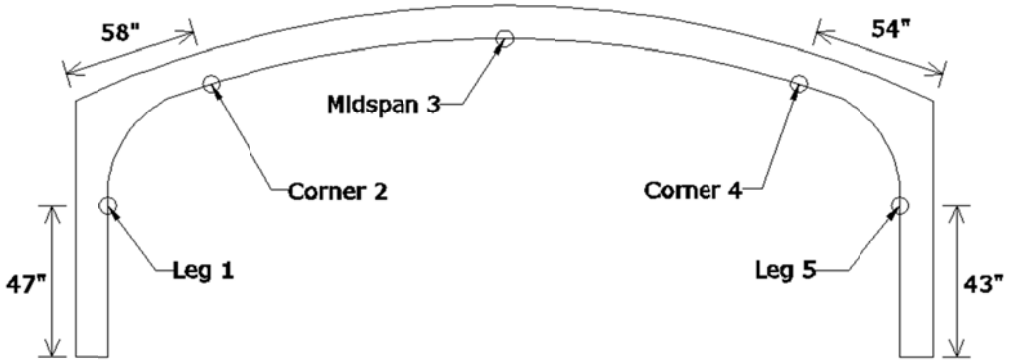

Figure 4-2 20 ft Cross Section Layout

The first three wirepots were placed in positions to measure the maximum deflections that the bridge experienced. Therefore, one was placed vertically at midspan to measure vertical deflection, and the other two were placed horizontally at the top of the walls to measure lateral deflection. After initial testing, it was observed that the maximum lateral deflections occurred within the wall, and not at the top. So for the final test, a fourth and fifth wirepot were placed horizontally at a point 48in above the bottom of the bridge, near cross sections one and five.

In addition, four load cells were used to measure the horizontal reaction at the base of the bridge. At the base of each leg, two load cells were used to restrain the lateral movement of the leg. This was done to effectively create a pinned support condition, like that experienced in the field. A sketch of the wirepot and load cell layout can be seen in Figure 4-3.

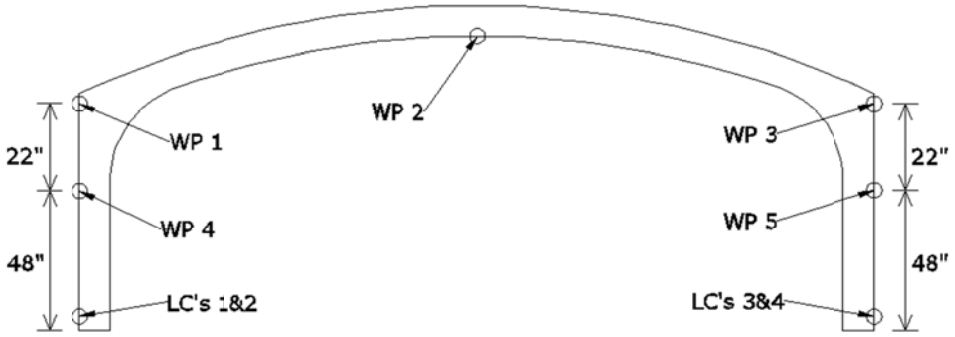

Figure 4-3 20 ft Wirepot and Load Cell Layout

4.2.2 Sister Bar Strain Gages

The sister bar strain gages were created by bonding an electrical resistance strain gage to the smooth, treated surface in the middle of a three foot long #4 bar. Prior to casting, these bars were tied to the normal reinforcement cage at the appropriate locations. Care was taken during

casting, storage, and shipment of the unit to ensure that unnecessary stress was not put on the wiring. A completed and installed sister bar can be seen in Figure 4-4.

Figure 4-4 Sister Bar Installed in Reinforcement Cage

Creating the sister bar strain gages consisted of first preparing a smooth, treated surface on the bar, then installing the strain gage. First, in the middle of a three foot long #4 deformed bar, a section of adequate width and length was ground smooth using a circular grinding wheel and sandpaper. The goal was to remove as little steel as possible, so as to have a minimal impact on the area of the bars. Next, the smoothed surface was prepared in accordance with techniques prescribed by Vishay Micro-Measurements. These steps consisted of degreasing with CSM-2 Degreaser, wet sanding with 320 grit sandpaper and M-Prep Conditioner A, surface conditioning with M-Prep Conditioner A, and neutralizing with M-Prep Neutralizer 5A.

Following surface preparation, a 250LW strain gage from Vishay Micro-Measurements was installed on the surface. The installation process followed the procedure described by Vishay Micro-Measurements. The process consisted of picking up the gage with PCT-2M gage installation tape, lining the gage up properly over the smoothed surface, peeling the tape and gage back just far enough to expose the entire bottom of the gage, applying a single coat of 200 Catalyst-C to the bottom surface of the strain gage, and putting a small dot of M-Bond 200 adhesive on the smoothed surface at the base of the strain gage. Then, in one motion, sliding the thumb over the tape to press the strain gage into the adhesive, spreading the adhesive while ensuring no air bubbles are formed between the gage and the smoothed surface. Pressure was held on the gage with the thumb for upwards of ten seconds before being released. The next day, after the adhesive has completely set, the tape was peeled back and removed. A small section of Mastic tape was placed under the lead wires to prevent them from touching the steel surface. A coat of M-Coat B Nitrile rubber was applied over the gage to provide protection and water-tightness, followed by another small section of Mastic tape over the gage to provide additional

protection. Finally, heat shrink tubing and electric tape were placed around the gage area to provide more protection and water-tightness.

Prior to placement, each sister bar strain gage was checked with a P3 Strain Indicator and Recorder to make sure the gages were working. It was found that two gages in different cross sections were faulty at this point.

4.2.3 Concrete Surface Strain Gages

Once the bridge was in the lab, concrete surface electrical resistance strain gages were attached to the bridge surface. The area where the strain gage was to be installed was firmly brushed with a metal wire brush, and then an air hose was used to remove excess concrete dust from the surface. Next, a back-coat of M-Bond GA-2 Adhesive was applied to the surface, ensuring all holes were filled and a relatively smooth surface was formed. The next day, after the adhesive cured, the back-coat layer was sanded smooth down to nearly the concrete surface, and then a damp paper towel was used to remove dust from that surface. A 20CLW strain gage with a two inch gage length from Vishay Micro-Measurements was picked up using PCT-2M gage installation tape. Finally, the gage was installed by applying a thin layer of five minute epoxy to the back-coat surface and pressing and holding the gage into place for upwards of five minutes, while ensuring no air bubbles were allowed to form. The piece of tape was left in place to provide some minimal amount of protection to the gage and because removal of the tape risked debonding the strain gage. An installed concrete surface strain gage can be seen in Figure 4-5.

Figure 4-5 Concrete Strain Gage

Concrete gages were also checked with the P3 Strain Indicator, and all gages were found to be working satisfactorily.

4.2.4 Displacement Wirepots

WDS P-60 series draw wire sensors with a range of 1000mm (39in) from Micro-Epsilon were used to measure deflections of the bridge unit. From henceforth, these sensors will be referred to as wirepots. The wirepots were attached to the bridge by drilling a small hole into the concrete, tapping in a light duty plug anchor, screwing in a small eyebolt and attaching the end of the wirepot string to the eyebolt. For wirepots measuring lateral deflection, holes were drilled into the side of the bridge unit, as seen in Figure 4-6. For the wirepot measuring vertical deflection at midspan, the hole was drilled in the bottom of the bridge arch. The lateral wirepot units were mounted to the lateral resistance frame to serve as a fixed point. The vertical wirepot was mounted to a frame built to house the wirepot and gage wire hookups around the center actuator.

Figure 4-6 Displacement Wirepot

4.2.5 Load Cells

Four LPSW-B model load cells from Load Cell Central were used to measure the horizontal reaction at the base of the bridge unit. Each load cell has a 50,000lb capacity. The four load cells were simply placed in between the bridge and the HSS section that served as our base horizontal reaction, with a 6in x 6in x 0.25in plate bearing between the load cell contact point and the concrete surface to prevent damage due to the concentrated force of the load cell. One of the installed load cells can be seen in Figure 4-7.

Figure 4-7 Load Cell

4.3 Testing Setup and Equipment

This section contains some details on testing setup outside of instrumentation. It includes details on the various loading frames used for testing, the actuators used to apply the load, and the data acquisition system.

4.3.1 Lateral Resistance Frame

For service load testing, a lateral resistance system was devised to attempt to represent lateral soil pressures that would arise due to horizontal displacement of the bridge legs. This system was composed of four HSS 6x6x0.5 sections, two per wall, bearing at the top and middle of the bridge walls, tensioned together by multiple 12ft long threaded rods on either side of the bridge, which ran along the bridge length from one HSS to the other. In between the 12ft threaded rods was a three foot threaded rod with strain gages attached to it. Coupling nuts were used to link the 12ft threaded rods with the three foot gaged rods. All threaded rods were 1.125in diameter rods. The three foot gaged rods were used to calculate the force in each rod, and therefore the lateral force being exerted on the bridge unit. Each gaged rod had two strain gages attached at the same location on opposite sides of the cross section, so that the effects of the moment in the rod could be accounted for when calculating the tension in the rod. An image of the four gaged rods can be seen in Figure 4-8. Increasing or decreasing the lateral force on the bridge was achieved by tightening or loosening the nuts holding the rod assembly to the HSS section. A wood framing platform, which was also used to mount horizontal wirepots and gage wire hookups, was built in order to hold the HSS sections at the proper height during testing. An image of the lateral resistance frame near the legs can be seen in Figure 4-9, while an image showing the threaded rods spanning the bridge can be seen in Figure 4-10.

Figure 4-8 Three Foot Gaged Thread Rods

Figure 4-9 Lateral Resistance Frame near Bridge Legs

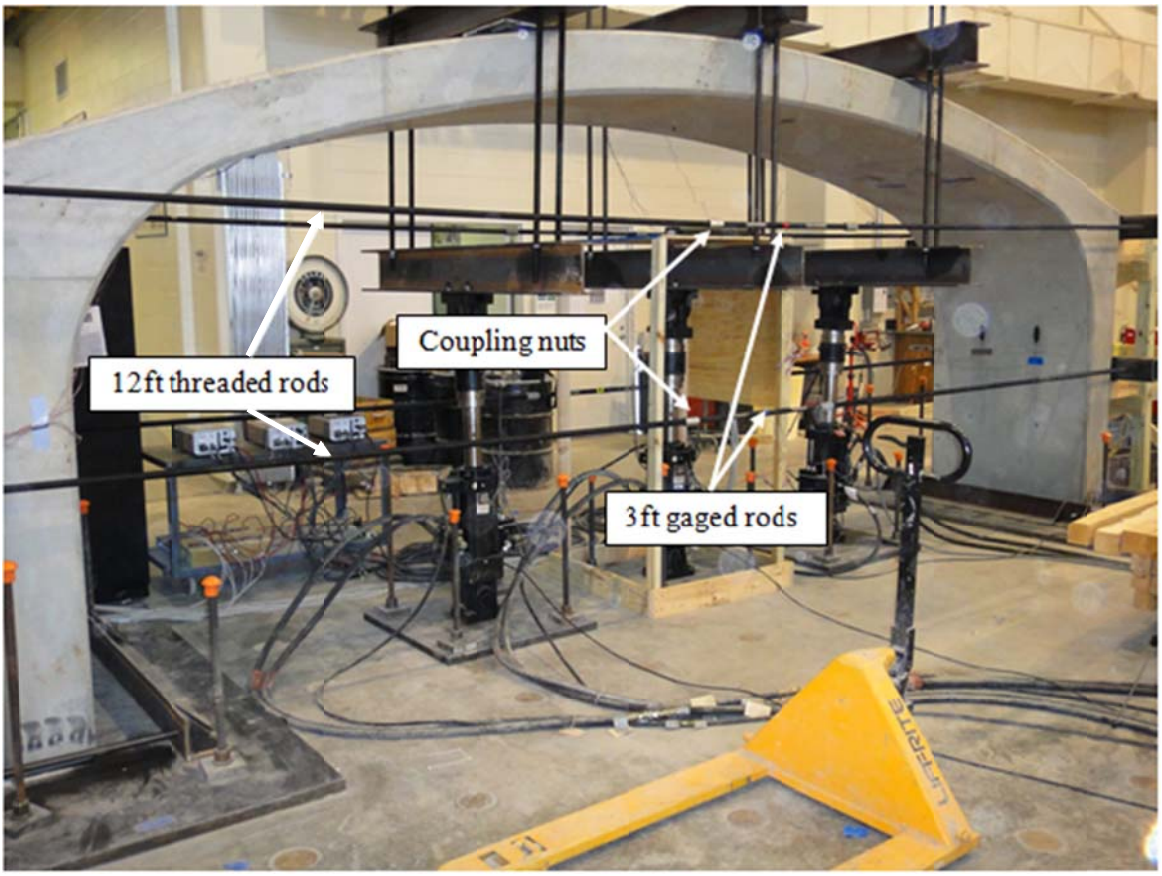

Figure 4-10 Lateral Resistance Frame Spanning Bridge Unit

4.3.2 Load Framing System

The load frame designed for this project consisted of three actuators pulling down on the bridge unit from underneath. The frames with the three actuators can be seen in Figure 4-11. A W8x35 beam lied on top of the bridge unit spanning the width of the section. Two 1.125in diameter threaded rods ran through each end of the W8x35 beam to another W8x35 beam, which was attached to the actuator at the midspan of the beam. The actuator was attached to a 32in x 32in x 1.5in baseplate, which was tensioned to the laboratory strong floor. Based on the layout of anchor points in the strong floor, the three actuators were spaced at four foot intervals, with the middle actuator located at midspan of the bridge unit. For the two outer actuators, roller plate units, which can be seen in Figure 4-12, were placed underneath the top W8x35 beams in order to insure that the actuator and load path remained vertical even on the sloped concrete surface. To ensure an even bearing surface, neoprene bearing pads were used on top of the concrete bridge surface.

Figure 4-11 Actuator Loading Frames

Figure 4-12 Illustration of Rollers

The baseplates for the bridge unit, seen in Figure 4-13, consisted of two 8ft x 4ft x 1.5in A36 steel plates, with an L6x6x0.5 angle welded onto each plate. Two 1.125in diameter threaded rods ran from the ends of the angle to an HSS6x6x0.5, which provided a horizontal reaction force at the base of the bridge. The horizontal restraint of the bottom of the leg was provided to simulate field conditions, in which the bridge units are placed into keyed footings.

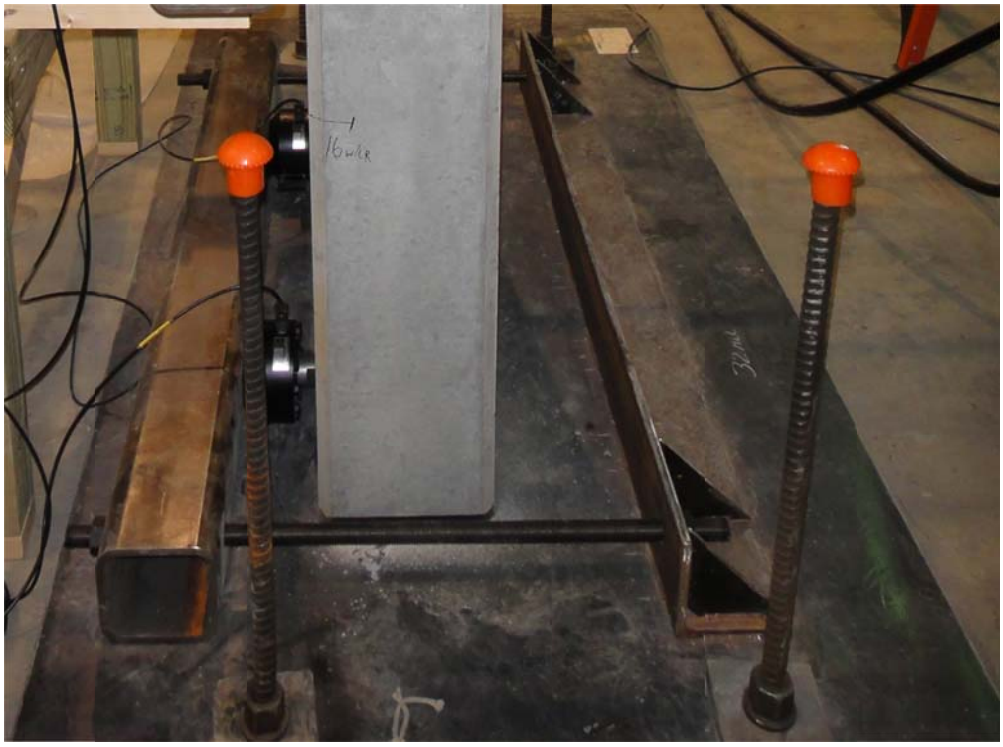

Figure 4-13 Bridge Baseplate

4.3.3 Actuators

The actuators used are model number 243.35 Single Ended Actuators from MTS. They have an 82 kip capacity in compression and a 54 kip capacity in tension with a ten inch total stroke. The load framing system was such that the actuators were in tension, giving them a capacity of 54 kips per actuator. MTS Model 407 controllers were used to control each actuator independently using displacement control.

4.3.4 Data Acquisition

A Pacific Instruments 6000 Data Acquisition System was used for collecting data. A sample rate of one sample per second was used for all testing. Data was monitored throughout testing and saved and recorded after each test was finished.

4.3.5 Additional Vertical Loading Frame

For the second ultimate load test, additional vertical load was needed to fail the bridge unit. This was supplied by spanning two L5x5x0.5 angles across the width of the bridge on either side of the midspan actuator. These angles were then tied to the floor using the 1.125in diameter threaded rods used for the lateral resistance system. The four gaged threaded rods were used to calculate the load in each rod, and therefore the additional load being applied to the bridge. Load

was applied by tightening the bolts holding the assembly together. This additional loading frame is shown in Figure 4-14.

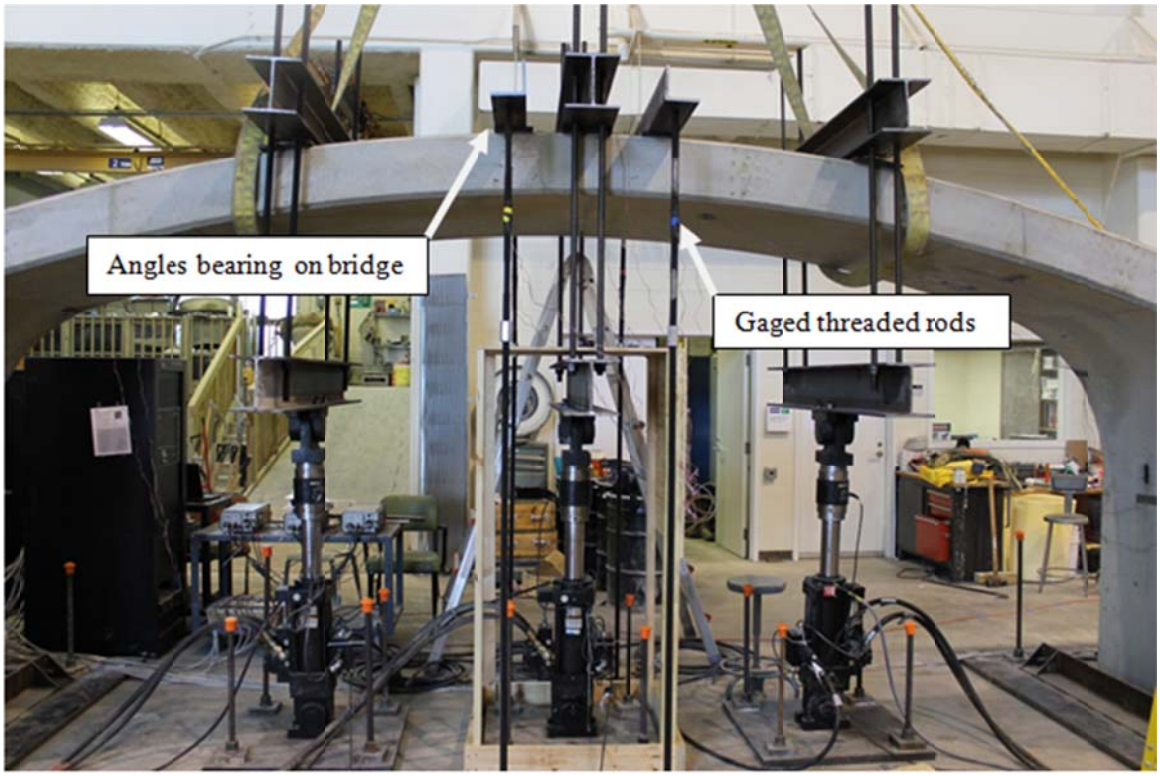

Figure 4-14 Additional Vertical Load

4.4 Testing Procedure

This section consists of the procedure used during testing. For this bridge unit, three separate tests were performed. The first test was a service level test using the lateral resistance frame. The second test was an ultimate level test without the lateral resistance frame. After being unable to achieve the ultimate load, a third test was needed. The third test was another ultimate level test using additional vertical loading. Information about the calibration of gaged threaded rods and concrete material property testing are also included.

4.4.1 Calibration of Gaged Threaded Rods

In order to accurately translate the measured strains in the three foot gaged rods into force, each rod was calibrated using a tension testing machine. Using a Tinius-Olsen Universal Testing Machine, as well as the P3 Strain indicator, tensile force and strains were measured every 100lbs up to a load of 2,000lbs, and this data was used to plot a force versus average strain graph. This process was repeated a minimum of five times for each rod, in order to gather sufficient data. It was discovered that each rod had a unique slope, which was then used to calculate the

force in the rods during bridge testing. An image of the gaged threaded rod calibration setup can be seen in Figure 4-15.

Figure 4-15 Gaged Threaded Rod Calibration

4.4.2 Concrete Cylinder Testing

Nine concrete cylinders were prepared when the bridge unit was cast. The cylinders were eight inches long with a four inch diameter. These cylinders were kept under the same conditions as the bridge unit until the unit was shipped. At that point, the cylinders were kept indoors at the production plant in order to simulate the laboratory conditions experienced by the bridge unit. The cylinders were shipped to Auburn University and strength and modulus tests were performed on these cylinders on August 15, 2011. Compressive strength tests conformed to ASTM C39, Standard Test Method for Compressive Strength of Cylindrical Concrete Specimens (ASTM International 2005), and modulus of elasticity tests conformed to ASTM C469, Standard Test Method for Static Modulus of Elasticity and Poisson's Ratio of Concrete in Compression (ASTM International 2002). Testing consisted of loading the cylinder up to roughly 40% of f'c with the compressometer attached in three cycles per cylinder to determine the modulus, followed by removing the compressometer and loading the cylinder until it fails to determine the compressive

strength. An image showing the test machine can be seen in Figure 4-16, and an image of the compressometer can be seen in Figure 4-17. A typical failed cylinder can be seen in Figure 4-18.

Figure 4-16 Concrete Cylinder Testing Machine

Figure 4-17 Compressometer

Figure 4-18 Failed Cylinder

4.4.3 Service Level Test

On the morning of August 3, 2011, a service level load test was performed on the 20 ft bridge unit. Load was applied using the actuators up to 16 kips per actuator, slowly moving in four kip increments. Each actuator was independently controlled, and the operators attempted to increase load at the same rate, applying a uniform load distribution in each actuator. At each load increment, the force in the lateral resistance frame had to be reduced to compensate for the buildup of force in the threaded rods. More details on the reasoning for this can be found later in section 4.5.8. Force in the threaded rods was reduced by loosening the nuts that attached the threaded rods to the HSS sections bearing against the bridge legs. Forces in the rods were small enough that loosening could be performed using simple adjustable wrenches. Rods on either side of the bridge attached to the same HSS were loosened at the same time in order to maintain a uniform load distribution along the concrete surface. At each load increment, the lateral resistance frame was adjusted to apply horizontal loads that would be typical of lateral earth pressures in backfill. After both the lateral restraints and actuator loads were stabilized at the correct level, load was held for several seconds to allow continuous data acquisition before proceeding to the next load increment. After the 16 kips per actuator maximum load increment, the load was removed, lateral resistance frame dismantled, and the hydraulics shut off.

4.4.4 First Ultimate Load Test

On the afternoon of August 3, 2011, an ultimate level load test was performed on the 20 ft bridge unit. The lateral resistance frame was removed, so that the only load applied to the structure was from the actuators pulling down. It was observed during the service level test that horizontal deflections were not maximum at the top of the walls, due to the side walls themselves experiencing flexure. To account for this, two rotational dial gages were arranged to measure deflections at approximately midheight of the legs. It was observed that measurements from wirepot gages added prior to the second ultimate load test showed approximately the same behavior as the dial gages, but at greater accuracy. Therefore, the dial gage data is not shown or discussed. The bridge was loaded using the actuators as before, at increments of two kips per actuator. The load was brought up to approximately 53 kips per actuator, at which point the actuators were maxed out and could not apply anymore load.

In an attempt to fail the bridge unit, the load was dropped down to 40 kips per actuator, and two concrete blocks, each weighing roughly 1,900lbs, were placed on either side of the midspan actuator. An image of the test with the concrete blocks can be seen in Figure 4-19. The load was then increase back to 53 kips per actuator, but the additional weight of the concrete blocks was not enough to fail the bridge unit. The concrete blocks and actuator load was removed and hydraulics turned off. The effects of this reloading using the concrete blocks was negligible, and is not did not impact the results of the test.

Figure 4-19 Addition of Concrete Blocks for Loading

4.4.5 Second Ultimate Load Test

On August 10, 2011, a second ultimate level load test was performed on the 20 ft bridge unit. This test was performed using the actuators as well as the additional vertical loading frame consisting of angles and threaded rods. Two additional displacement wirepots were added at a height of 48 in on the side walls of the bridge unit in order to measure the horizontal displacement in the walls relative to the horizontal displacement at the top of the walls.

In anticipation of failure, the crane in the laboratory was centered over the bridge, with straps placed loosely underneath the bridge to "catch" the bridge. The ten ton capacity laboratory crane was manually controlled, and had enough capacity to keep the arch from falling on the testing equipment should a complete collapse of the structure occur. An image showing how the crane straps were position can be seen in Figure 4-20.

Figure 4-20 Crane Support Illustration

The load in the actuators was gradually brought up to 50 kips per actuator and held at that load. Load was then applied using the angles and threaded rods by tightening the nuts connecting the rods to the angle while preventing the entire threaded rod assembly from rotating by gripping the coupling nut connected the two threaded rod segments. An image showing the tightening process can be seen in Figure 4-21. Each rod was brought up to a tensile force of five kips, thus providing an additional 20 kips of force on the structure. To prevent uneven loading across the width of the bridge, threaded rods attached to the same angle were tightened at the same time. Increasing load on the rods, however, relieves some of the load on the actuators. So after each rod was brought up to full force, the actuators were brought back up to 50 kips each. However, this then relieved some of the force in the threaded rods, which were then brought back to five kips each. This iterative process was repeated for several cycles, with the force in the rods being increased to 11 kips per rod at their maximum, and the force in the actuators being increased to 52 kips per actuator at their maximum. Eventually, during a cycle of reapplying load with the actuators, the bridge unit collapsed due to a shear failure in the arch near one of the corners.

Figure 4-21 Tightening of Additional Vertical Loading Frame

4.5 Analysis, Results, and Discussion of Testing

This section contains the measured data as well as calculated results from the 20 ft bridge test. For analysis purposes, the bridge is divided into five instrumented cross sections based on the strain gage layout. Two cross sections are on the legs, two are near the corners, and one is at midspan. The cross sections are the same as those in Figure 4-2.

4.5.1 Concrete Material Properties

Cylinder tests revealed the concrete to have a compressive strength, f'c, of 12,500 psi. Modulus of elasticity tests show the concrete to have a modulus, Ec, of 5,950 ksi. This compressive strength value is quite high. Typical 28-day compressive strength values are 6,000 psi to 7,000 psi. The high compressive strength value is a function of the fast setting concrete used for this precast unit, as well as time between casting and testing, which was roughly five months.

4.5.2 Strains

Strains at the same location within each cross section were approximately equal, meaning sister bar strain gages agreed with each other at each cross section, and the same with concrete surface strain gages. This observation indicated two very important things. First, load testing did not cause any torque in the bridge. Second, the strain gages were measuring strains properly. In addition to the two sister bar strain gages that were faulty after casting of the bridge, two other

gages became faulty during the course of the three tests, drastically rising and flattening at a peak strain orders of magnitude higher than other gages. In such cases, those particular strain gages were neglected for calculating moments and axial forces. At all cross sections, at least one sister bar strain gage measured properly.

It was observed that very small strains were measured at the corner cross sections, locations two and four. In some cases these cross sections measured strains opposite the anticipated sign, for example, concrete gages in tension. It was determined that the location of these gages was further out on the arch than intended, near the inflection points. For these gages, uncracked section analysis similar to what was used for the field test was used to determine moments and axial forces.

Near the very end of testing, just prior to failure of the bridge unit, some sections measured a strain higher that the assumed reinforcement yield strain of 0.00207. However, this yielding did not significantly affect the calculated internal forces.

4.5.3 Moment and Axial Force Calculations from Strains

Using the strains measured on the concrete compressive surface and within the cross section near the steel, moments and axial forces were calculated. Assuming plane sections remain plane, a linear strain distribution was used across the entire concrete section. This strain distribution and its curvature were used to find the neutral axis, a distance "c" from the concrete compressive surface, as well as strains in the concrete and steel. Stresses in both the tension and compression steel were calculated using a modulus of elasticity of 29,000 ksi, with a yield plateau of 60 ksi. Concrete tension stresses were calculated using the modulus of elasticity of the concrete up to the calculated rupture stress, f_r, which is 840 psi. Concrete compressive stresses were calculated using an assumed stress-strain curve taken from Wight and MacGregor which uses the measured strength and modulus of the concrete to calculate a stress-strain relationship for concrete compressive strengths from 2,000 psi to 18,000 psi (Wight and MacGregor 2009). The relationship between concrete stress, fc, and strain, εc, is as follows:

$$\frac{fc}{f'c} = \frac{n*\left(\frac{\varepsilon c}{\varepsilon o}\right)}{n-1+\left(\frac{\varepsilon c}{\varepsilon o}\right)^{nk}} \quad (4\text{-}1)$$

where

f'c = peak stress obtained from a cylinder test

εo = strain at peak stress

n = curve fitting factor

k = slope controlling factor

The curve fitting factor is found by using the following equation:

$$n = 0.8 + \left(\frac{f'c}{2{,}500}\right) \tag{4-2}$$

The slope controlling factor, k, is equal to 1.0 when εc ≤ εo, but for εc > εo,

$$k = 0.67 + \left(\frac{f'c}{9{,}000}\right) \geq 1.0 \tag{4-3}$$

The strain a peak stress is calculated using the following:

$$\varepsilon o = \frac{f'c}{Ec}\left(\frac{n}{n-1}\right) \tag{4-4}$$

where

Ec = compressive modulus of elasticity of concrete

The stress distribution along the cross section was then used to calculate the four internal forces, concrete compressive force (Cc), concrete tension force (Tc), steel compressive force (Cs), and steel tension force (Ts). The steel forces Cs and Ts were calculated by simply multiplying the stress by the area of steel at each location. The concrete tension force was calculated using a triangular stress distribution multiplied by the width of the cross section. The concrete compressive force was calculated by dividing the compressive stress distribution into five equal parts by height, taking the average stress in each part, multiplying the average stress of each part by its height and the width of the cross section, and then summing the forces in each part. The location of Cc, a distance "g" from the edge of the compression surface, was determined by taking the sum of the compressive forces multiplied by their locations, and dividing it by the total force, Cc. An illustration of this is provided in Figure 4-22.

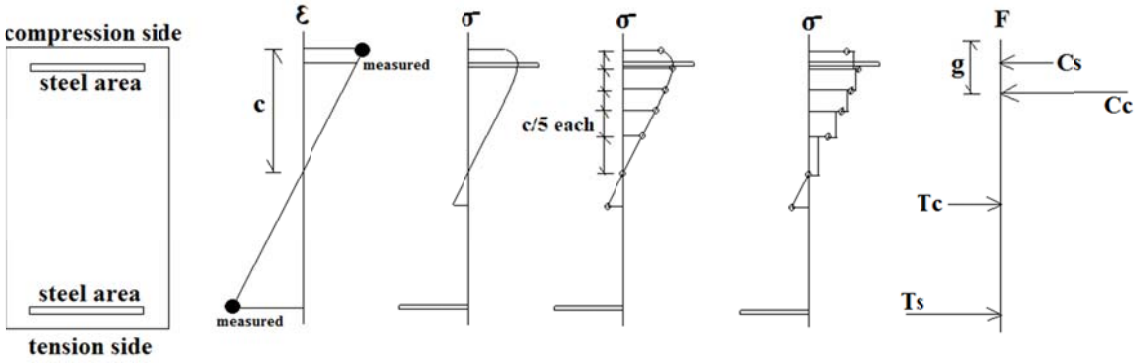

Figure 4-22 Strain and Stress Distribution

Axial forces and moments were then calculated by taking the sum of the forces, and taking the sum of the moments due to the forces about midheight of the cross section, respectively. Moments and axial forces were calculated using the full width of the unit. It is worth pointing out that when the two measured strains have the same sign, or when the curvature

is opposite of what would be expected, this analysis returns faulty results. However, this generally happens only at very low load levels. It is also worth noting that the concrete tension force calculation does not factor in when the bridge was loaded, cracked, unloaded, and then reloaded again. However, the concrete tension force does not have a substantial effect on the axial force or moment calculations above a relatively low load level.

It was found that cross section two and cross section four were placed near the inflection point. They therefore experienced relatively low strains and curvature opposite of what was expected. For these sections, an analysis similar to what was used on the 42 ft field test was used. Calculations of moment and axial force in the cross sections were done assuming a linear elastic, homogeneous, rectangular cross section. Using the strains from the two strain gages and their locations in the cross section, a linear strain profile was assumed. The strain profile was then turned into a stress profile using the modulus of elasticity of the concrete. The average of the two stresses on the top and bottom of the cross section was used as the axial stress. The axial stress was then multiplied by the area of the cross section to determine the axial force. The difference between the average stress and one of the extreme fiber stresses was used as the bending stress. The bending stress was then multiplied by the moment of inertia and divided by half of the section thickness to determine the moment. This is based on the linear elastic behavior, stress = My/I.

4.5.4 Moments and Axial Forces

Moments in the five cross sections during the service load test, first ultimate load test, and second ultimate load test can be seen in Figure 4-23, Figure 4-24, and Figure 4-25 respectively. Moments were calculated using the full four foot width of the section. Note that the sign associated with the moment is relative to the position of the concrete and sister bar strain gages. Therefore a positive sign means that the moment is such that tension is in the sister bars and compression is in the concrete surface gages. Also note that for each of the service load test and first ultimate test graphs, the moment builds up to a peak at the peak load, and then follows an unloading curve back to a non-zero number. This represents the permanent strain that the section sustains due to loading. This fictitious moment is subtracted out for the subsequent test because while there is permanent deformation, all loading is removed, so the moment due to load is still simply the dead weight of the bridge. The second ultimate test graph does not contain this unloading curve, because the bridge was loaded up to its ultimate load, at which point failure occurred.

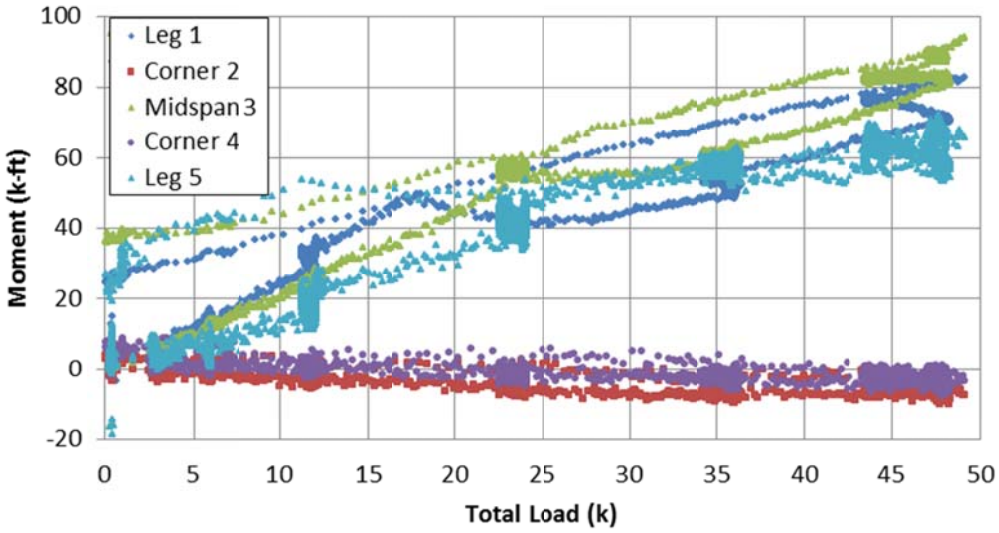

Figure 4-23 Moment - Service Load Test

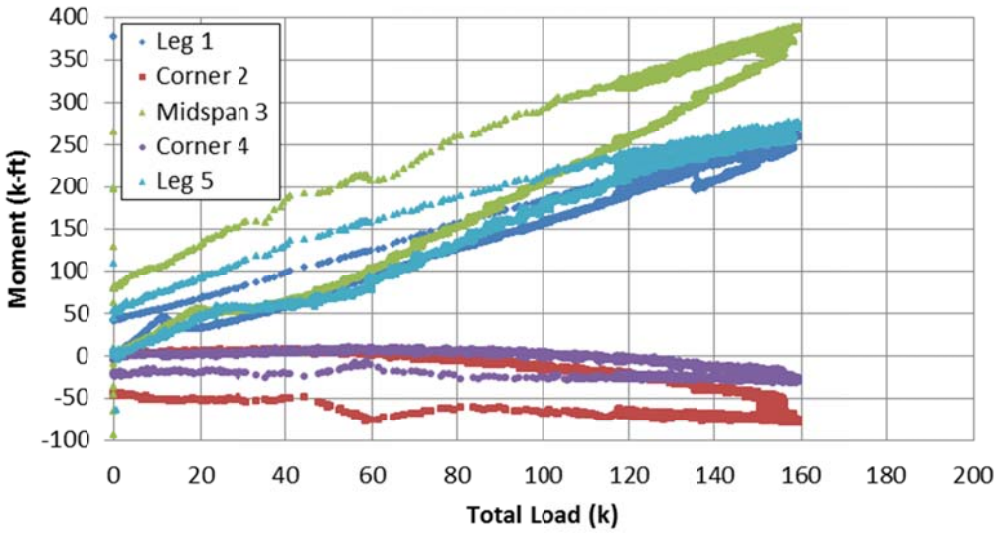

Figure 4-24 Moment - First Ultimate Load Test

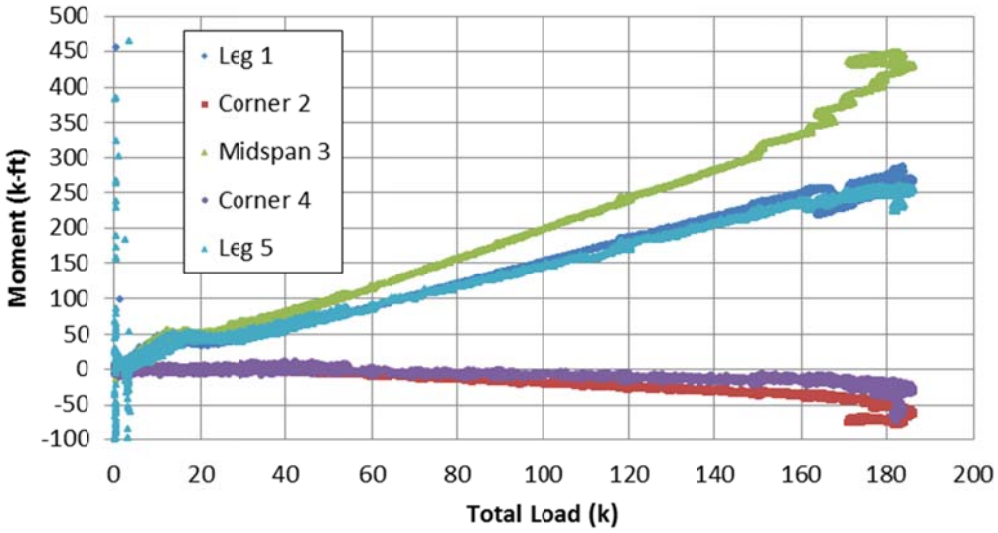

Figure 4-25 Moment - Second Ultimate Load Test

Calculated axial forces were determined to be far beyond theoretical values. It was found that the axial force calculation is extremely sensitive to even minor changes in measured strain. As such, the values that were calculated were deemed too inaccurate to report. These large forces, however, do not significantly affect the stress in the cross section, due to the large cross sectional area of the four foot wide bridge unit. For example, at 160 kips of total load, the strain analysis predicts an axial force of 380 kips in each of the leg cross sections, which is not feasible using statics. However, this represents a compressive force of only $0.06f'_cA_g$, and is therefore negligible.

4.5.5 Horizontal Reactions

Load cell reactions at the base of the bridge legs during the service load test, first ultimate load test, and second ultimate load test can be seen in Figure 4-26, Figure 4-27, and Figure 4-28 respectively. Note that for each of the service load test and first ultimate test graphs, the load cell reaction builds up to a peak at the peak load, and then follows an unloading curve back to a non-zero number. This represents the permanent deformation that the bridge sustains due to loading, causing an increase in the horizontal reactions. The second ultimate test graph does not contain this unloading curve, because the bridge was loaded up to its ultimate load, at which point failure occurred.

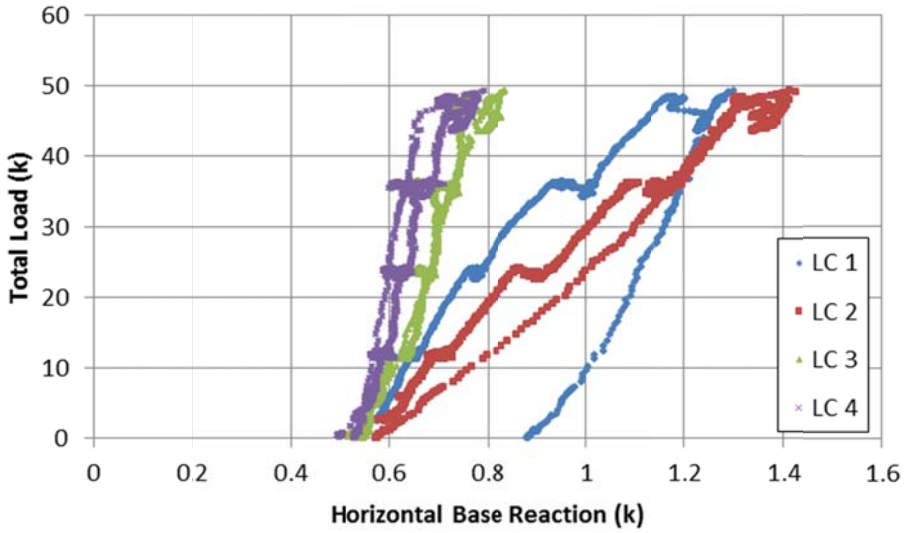

Figure 4-26 Load Cell Reaction - Service Load Test

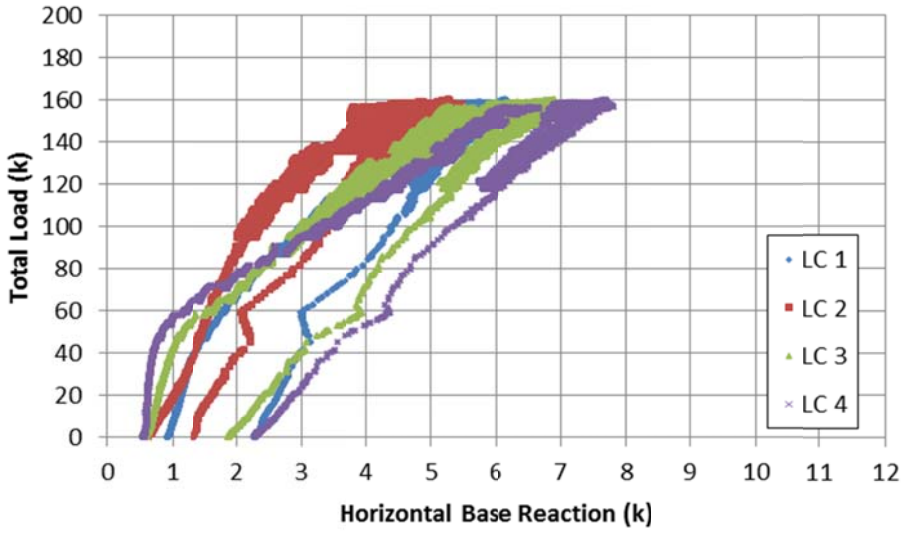

Figure 4-27 Load Cell Reaction - First Ultimate Load Test

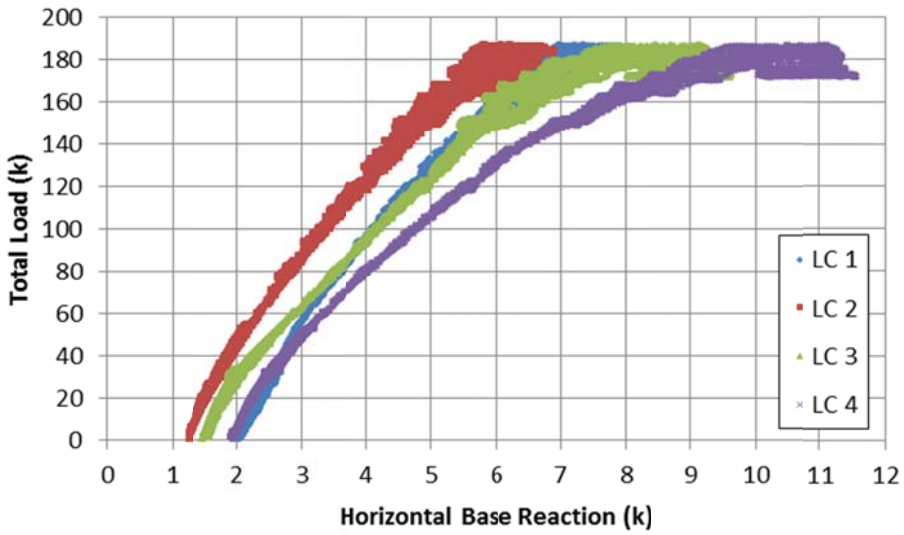

Figure 4-28 Load Cell Reaction - Second Ultimate Load Test

The forces in the load cells are small compared to the total load on the bridge. This is due to the horizontal friction force between the baseplate and the bridge. In addition to providing the vertical support of the legs, the bearing surface of the concrete bridge on the steel baseplate resists the bridge legs sliding outward through friction. Therefore, a smaller portion of the horizontal reaction goes into the load cells.

4.5.6 Displacement Wirepots

Individual wirepot displacements during the service load test, first ultimate load test, and second ultimate load test can be seen in Figure 4-29, Figure 4-30, and Figure 4-31 respectively. Note that for each of the service load test and first ultimate test graphs, the displacement builds up to a peak at the peak load, and then follows an unloading curve back to a non-zero number. This represents the permanent deformation that the bridge sustains due to loading. The second ultimate test graph does not contain this unloading curve, because the bridge was loaded up to its ultimate load, at which point failure occurred.

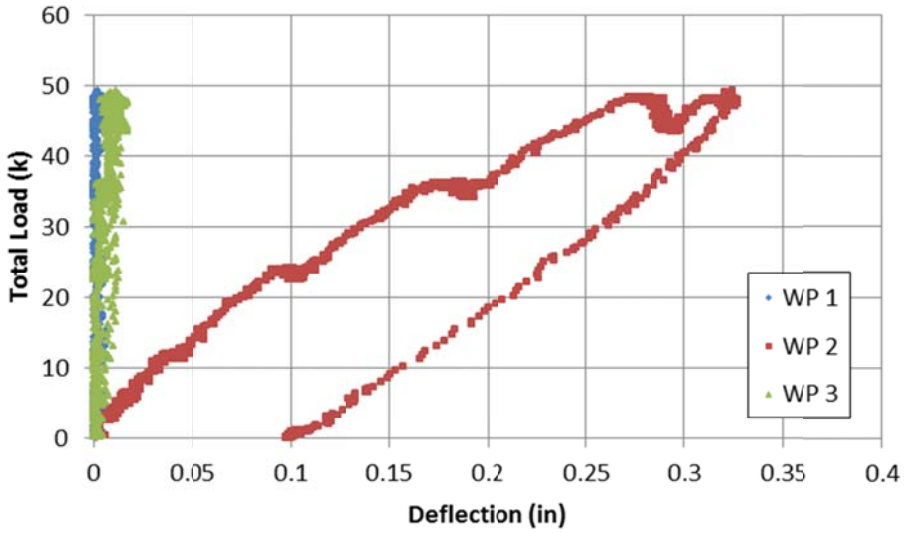

Figure 4-29 Deflection - Service Load Test

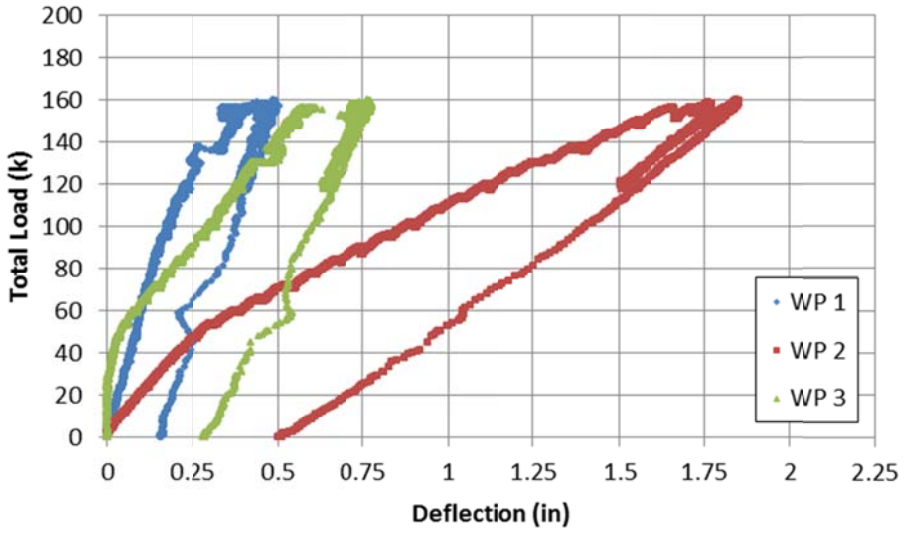

Figure 4-30 Deflection - First Ultimate Load Test

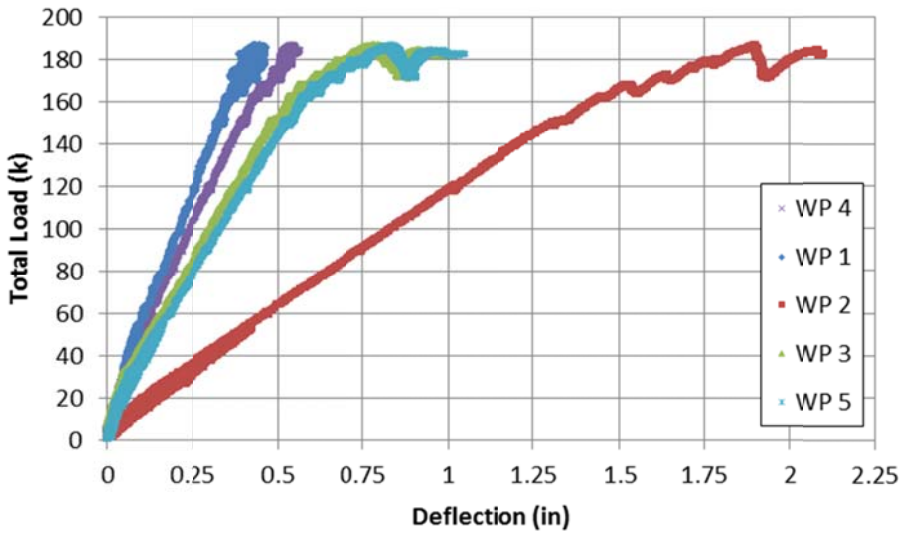

Figure 4-31 Deflection - Second Ultimate Load Test

Larger displacements at midheight of the legs, compared to displacements at the top of the legs, indicate that the legs were flexible compared to the axial stiffness of the arch. The long legs, which contain less reinforcement than the arch, bowed significantly. Care should be taken to design the leg dimensions and reinforcement to ensure that unit behavior is controlled by the behavior of the arch itself.

The shape of the deflection curves indicates stiff behavior. In all three tests, deflections increase at an approximately linear rate, and there is very little flattening of the curve prior to failure in the final test, indicating a lack of ductility. The small deflections, even at ultimate load, also show the bridge unit to be very stiff. A vertical deflection of 2.10 in is measured at failure. This ultimate load deflection translates to roughly L/120. In addition, the unrestrained lateral deflections of the bridge walls were relatively small, maximum being 1.04 in at wirepot five. Due to these small deflections, passive pressure in the backfill soil would not develop, but the soil would remain in an at rest pressure condition. Therefore, for the smaller, stiffer 20 ft span, backfill soil would not significantly aid the ultimate strength of the bridge.

4.5.7 Observed Bridge Behavior and Failure

Initial cracking was observed around 48 kips total load, with many thin cracks opening in the high moment areas. This initial cracks took place during the service load test, and were basically equal on either end of the bridge unit. An image showing these initial cracks in one of the legs, near one of the corners, and at midspan can be seen in Figure 4-32, Figure 4-33, and Figure 4-34, respectively. The crack location is emphasized with the use of a permanent marker, and the extent of the crack is noted with the load in each actuator at that time. However, these

flexural cracks did not significantly propagate or widen throughout testing, because the bridge redistributed the load to the uncracked concrete. Furthermore, the lack of crack widening indicates that the reinforcement did not yield . More hairline cracks appeared as testing progressed, but crack sizes did not become significant until near ultimate loading.

Figure 4-32 Initial Cracks in Leg

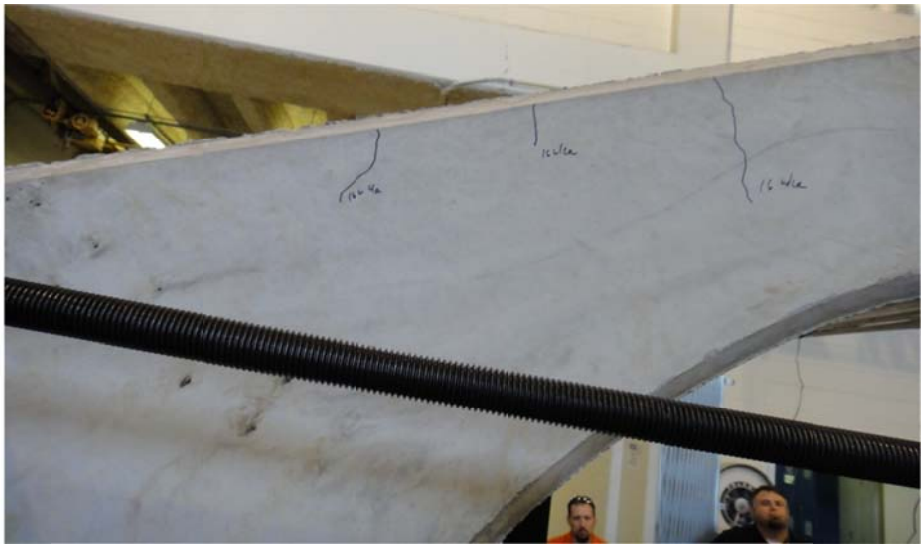

Figure 4-33 Initial Cracks near Corner

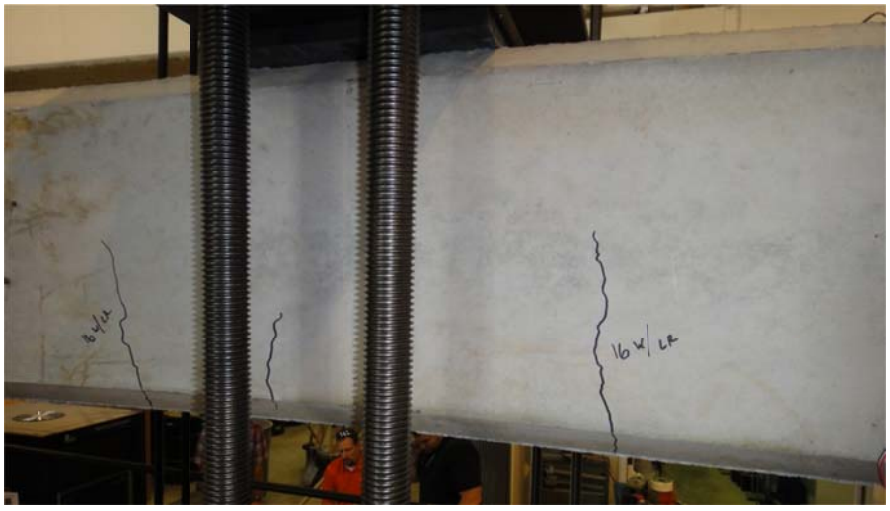

Figure 4-34 Initial Cracks at Midspan

The first significant crack occurred at a load of 120 kips total. This crack ran straight through the corner of the bridge at its thickest point. The crack continued through the corner, beginning to run down the leg with the reinforcement. An image of the crack forming at 120 kips of load can be seen in Figure 4-35, while an image of the crack propagating and widening at 156 kips can be seen in Figure 4-36. A crack similar to this one opened up in the opposite corner as well.

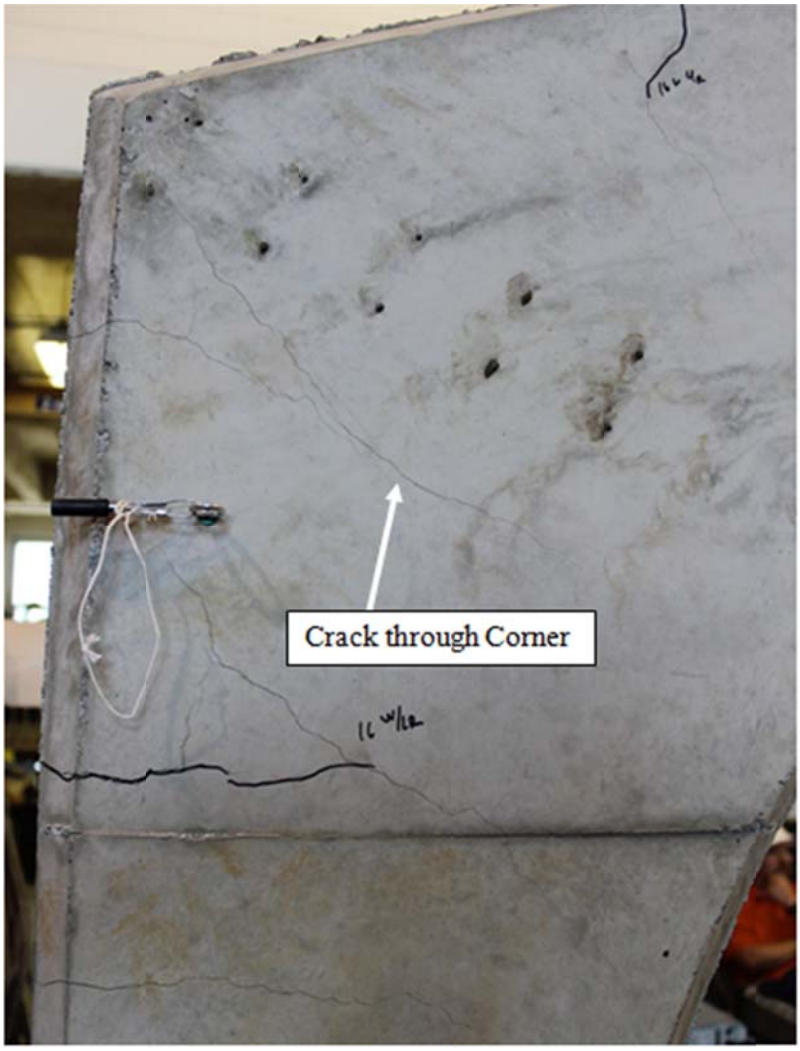

Figure 4-35 Corner Crack at 120 kip Total Load

Figure 4-36 Corner Crack at 156 kip Total Load

The critical shear crack that would be the failure mechanism did not appear until approximately 175 kips of total load. This crack was a shear crack running through the arch close to the corner of the bridge. Figure 4-37 shows the crack forming, Figure 4-38 shows the crack immediately prior to failure, and Figure 4-39 shows the failure mechanism.

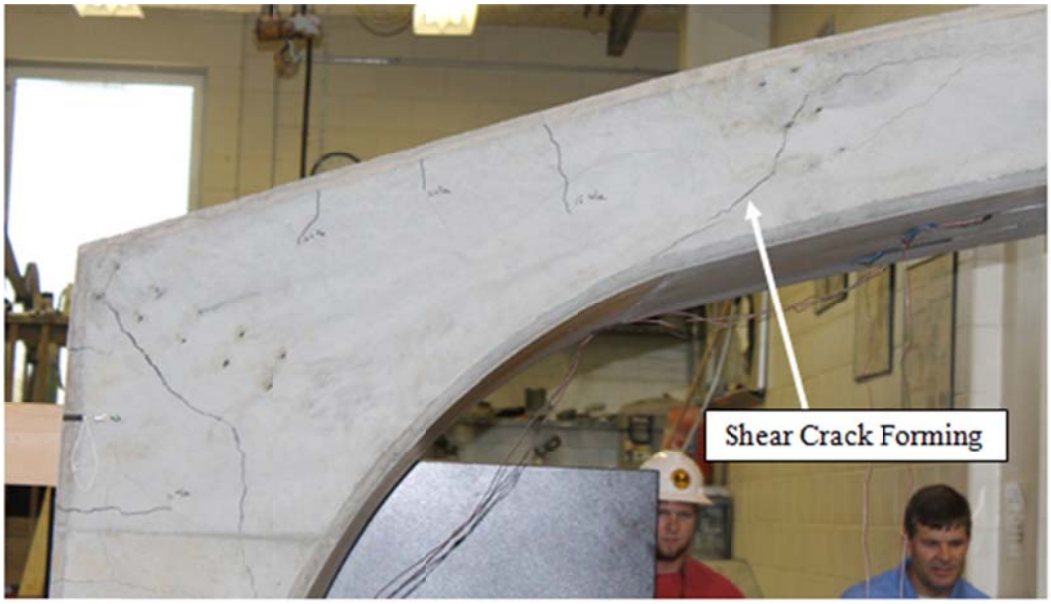

Figure 4-37 175 kip Total Load

Figure 4-38 Immediately Prior to Failure

Figure 4-39 Failure Mechanism

The 20 ft span failed under a total applied load of 182.1 kips. The failure mechanism was a shear crack near the corner on the arch itself. The shear crack opened up on the side of the bridge containing cross sections four and five, wirepots three and five, and load cells three and four. The load configuration can be seen below in Figure 4-40. A picture of the failed structure can be seen in Figure 4-41.

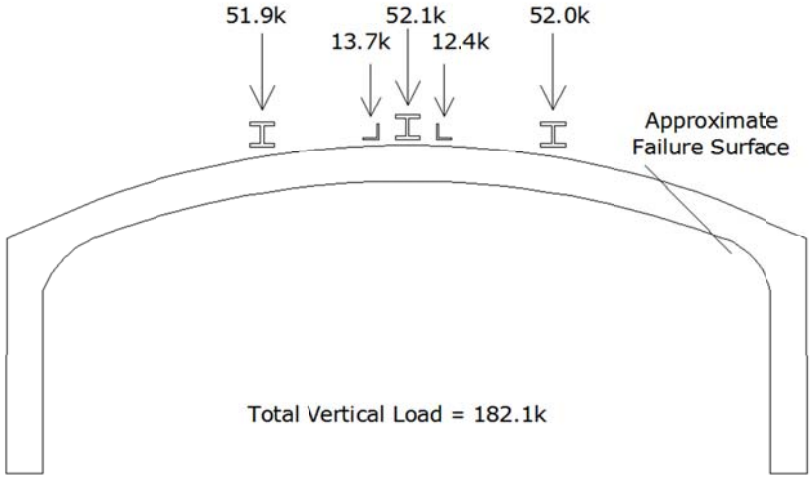

Figure 4-40 Failure Load Configuration

Figure 4-41 Failed Structure

The shear failure mechanism of the bridge was unexpected. A general flexural failure caused by hinges forming near the corners and at midspan was considered more likely. However, due to the stiffness of the concrete and large amounts of reinforcement steel, especially at midspan, steel did not significantly yield, causing a different failure mechanism.

The failure mechanism was not ductile and developed quickly. The bridge failed rapidly and could not carry its own dead weight after failure. While flexural cracks did develop in the walls, corners, and midspan of the bridge, none of them opened up very much after forming, due to the bridge redistributing the load to stiffer sections. Overall, the flexural stiffness of this shorter span bridge forced the bridge to be controlled by shear strength of the concrete. The relatively thin section, containing no shear reinforcement, was not large enough to resist the large shear forces developed during the test.

4.5.8 Lateral Resistance Frame – Reactions and Effects

Based on an approximate soil unit weight of 100 pcf with a lateral earth pressure coefficient of 0.3, ten feet of backfill soil would cause a pressure of 300 psf at the top of the leg, and 486 psf at the base of the leg, with a linear pressure distribution along the leg. By dividing this pressure distribution into three areas tributary to the base load cells, the middle HSS restraint, and the top HSS restraint, it was determined that each middle rod needed a tension force of approximately 1460 lbs, while each top rod needed a tension force of approximately 520 lbs. An illustration showing how this theoretical earth pressure distribution is converted into loads for the lateral resistance frame can be seen in Figure 4-42.

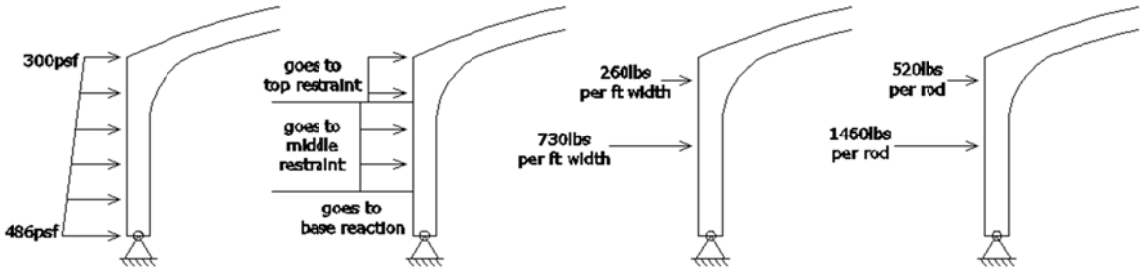

Figure 4-42 Lateral Resistance Frame Force Calculation

The lateral resistance frame consisted of measurements from four rods. The frame consisted of a restraint at the top of the walls, and a restraint at the middle of the walls, with each restraint having two rods, one on either side of the bridge. Therefore, the rods are named according to their location, top right, top left, middle right, and middle left. "Left" and "right" in this case simply relate which side of the bridge the rod was on, and do not have a specific orientation. The forces in the rods can be seen in Figure 4-43. It is noted that the rod forces are approximately equal at each vertical location, meaning that neither the left nor the right side has more force on it. As load is applied to the bridge unit, the walls deflect laterally, causing the force in the rods to increase. However, the force in the rods increases in accordance with the stiffness of the steel, so at each four kip per actuator interval, the force in the rods is reduced and brought back down to levels that would be applied by the design backfill soil.

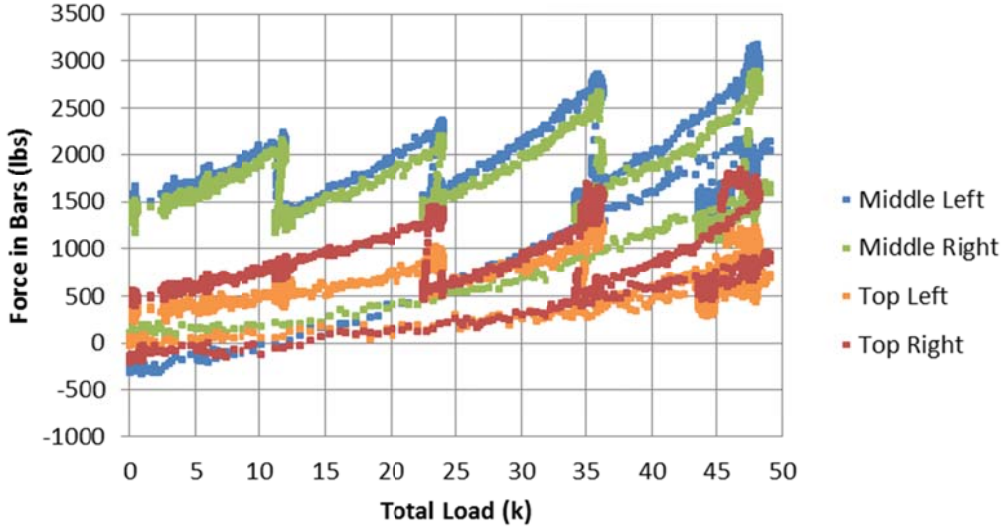

Figure 4-43 Force in Lateral Resistance Frame

The effect of the lateral resistance frame on the measured displacements is basically negligible. While the lateral resistance frame does reduce the lateral displacement of the corners, these displacements are already very small. The lateral resistance frame had virtually no effect on

the vertical displacement of midspan. A comparison of the measured displacements at wirepot one between the three tests showing the impact of the lateral resistance frame can be seen in Figure 4-44. A similar comparison graph for wirepot two, which measured midspan deflection, can be seen in Figure 4-45.

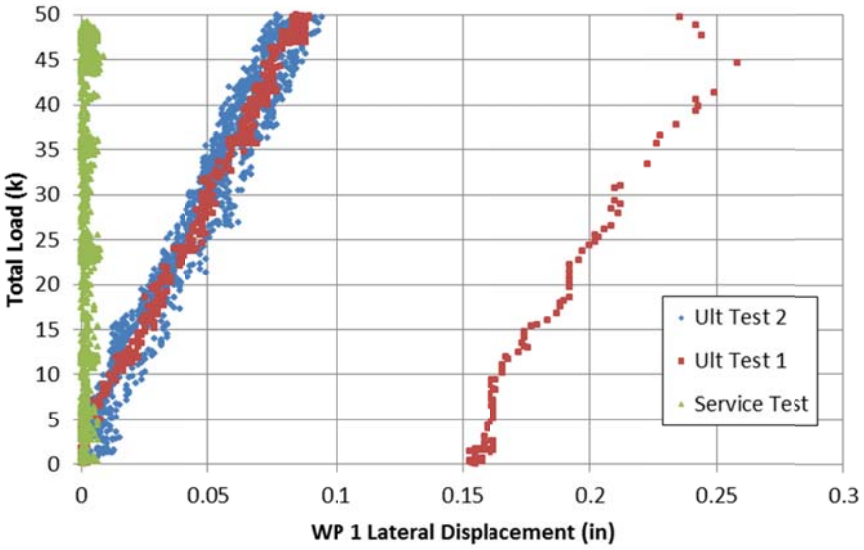

Figure 4-44 Lateral Displacement Comparison

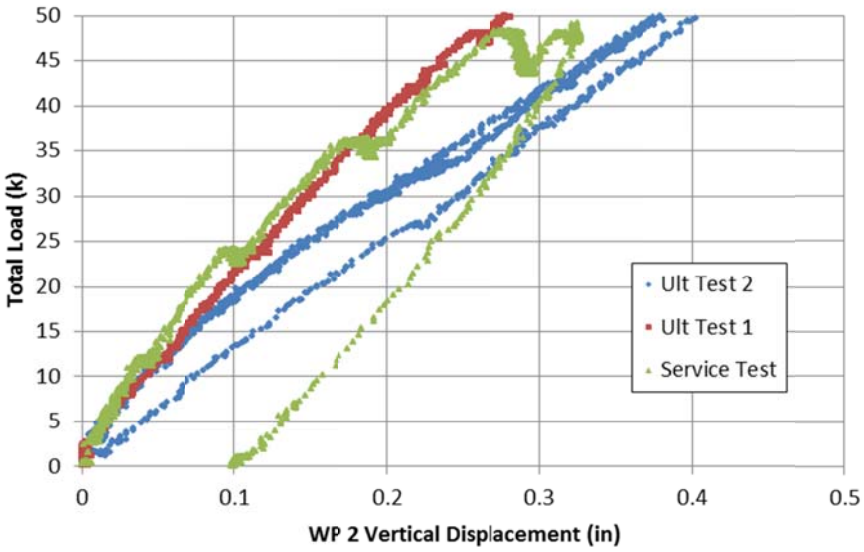

Figure 4-45 Vertical Displacement Comparison

Similarly, the lateral resistance frame had virtually no effects on the moments in the bridge unit. A comparison of moment at midspan between the three tests can be seen in Figure 4-46.

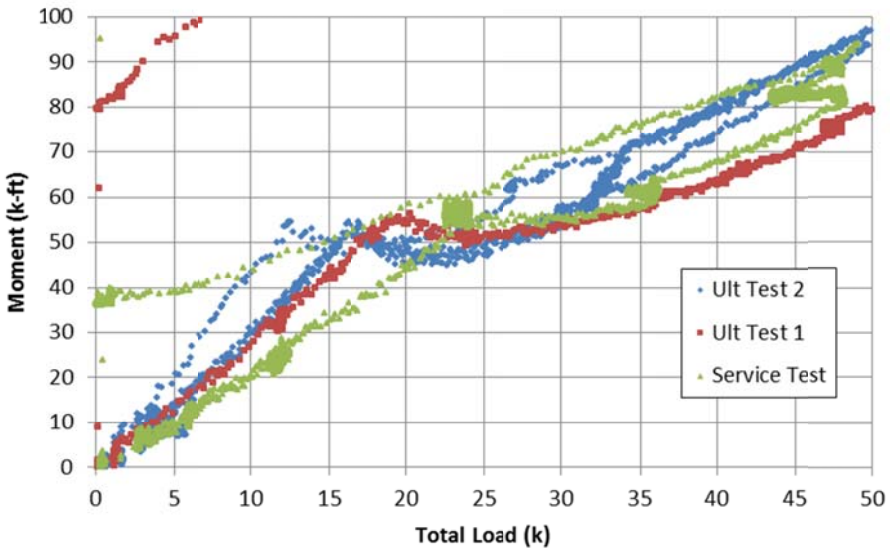

Figure 4-46 Service Load Midspan Moment Comparison

In summary, the lateral resistance frame did not affect any measured property other than lateral displacements at the top of the legs.

4.5.9 Effects of Multiple Ultimate Load Tests

One of the initial concerns with having to perform a second ultimate level test one week after the first ultimate test was the potential loss of stiffness and strength in the system. While there was some loss of stiffness in the bridge, it was not much. This loss of stiffness can be seen in the moment vs. load graphs of the two tests as a general decrease in the slope of the graph between the two tests. A comparison between the midspan moment vs. load graphs between the two tests can be seen in Figure 4-47. Furthermore, the section was still able to sustain a higher moment and a higher load, so a significant portion of the stiffness and strength of the bridge was not lost due to the need to unload and reload the bridge in a second test.

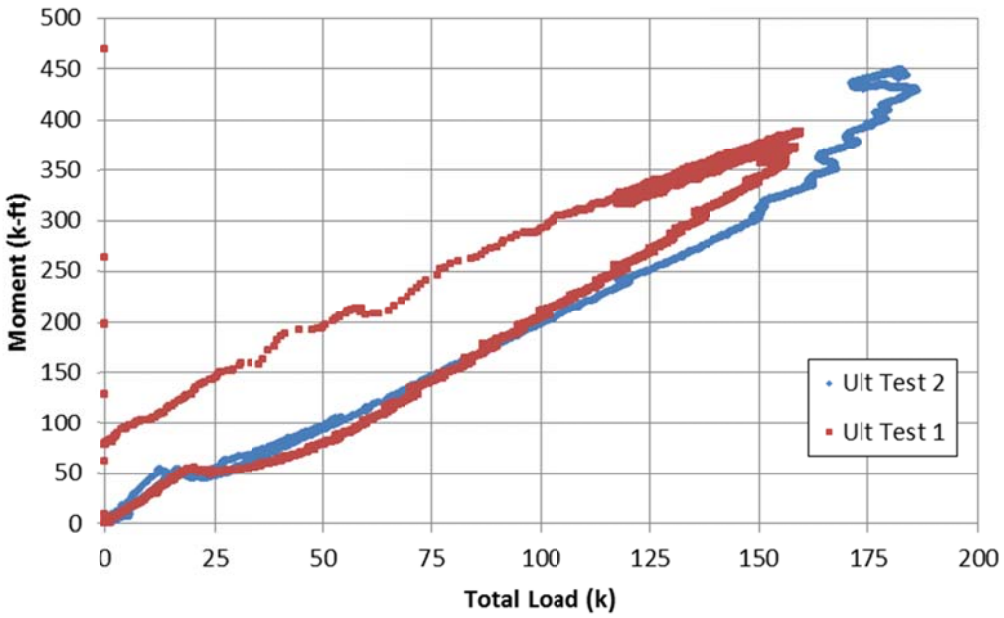

Figure 4-47 Ultimate Load Midspan Moment Comparison

4.6 Chapter Summary

The 20 ft bridge unit appeared to have plenty of strength, but did not fail with a ductile mechanism. While flexural cracking did occur in the high moment areas at early loading stages, these cracks did not significantly widen or propagate during testing, due to the bridge unit redistributing load around the cracks and the reinforcement not yielding. The bridge unit held 182.1 kips of force before failure. Immediately prior to failure, maximum deflections were 2.1 in downward at midspan, and 1.04 in laterally in the walls. The failure mechanism was a shear failure of the concrete, with a shear crack running through the thickness of the unit near the corner.

The lateral resistance frame did not significantly affect moments or displacements.

Chapter 5 Laboratory Test – 36 ft Span

5.1 Introduction

A 36 ft span bridge unit was used for a laboratory test of the Foley Arch precast arch culvert bridge system. The single unit of a multi-unit bridge was designed for five feet of backfill plus live load. The unit has a 36 ft clear span, an inside clear height of nine feet at midspan, and is four feet wide. An image of unit overall dimensions taken from the design drawings can be seen in Figure 5-1. An image of the reinforcement layout in half of the unit can be seen in Figure 5-2, with the exact reinforcement used detailed in Table 5-1. The reinforcement layout in the two halves of the unit was mirrored. Note that transverse steel runs parallel to the roadway, meaning that it is the primary flexural resistance steel.

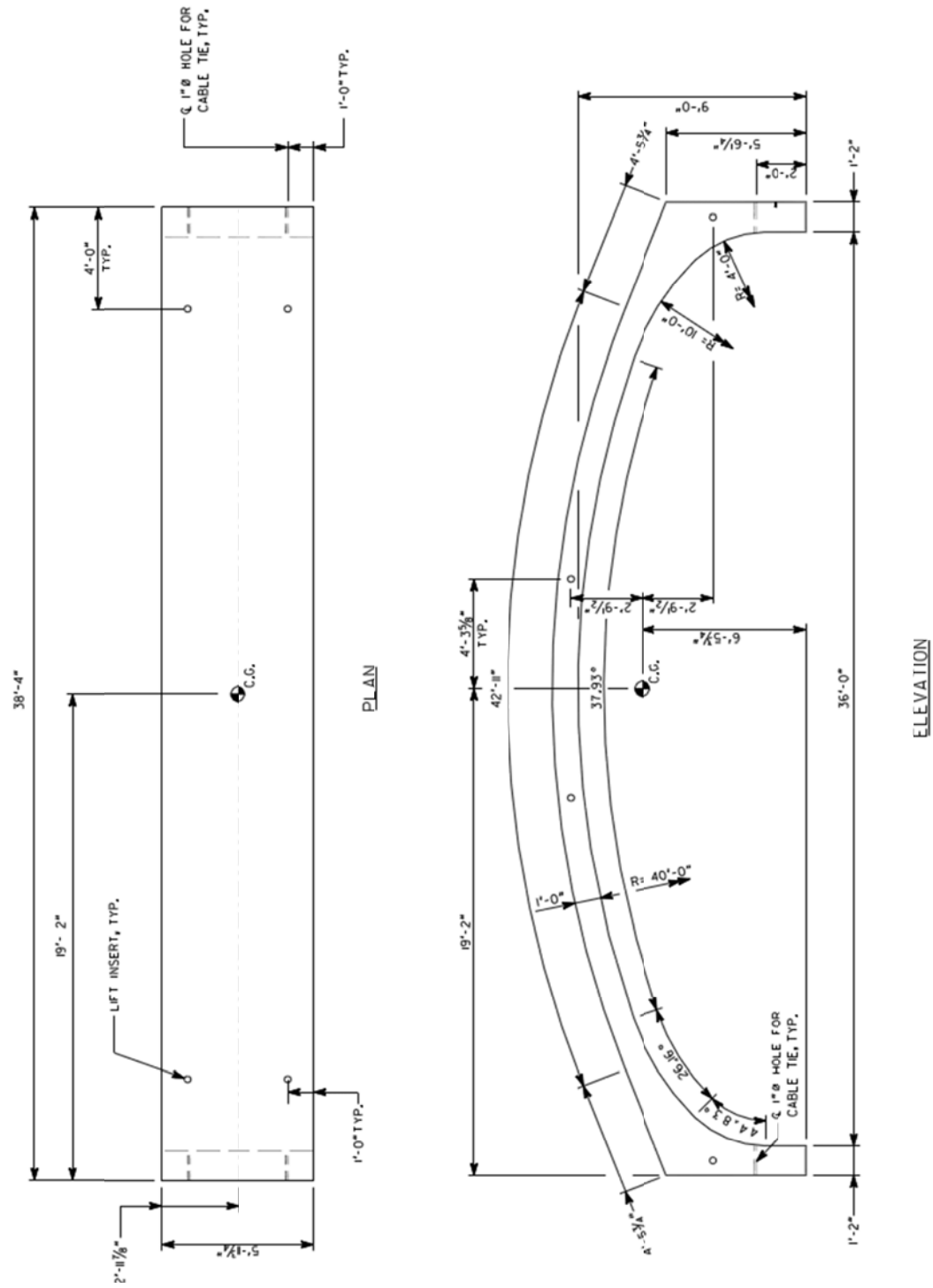

Figure 5-1 36 ft Bridge Unit Overall Dimensions (FoleyArch 2011)

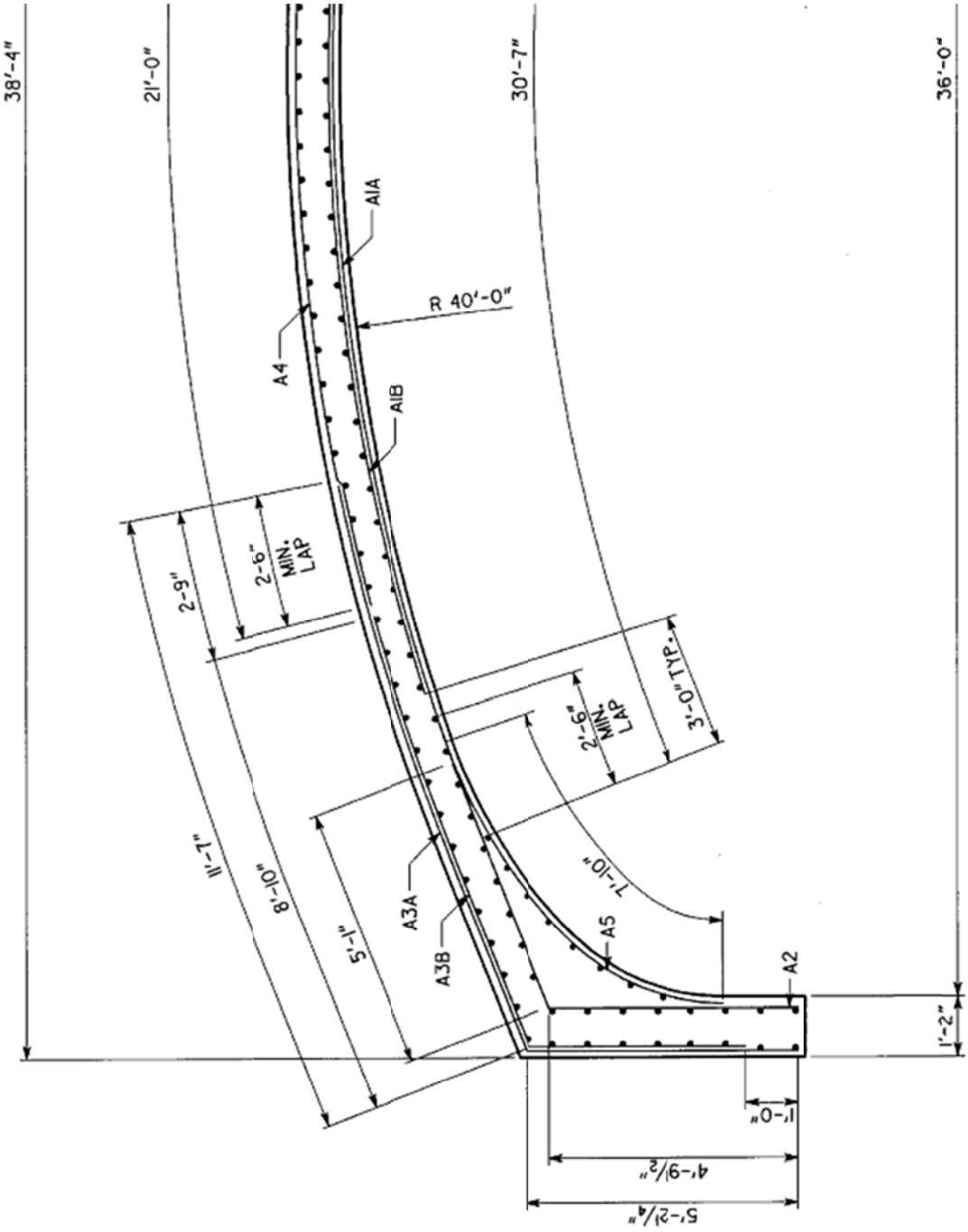

Figure 5-2 36 ft Bridge Unit Reinforcement Layout (FoleyArch 2011)

Table 5-1 36 ft Bridge Unit Reinforcement Details (FoleyArch 2011)

Designation:	Mesh Size	Length (ft)	Transverse Area Supplied (in2/ft)	Longitudinal Area Supplied (in2/ft)
A1A	D10xD10 2x3.8	24'-0"	0.6	0.315
A1B	D13.2xD5.5 2x16	30'-0"	0.792	0.041
A2	D5.5xD10 2x8	9'-9"	0.33	0.15
A3A	D10xD10 2x8	16'-1"	0.6	0.15
A3B	D10xD5.5 2x16	13'-1"	0.6	0.041
A4	D5.5xD10 2x3.8	26'-0"	0.33	0.315
A5	D5.5xD10 2x8	7'-10"	0.33	0.15
Design based on uncoated reinforcing meeting ASTM A-615, Grade 60, fy = 60,000psi				
Minimum Yield Strength for welded wire fabric shall be 65,000 psi				

The bridge unit was cast on December 1, 2011 at the Foley plant in Winder, GA, and shipped to Auburn University on December 14, 2011. The unit was shipped on its side and brought to Scott Bridge Company of Opelika, AL, where it was taken off the truck with a crane, rotated so that it was standing upright, and then placed back on the truck with the forward most leg on rollers. The unit was then brought to the Structures Research Laboratory at Auburn University, where, with the use of the laboratory crane and a forklift, the rear end of the bridge was lifted and the bridge was rolled into the lab. The weight of the unit was more than the laboratory crane's capacity, so positioning the bridge was done by placing one end on rollers, lifting up the other end, and using the forklift to push or pull the bridge into place. This process caused some minor cracking in the unit, as well as some slight misalignment of the legs, which will be discussed more in section 5.5.8.

A single load test was performed on the bridge on January 6, 2012. At ultimate load conditions, the unit held more than 151 kips before failing.

This chapter details how the 36 ft unit was tested, as well as the results of that testing. It contains sections on the instrumentation, setup, and procedure used for testing. It also contains analysis and results from testing, followed by discussion of those results

5.2 Instrumentation

This section contains a detailed description of the instrumentation used on the 36 ft span bridge unit. It also contains details about the different types of instruments used, including how each was installed.

5.2.1 Instrumentation Layout

The 36 ft clear span bridge unit was instrumented with 15 sister bar strain gages, ten concrete surface strain gages, three displacement potentiometers, or wirepots, and four load cells.

Strain gages were placed at seven cross section locations on the bridge: at midspan, at the corners where the arch section began to increase in thickness, within the thicker corner sections, and on the legs where the section began to increase in thickness. The layout of the instrumented cross sections can be seen in Figure 5-3. Two sister bar gages were placed at each location and tied to the reinforcing cage. Three sister bar gages were used at midspan. These sister bar gages were tied on the side of the cross section that would be the expected tension side, meaning the inner side of the bridge at midspan, and the outer side of the bridge at the corners and legs. Two concrete surface strain gages were placed at each cross section, at third points along the width, on the concrete surface expected to be in compression, meaning the outer side at midspan, and the inner side at the corners and legs

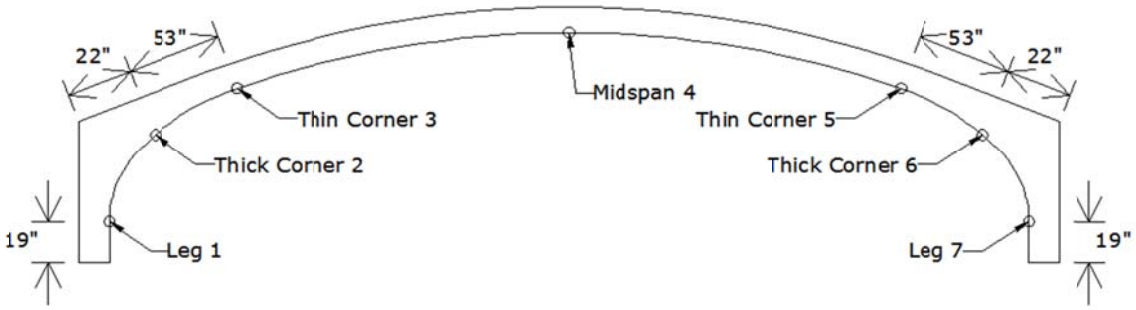

Figure 5-3 36 ft Cross Section Locations

The three wirepots were placed in positions to measure the maximum deflections that the bridge experienced. Therefore, one was placed vertically at midspan to measure vertical deflection, and the other two were placed horizontally at the top of the walls to measure lateral deflection.

In addition, four load cells were used to measure the horizontal reaction at the base of the bridge. Two load cells were placed on the exterior side of each leg, bearing against the leg to provide lateral restraint. This was done to effectively create a pinned support condition, like that experienced in the field. An image of the wirepot and load cell layout can be seen in Figure 5-4.

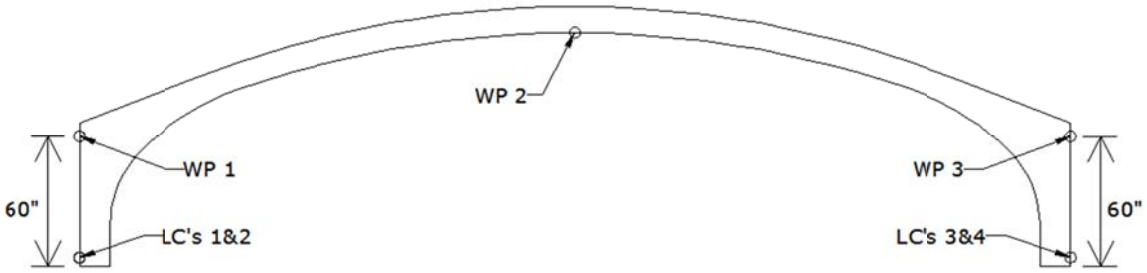

Figure 5-4 36 ft Wirepot and Load Cell Layout

5.2.2 Sister Bar Strain Gages

The sister bar strain gages were created using the same method and materials described in Chapter 4. For details, see section 4.2.2.

Prior to placement, each sister bar strain gage was checked with a P3 Strain Indicator and Recorder to make sure the gages were working. It was found that only one gage was faulty at this point.

5.2.3 Concrete Surface Strain Gages

The concrete surface strain gages were created using the same method and materials described in Chapter 4. For details, see section 4.2.3.

Concrete gages were also checked with the P3 Strain Indicator, and all gages were found to be working satisfactorily.

5.2.4 Displacement Wirepots

WDS P-60 series draw wire sensors from Micro-Epsilon were used to measure deflections of the bridge unit. From henceforth, these sensors will be referred to as wirepots. The wirepots were attached to the bridge by drilling a small hole into the concrete, tapping in a light duty plug anchor, screwing in a small eyebolt and attaching the end of the wirepot string to the eyebolt. For wirepots measuring lateral deflection, holes were drilled into the side of the bridge unit. For the wirepot measuring vertical deflection at midspan, the hole was drilled in the bottom of the bridge arch. The lateral wirepot units were mounted to the lateral resistance frame to serve as a fixed point, even though the frame itself was not used during testing. The vertical wirepot was mounted to a frame built to house the wirepot and gage wire hookups around the center actuator.

5.2.5 Load Cells

Four LPSW-B model load cells from Load Cell Central were used to measure the horizontal reaction at the base of the bridge unit. Each load cell has a 50,000lb capacity. The four load cells were simply placed in between the bridge and the HSS section that served as our base horizontal reaction, with a 6in x 6in x 0.25in plate bearing between the load cell contact point and the concrete surface to prevent damage due to the concentrated force of the load cell.

5.3 Testing Setup and Equipment

This section contains some details on testing setup outside of instrumentation. It includes details on the loading frame used for testing, the actuators used to apply the load, and the data acquisition system.

5.3.1 Load Framing System

The load frame used for testing the 36 ft bridge unit is the same frame used during the 20 ft bridge unit test. Details on the load frame can be found in 4.3.2. Once again, the three actuators were spaced at four feet, with the middle actuator corresponding to midspan.

5.3.2 Actuators

The actuators used are model number 243.35 Single Ended Actuators from MTS. They have an 82 kip capacity in compression and a 54 kip capacity in tension with a 10 in total stroke. The load framing system was such that the actuators were in tension, giving them a capacity of 54 kips per actuator. MTS Model 407 controllers were used to control each actuator independently using displacement control.

5.3.3 Data Acquisition

A Pacific Instruments 6000 Data Acquisition System was used for collecting data. A sample rate of one sample per second was used for all testing. Data was monitored throughout testing and saved and recorded after the test was finished.

5.4 Testing Procedure

This section consists of the procedure used during testing. For this bridge unit, a single ultimate load level test was performed.

5.4.1 Concrete Cylinder Tests

Eight concrete cylinders were created when the bridge unit was cast. The cylinders were eight inches long with a four inch diameter. These cylinders were kept under the same conditions as the bridge unit until testing. Strength tests were performed on two of the cylinders at Auburn Universtiy on January 6, 2012. Strength and modulus tests were performed on the remaining cylinders on January 9, 2012. Compressive strength tests conformed to ASTM C39 (ASTM International 2005), and modulus of elasticity tests conformed to ASTM C469 (ASTM International 2002). For more details on how cylinder tests were performed, see section 4.4.2 in Chapter 4.

5.4.2 Steel Reinforcement Tensile Testing

In order to better understand the stress-strain behavior of the reinforcement used for this bridge unit, seven bars taken from steel reinforcement samples were tested in a tension testing machine. Four of the bars were cut from extra mats prior to casting. These bars are the same size, D10 bars, as the bars used as primary negative moment reinforcement in the legs and the corners. The remaining three bars were cut directly from the bridge unit during demolition after

testing was completed. These larger D13.2 bars were cut from the primary positive moment reinforcement used at midspan. The D13.2 samples used for testing were removed from the bridge unit at approximately quarterspan, in order to obtain samples that had not been significantly strained during testing.

Tension testing was done using a Tinius-Olsen Universal Testing Machine at Auburn University, which both applied and measured the tensile force put into the specimen. This is the same machine used for calibration of the gaged threaded rods, as discussed in chapter four. Deformations in the steel samples were measured using a model 3542 axial extensometer from Epsilon Technology Corp, shown in Figure 5-5, which had an initial gage length of one inch. Each bar was run through at least one test in the linear elastic range, followed by a test running through failure. To prevent damage to the extensometer, it was removed as the sample bar neared failure. Tensile forces were converted to stresses using the nominal area of the bar, and deformations were converted to strains using the known initial gage length.

Figure 5-5 Extensometer

5.4.3 Ultimate Load Test

On January 6, 2012, an ultimate level load test was performed on the 36 ft bridge section. Each actuator was independently controlled, and the operators attempted to increase load at the same rate, applying a uniform load distribution in the actuators. An initial preliminary load test was performed as part of the ultimate load test. For this preliminary load portion, the load was applied in four kip per actuator increments, up to 16 kips per actuator. After this, the load was removed and the test reset for the ultimate load level portion.

The lateral resistance frame used for the 20 ft bridge unit service load test was not used at all on the 36 ft unit. Due to the negligible effects it had on the 20 ft unit, as well as the shortened leg height of the 36 ft unit, which would not deflect as much as longer leg heights, it was determined that the lateral resistance frame would not have an impact on the 36 ft unit's behavior.

In anticipation of failure, the crane in the laboratory was centered over the bridge, with straps placed loosely underneath the bridge to "catch" the bridge. The ten ton capacity laboratory crane was manually controlled, and had enough capacity to keep the arch from falling on the testing equipment should a complete collapse of the structure occur.

For the ultimate load test, load was applied slowly and evenly in the same manner as the preliminary load test. Near the end of the actuators' capacity, the bridge failed when a hinge formed near the corner within the arch, in between the two gage locations in that corner.

5.5 Analysis, Results, and Discussion of Testing

This section contains the measured data as well as calculated results from the 36 ft bridge test. For analysis purposes, the bridge is divided into seven instrumented cross sections based on the strain gage layout. Two cross sections are on the legs, two are near the corners where it is thicker, two are near the corners where the thinner arch begins, and one is at midspan. The cross sections are the same as those in Figure 5-3.

5.5.1 Concrete Material Properties

Cylinder tests revealed the concrete to have a compressive strength, f'c, of 7,040 psi. Modulus of elasticity tests show the concrete to have a modulus, Ec, of 4,100 ksi. This compressive strength value is fairly typical of precast, three-sided arch units, which have a typical 28 day compressive strength of 6,000 psi to 7,000 psi.

5.5.2 Steel Reinforcement Testing

It was found that reinforcement had both sufficient strength as well as ductility. A graph showing the full stress-strain curves for each of the seven steel samples can be seen in Figure 5-6. Data showed that the modulus of elasticity was approximately 26,500 ksi, however, which is unusual for steel. Data showed that the steel stress-strain curve increases linearly before beginning to flatten out at a yield plateau. Specimens did not exhibit strain hardening, increasing strength after yielding, but instead continued to deform with very little strength increase prior to break. In addition to the smaller modulus of elasticity, one other anomaly was noted. It was found that yielding of the smaller D10 bars was around 70 ksi, while the larger D13.2 bars did not yield until roughly 90 ksi, which is very high for this steel. However, due to the range of strains measured during testing, this anomaly did not prove to be significant.

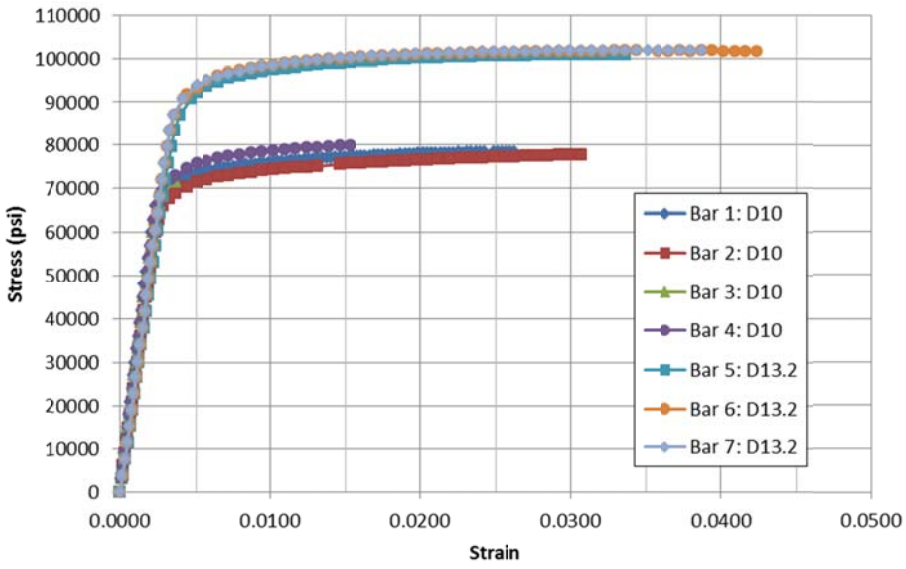

Figure 5-6 Steel Reinforcement Testing Results

5.5.3 Strains

Strains at the same location were close to each other, which indicated two very important things. First, load testing did not cause any torque in the bridge. Second, the strain gages were measuring strains properly. Other than the one sister bar strain gage that was faulty after casting of the bridge, no other strain gages became faulty during the course of the test.

The highest strains were measured in cross sections three, four, and five, as expected. Steel strains in all three of these cross sections were high enough to cause yielding, with the maximum strains being around 0.0035, which occurred in cross section five right before failure. Steel strains in cross sections one, two, six, and seven did not reach yielding.

5.5.4 Moment and Axial Force Calculations from Strain

Moments and axial forces are calculated in the same way as in Chapter 4. The only notable differences are that the concrete rupture stress, f_r, is 630 psi, and all cross sections were analyzed using the cracked section analysis described in Chapter 4, as opposed to the gross concrete section analysis described in Chapter 3. For more details on how moments and axial forces are calculated, see section 4.5.3.

Another notable difference is the use of a different stress-strain relationship for steel. Based on tensile tests of samples similar to the steel used in the bridge unit, as well as the range of measured strains during the test, the steel stress-strain relationship was modeled as a two part function. Steel stress, σ, versus steel strain, ε, is calculated using the following two part equation:

$$\sigma = 26{,}500ksi * \varepsilon \ \leq (5{,}000ksi * \varepsilon) + 53.5ksi \qquad (5\text{-}1)$$

A graph containing these two equations as well as the results from the aforementioned tensile tests can be seen in Figure 5-7.

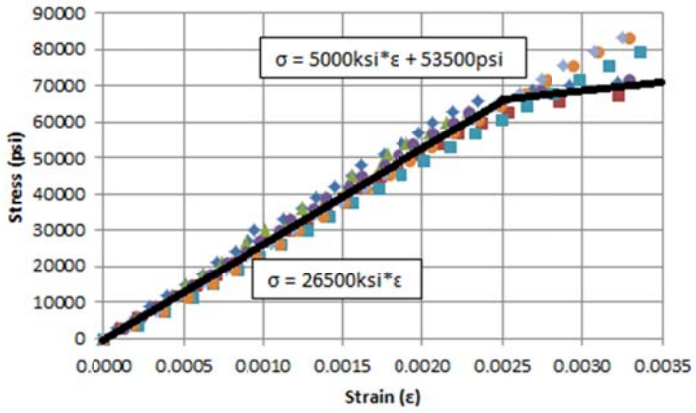

Figure 5-7 Steel Stress vs. Strain

5.5.5 Moments and Axial Forces

Moments in the seven cross sections during the ultimate load test can be seen in Figure 5-8. Moments in cross sections two and six are the highest due to the thicker, stiffer cross section within the corner of the bridge. Note that the sign associated with the moment is relative to the position of the concrete and sister bar strain gages. Therefore a positive sign means that the moment is such that tension is in the sister bars and compression is in the concrete surface gages. Also note that, due to the preliminary loading portion of the test, there are loading, unloading, and reloading portions of the graph. The unloading curve for each cross section does not return to zero, indicating that there is permanent strain deformation, which is expected. After load is removed, the fictitious moment caused by the permanent strain is subtracted out before beginning the reloading portion of the graph.

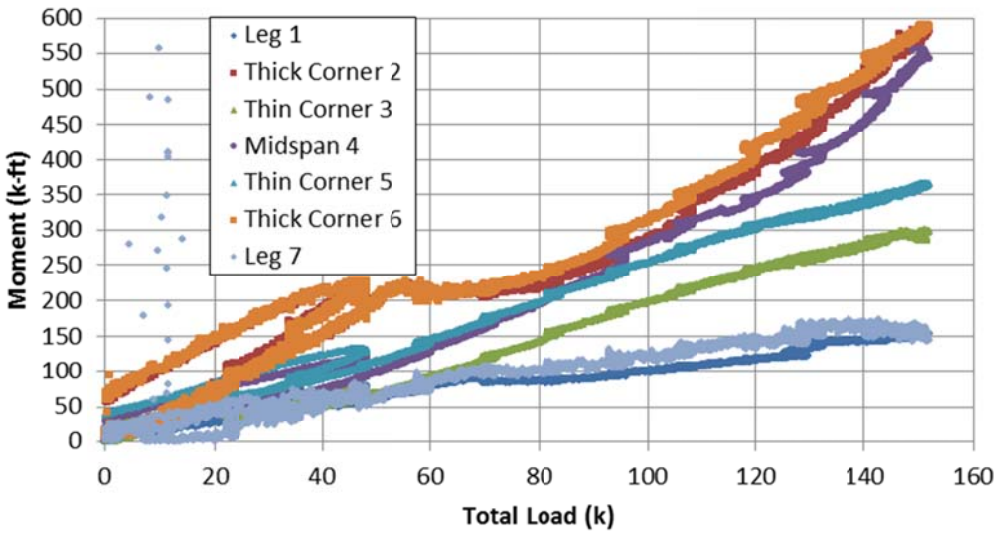

Figure 5-8 Moment vs. Load

As with the 20 ft span in Chapter 4, calculated axial forces were determined to be far beyond theoretical values. It was found that the axial force calculation is extremely sensitive to even minor changes in measured strain. As such, the values that were calculated were deemed too inaccurate to report. These large forces, however, do not significantly affect the flexural strength of the cross section, due to the large cross sectional area of the four foot wide bridge unit.

5.5.6 Horizontal Reactions

Load cell reactions at the base of the bridge legs during the ultimate load test can be seen in Figure 5-9. Note that, due to the preliminary loading portion of the test, there are loading, unloading, and reloading portions of the graph. The unloading curve for each load cell does not return to zero, indicating that there is permanent deformation, which is expected. However, upon reloading, each load cell quickly returns to the initial loading curve, and continues along the same path as initial loading.

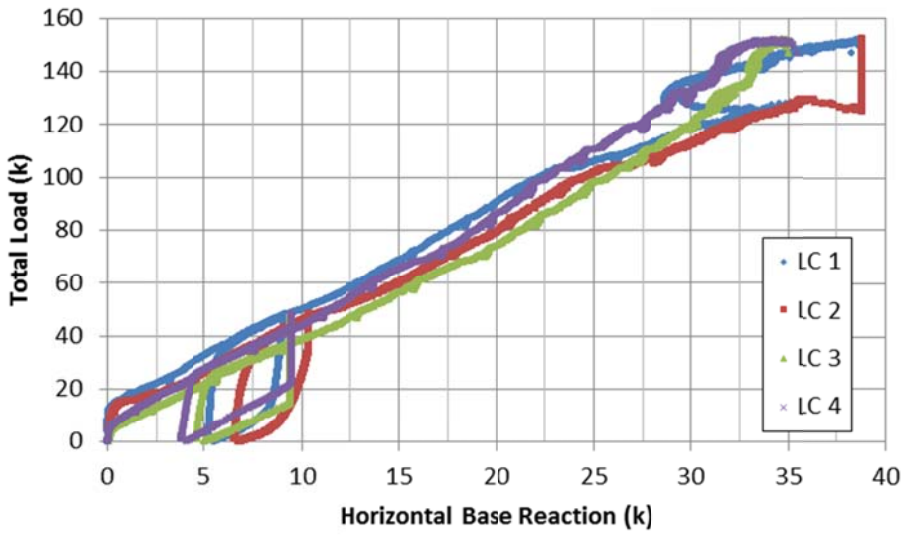

Figure 5-9 Load Cell Reaction vs. Load

The forces in the load cells are much higher in the 36 ft span bridge unit compared to the 20 ft span bridge unit. This is due to the slightly angled legs and their smaller bearing surface on the baseplate, creating less horizontal friction force between the baseplate and the bridge. Therefore, a higher portion of the horizontal reaction goes into the load cells. Another possible reason for the increase in load cell forces is the relative stiffness of the 36 ft arch compared to the 20 ft arch. The 36 ft arch allowed for much greater rotation of the corners, which would increase the amount of lateral force at the base of the bridge unit.

5.5.7 Displacement Wirepots

Individual wirepot displacements during the ultimate load test can be seen in Figure 5-10. Note that, due to the preliminary loading portion of the test, there are loading, unloading, and reloading portions of the graph. The unloading curve for each wirepot does not return to zero, indicating that there is permanent deformation, which is expected. However, upon reloading, each wirepot quickly returns to the initial loading curve, and continues along the same path as initial loading.

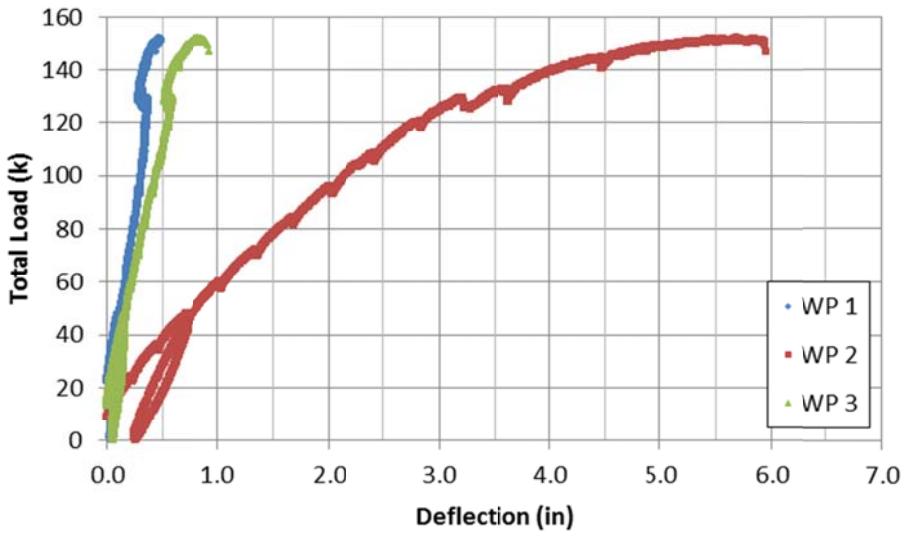

Figure 5-10 Deflection vs. Load

With 5.96 in of vertical deflection at failure, the bridge was fairly flexible. This ultimate load deflection translates to roughly L/70. However, due to the relatively short legs, the unrestrained lateral deflections of the bridge walls were relatively small, maximum being 0.93 in at WP 3. Due to these small deflections, passive forces in the backfill soil would not develop. Therefore, for the 36 ft span, backfill soil would not significantly aid the ultimate strength of the bridge with its current leg height.

5.5.8 Observed Bridge Behavior and Failure

Due to issues shipping and handling the much larger and less stiff 36 ft span bridge unit, some cracking and spalling of the bridge occurred before testing was begun. During the process of getting the bridge into the lab and onto the baseplates, initial flexural cracks formed at midspan and near the corners, but were still small prior to testing. More significantly, the bridge legs were placed on the baseplates such that they were not completely vertical, but slightly angled outward. An exaggerated illustration of the angled bearing surface can be seen in Figure 5-11. This misalignment caused some spalling on the inside of the leg prior to testing, as can be seen in Figure 5-12. This misalignment also caused further spalling to occur during the test as more weight was placed on the bridge. An image of further spalling during testing on the opposite bridge legs can be seen in Figure 5-13. The spalling and initial cracking did not affect the ultimate strength of the bridge, however.

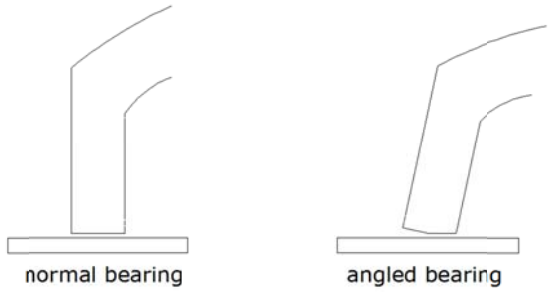

Figure 5-11 Exaggerated Angled Bearing Surface

Figure 5-12 Initial Spalling on Bridge Leg

Figure 5-13 Spalling at 96 kips Total Load

The first significant cracks occurred at midspan, followed by cracks developing near the corners. Several cracks formed near midspan, approximately spaced evenly at six inches. These cracks propagated up through the thickness of the bridge well past midheight before failure. An image illustrating the even spacing of the cracks near midspan can be seen in Figure 5-14. An image showing the midspan cracking pattern after failure can be seen in Figure 5-15. The cracks near the corners were also approximately evenly spaced at six inches. These cracks widened and extended until failure, indicating that some yielding of the steel reinforcement took place. An image of the largest corner cracks at 144 kips of total load can be seen in Figure 5-16.

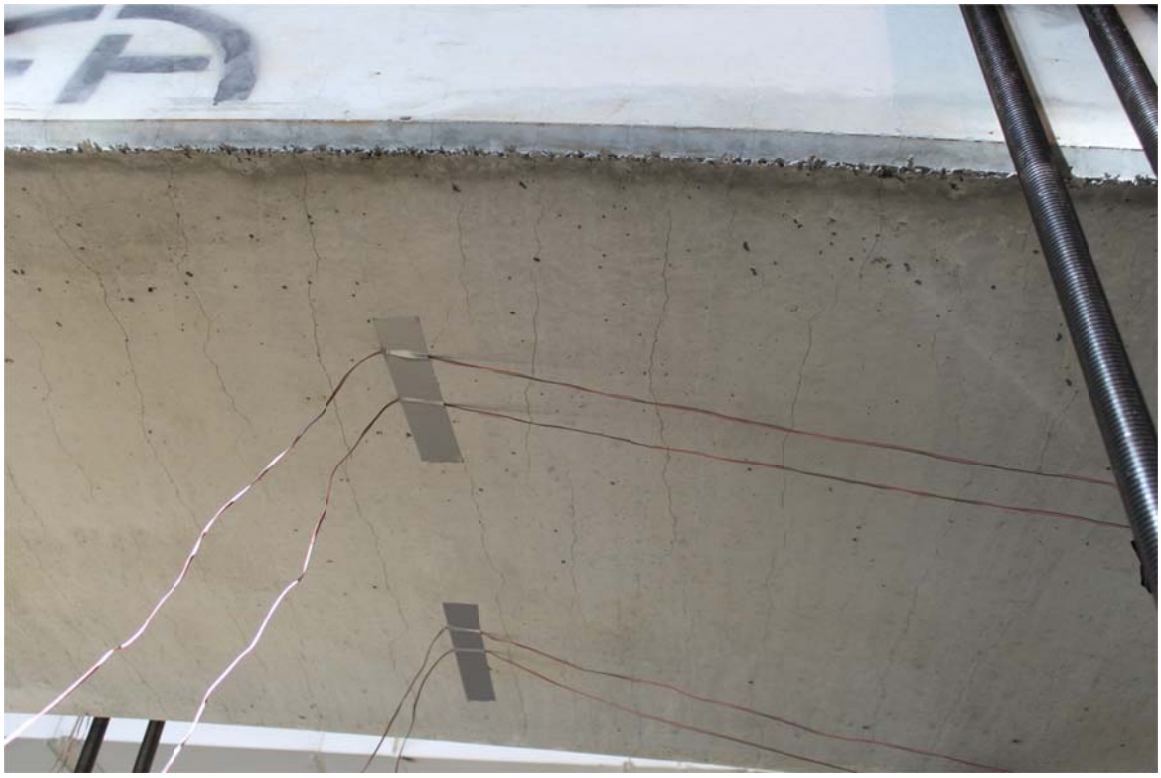

Figure 5-14 Midspan Cracking – 120 kips Total Load

Figure 5-15 Midspan Cracking – After Failure

Figure 5-16 Corner Cracks – 144 kips Total Load

The 36 ft span failed under a total applied load of 151.9 kips. The failure mechanism was flexural in nature, with a crack near the corner of the arch widening until the tension steel ruptured, which quickly caused the concrete to crush in compression. The remaining uncrushed concrete and compression steel allowed the bridge to continue carrying some load, but rupture of the tension steel meant that further loading of the bridge would be futile. An image of the eventual failure surface at a lower load level of 72 kips total load can be seen in Figure 5-17. An image of the failure mechanism immediately before and after failure can be seen in Figure 5-18 and Figure 5-19 respectively. An alternate image of the failure mechanism showing the crushing of the concrete can be seen in Figure 5-20. An image of the ruptured tension steel can be seen in Figure 5-21. The failure occurs between cross sections five and six, on the side of the bridge with wirepot three and load cells three and four. The ultimate load configuration can be seen in Figure 5-22.

Figure 5-17 Eventual Failure Surface – 72 kips Total Load

Figure 5-18 Immediately Prior to Failure

Figure 5-19 Immediately After Failure

Figure 5-20 Failure Mechanism – Crushed Concrete

Figure 5-21 Ruptured Tension Steel

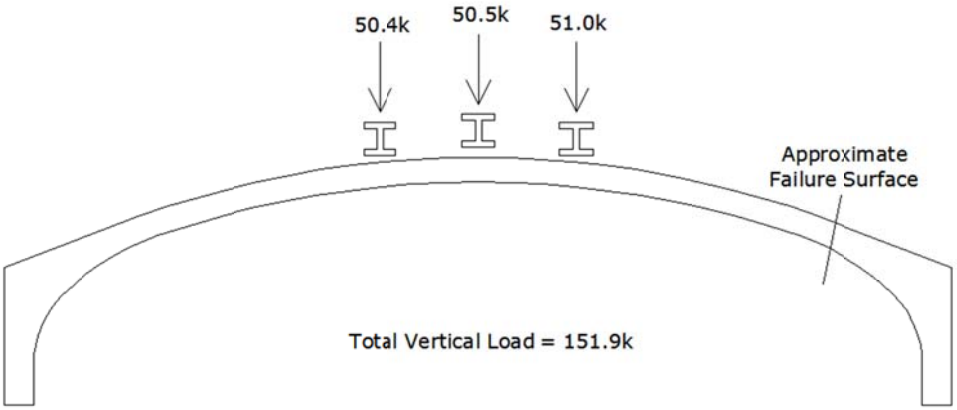

Figure 5-22 Failure Load Configuration

The flexural failure mechanism of the bridge was expected to occur near the corners. The failure mechanism was ductile and developed more slowly. The entire arch deformed considerably prior to the failure mechanism, which developed in one of the corners. The bridge could still carry some weight after failure, but would not have been able to hold nearly as much. The only surprise was the rupture of the tension steel prior to the crushing of the concrete. For greater ductility, the concrete should have crushed prior to steel rupture, allowing the bridge to form a hinge. If the steel had been more ductile, hinges would have formed in both corners and at midspan, providing more ductility and deformation in the bridge prior to failure.

It was noted that the failure mechanism passed through the location of the cast in place lifters used to lift the units during transportation. An image of one of these lifters on the concrete

surface can be seen in Figure 5-23. An image showing the failure surface passing through the lifter location can be seen in Figure 5-24. It was then recalled that during production of this unit, the reinforcement is cut at lifter locations in order to put the lifters in place. An image of this can be seen in Figure 5-25. This practice removed four bars from each mat, which translates to a loss of 17% of the reinforcement at that location for this particular bridge unit. This significantly weakened the ultimate load capacity of the cross section at the lifters, forcing the failure mechanism to occur at that spot. In order to prevent weakening of the structure, reinforcement bars should be properly spliced to the reinforcing mats at lifter locations to prevent a loss of effective steel area.

Figure 5-23 Lifter at Concrete Surface

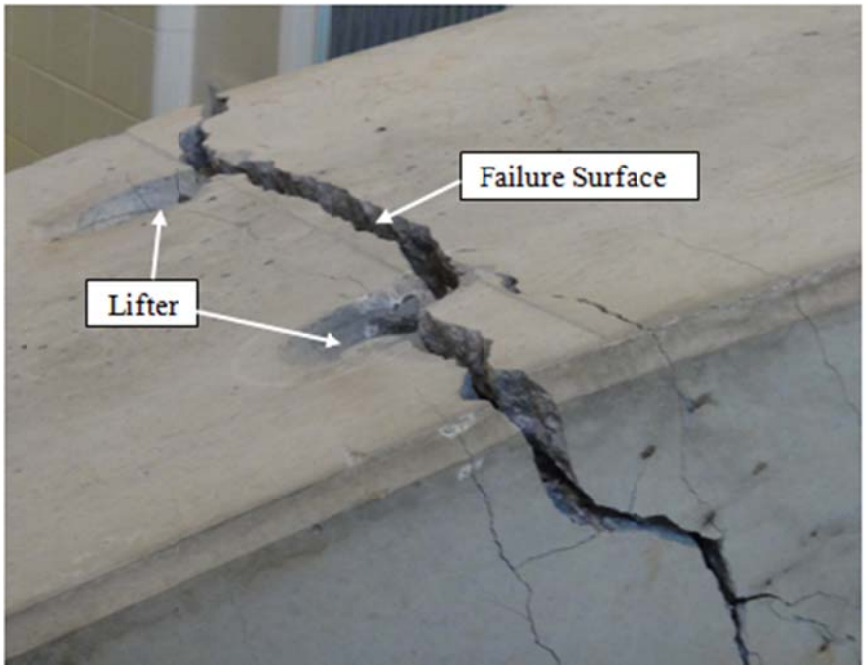

Figure 5-24 Failure Through Lifter Location

Figure 5-25 Reinforcement Cut at Lifter Location

5.5.9 Observations During Bridge Demolition

During the demolition and removal of this bridge unit from the laboratory, a unique failure of the concrete arch was observed. The unit was demolished by dividing it into three separate parts: two leg portions and the arch. After the first leg portion was separated, the second leg portion and arch were broken apart by cutting the top steel near the corner and lifting the arch to allow forcing a failure surface to form there. As the arch was being lifted, the two bottom layers of steel in the arch began to "unzip" from each other. An image of the two layers of steel delaminating from each other can be seen in Figure 5-26. These two layers delaminated across the entire arch until the bottom layer of steel was completely separate from the arch. This occurred due to the tight spacing between bars in the mesh, two inches center-to-center, and the fact that the two layers of steel were cast on top of each other with no concrete cover between them. The spacing between bars within the same mesh and in different meshes should be increased to allow concrete to fully bond around each individual bar to prevent this plane of weakness. It is noted that this failure mechanism did not occur until demolition of the bridge unit, and that it appears that it might only occur if the bridge were being lifted up while missing the top layer of steel. An image of the demolished bridge unit can be seen in Figure 5-27.

Figure 5-26 Steel Layers Delaminating

Figure 5-27 Demolished Bridge Unit

5.5.10 Comparisons to 20 ft Bridge Unit

The 36 ft span bridge unit was much more flexible that the 20 ft span bridge unit. This is primarily due to the lower concrete strength, the larger clear span, and the fact that the 20 ft unit was designed for five more feet of backfill. As such, the 36 ft bridge unit held less load, developed higher moments, deflected significantly more in the arch, and had significantly more cracking prior to failure. The 20 ft bridge unit did develop higher moments in the legs, due to the 20 ft span having a higher arch stiffness to leg stiffness ratio than the 36 ft span. The failure mechanism of the 36 ft bridge is much more ductile, and therefore more desirable.

5.6 Chapter Summary

The 36 ft bridge unit appeared to have plenty of strength, and was more ductile. Initial flexural cracking occurred in the high moment areas during transportation and handling.

However, unlike the 20 ft span bridge unit, flexural cracks propagated, widened, and increased in number with a fairly uniform spacing underneath midspan and on top near the corners. The bridge unit held 151.9 kips of force before failure. Immediately prior to failure, maximum deflections were 5.96 in downward at midspan, and 0.93 in laterally in the walls. The failure mechanism was a flexural failure near one of the corners. The tension steel ruptured, quickly causing the concrete to crush in compression.

Chapter 6 Summary, Conclusions, and Recommendations

6.1 Summary

The use of precast, three-sided arch culverts has become fairly popular for new bridges and bridge replacements, but little research has been performed into the strength of these structures. Many have speculated that, due to arching action, large lateral earth pressures can be developed in the backfill behind the legs, and that these pressures allow the bridge to achieve strengths much larger than possible without the confinement of the backfill soil. The research in this thesis was performed to verify the behavior of these arch culverts through field testing of an existing bridge, as well as two ultimate load tests on bridge units.

It was discovered that, while the test bridges were capable of achieving very high strengths, they were too stiff to cause enough lateral deflection to activate passive earth pressures, and the earth pressures had a minimal effect. In addition, it was found that undesirable shear failures can occur in certain bridge designs, and the ductility of the steel used for reinforcement was not sufficient to allow flexural hinges to form.

6.2 Conclusions

Based on the field testing of a full 42 ft span bridge:

- The bridge had excellent service level behavior. While being subjected to two feet of backfill cover, as well as the load of a 56,820 lb truck, no cracking was observed in the structure and measured strains remained below the theoretical cracking strain.
- The largest lateral earth pressures were measured at the top of the side walls due to the arch thrusting outwards.
- Negligible lateral earth pressures were measured near the bottom of the side walls, indicating that the bridge supports act as a pinned connection.
- Lateral earth pressure magnitudes were relatively small and no passive earth pressures were activated in the backfill.
- Measurements during the backfill operation indicate no cracking in the structure, and that the presence of backfill causes a net compression throughout the bridge.

Based on the laboratory testing of a 20 ft span individual bridge unit:

- Due to their stiffness and strength, shorter spans designed for large amounts of fill could be subject to non-ductile shear failures in the concrete.

- Due to stiffness in both the legs and the arch, measured lateral deflections were small, indicating that passive earth pressures would not be developed in backfill soil.
- A critical area for failure is near the corners, where negative moment and shear are highest.

Based on the laboratory testing of a 36 ft span individual bridge unit:

- Longer spans behave much more flexibly, achieving much higher deflections before failure.
- Based on the observation that the tension steel ruptured prior to concrete crushing, ductility of steel reinforcement may not be high enough to fully develop hinges.
- Due to shortness of the legs, measured lateral deflections were small, indicating that passive earth pressures would not be developed in backfill soil.
- A critical area for failure is in the negative moment regions near the corners of bridge units.
- For heavier, longer span, more flexible bridge units, additional care should be taken during shipping and placement to prevent premature cracking.
- Steel reinforcement removed to place the lifters should be replaced and adequately developed in order to prevent loss of strength.

6.3 Recommendations

The following recommendations for further research were determined:

- Ultimate load testing of full sized bridges with backfill resistance
- Testing of longer span units with taller leg heights to research effect of lateral displacements and backfill pressure
- Comparison testing of similar units in both a laboratory and field setting

References

ASTM International. "C 39/C 39M Standard Test Method for Compressive Strength of Cylindrical Concrete Specimens." 2005.

ASTM International. "C 469 Standard Test Method for Static Modulus of Elasticity and Poisson's Ratio of Concrete in Compression." 2002.

Beach, Timothy J. "Load Test Report and Evaluation of a Precast Concrete Arch Culvert." *Transportation Research Record*, no. 1191 (1988): 12-21.

FoleyArch. "Auburn Test Specimen 36' Span x 9' Tall with 5 Feet of Fill." Calculations for Design of Precast Three Sided Arch Structure, 2011.

FoleyArch. "Bridge No. 145 over Wiley Branch Creek on SR 1121 (Cabarrus Station Road)." Calculations for Design of Precast Three Sided Arch Structure, 2010.

FoleyArch. "S.R. 54/Jonesboro Rd. Bike and Pedestrian Underpass." Shop Drawings, 2010.

McGrath, T.J., and E.P. Mastroianni. "Finite-Element Modeling of Reinforced Concrete Arch Under Live Load." *Transportation Research Record*, no. 1814 (2002): 203-210.

McGrath, Timothy J., Ernest T. Selig, and Timothy J. Beach. "Structural Behavior of Three-Sided Arch Span Bridge." *Transportation Research Record*, no. 1541 (1996): 112-119.

Wight, James K., and James G. MacGregor. *Reinforced Concrete Mechanics and Design.* 5th. Upper Saddle River, New Jersey: Pearson Education, Inc., 2009.

Zoghi, Manoochehr, and Daniel N. Farhey. "Performance Assessment of a Precast-Concrete, Buried, Small Arch Bridge." *Journal of Performance of Constructed Facilities*, August 2006: 244-252.

Appendix A: Gaged Threaded Rod Calibration

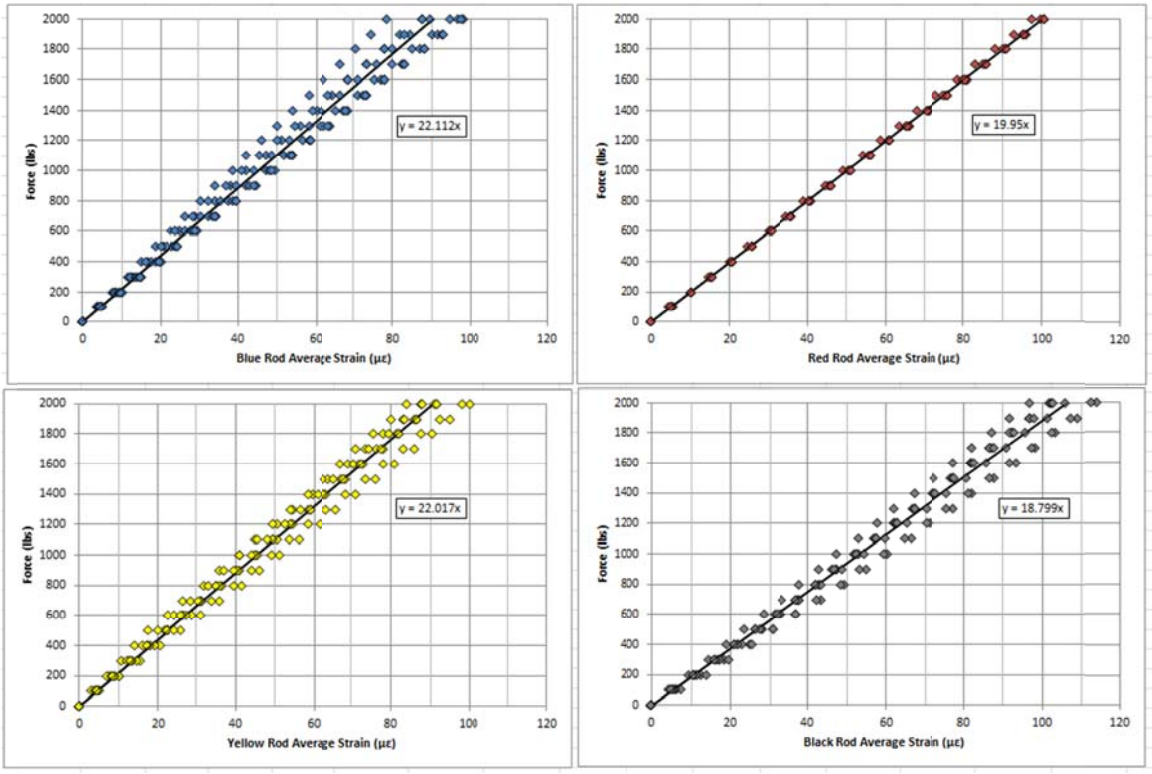

Figure A-0-1 Gaged Threaded Rod Calibration Graphs

Table B-1 Cylinder Test Data – 20 ft span

Performed 8-15-11
Luke Meadows
Jared Jensen

Cylinder Test Data - 20' Span

Sheet prepared by:
Luke Meadows

L= 8 in d= 4 in
A= 12.566 in2

Cylinder	Dial Gage (in)	Load (lb)	Strain	Stress (psi)	Modulus (ksi)	Break Load (lb)	Ult Strength (psi)
1	0.0004	2715	0.000025	216.05	5960.90	153820	12241
	0.0105	50000	0.000656	3978.87			
	0.0004	2605	0.000025	207.30	5974.77		
	0.0105	50000	0.000656	3978.87			
	0.0004	2255	0.000025	179.45	6018.89		
	0.0105	50000	0.000656	3978.87			
2	0.0004	2285	0.000025	181.83	6075.26	156245	12434
	0.0104	50000	0.000650	3978.87			
	0.0004	2465	0.000025	196.16	6052.34		
	0.0104	50000	0.000650	3978.87			
	0.0004	2835	0.000025	225.60	6005.23		
	0.0104	50000	0.000650	3978.87			
3	0.0004	2550	0.000025	202.92	5699.55	157160	12506
	0.0110	50000	0.000688	3978.87			
	0.0004	2495	0.000025	198.55	5706.16		
	0.0110	50000	0.000688	3978.87			
	0.0004	2350	0.000025	187.01	5723.57		
	0.0110	50000	0.000688	3978.87			
4	0.0004	2510	0.000025	199.74	6046.61	157790	12557
	0.0104	50000	0.000650	3978.87			
	0.0004	2620	0.000025	208.49	6032.61		
	0.0104	50000	0.000650	3978.87			
	0.0004	2485	0.000025	197.75	6049.80		
	0.0104	50000	0.000650	3978.87			
5	0.0004	2310	0.000025	183.82	6072.08	156985	12492
	0.0104	50000	0.000650	3978.87			
	0.0004	2420	0.000025	192.58	5998.09		
	0.0105	50000	0.000656	3978.87			
	0.0004	2380	0.000025	189.39	6063.17		
	0.0104	50000	0.000650	3978.87			
6	0.0004	2395	0.000025	190.59	5884.72	158700	12629
	0.0107	50000	0.000669	3978.87			
	0.0004	2440	0.000025	194.17	5879.15		
	0.0107	50000	0.000669	3978.87			
	0.0004	2530	0.000025	201.33	5925.56		
	0.0106	50000	0.000663	3978.87			
7	0.0004	2400	0.000025	190.99	5664.13	152740	12155
	0.0111	50000	0.000694	3978.87			
	0.0004	2415	0.000025	192.18	5662.35		
	0.0111	50000	0.000694	3978.87			
	0.0004	2515	0.000025	200.14	5650.45		
	0.0111	50000	0.000694	3978.87			
8	0.0004	2430	0.000025	193.37	5880.39	161050	12816
	0.0107	50000	0.000669	3978.87			
	0.0004	2400	0.000025	190.99	5884.10		
	0.0107	50000	0.000669	3978.87			
	0.0004	2230	0.000025	177.46	5848.33		
	0.0108	50000	0.000675	3978.87			
9	0.0004	2470	0.000025	196.56	6238.87	159950	12728
	0.0101	50000	0.000631	3978.87			
	0.0004	2390	0.000025	190.19	6249.37		
	0.0101	50000	0.000631	3978.87			
	0.0004	2290	0.000025	182.23	6262.50		
	0.0101	50000	0.000631	3978.87			

Average:	5944.78		12506.40
Stan Dev:	177.36		212.87

Table B-2 Cylinder Test Data - 36 ft span

Performed 1-9-12
Luke Meadows
Jared Jensen

Cylinder Test Data - 36' Span

Sheet prepared by:
Luke Meadows

L= 8 in d= 4 in
A= 12.566 in2

Cylinder	Dial Gage (in)	Load (lb)	Strain	Stress (psi)	Modulus (ksi)	Break Load (lb)	Ult Strength (psi)
1	0.0004	2010	0.000025	159.95	4242.85	85810	6829
	0.0103	35000	0.000644	2785.21			
	0.0004	2010	0.000025	159.95	4038.86		
	0.0108	35000	0.000675	2785.21			
	0.0004	2115	0.000025	168.31	4065.10		
	0.0107	35000	0.000669	2785.21			
2	0.0004	1670	0.000025	132.89	4080.49	87475	6961
	0.0108	35000	0.000675	2785.21			
	0.0004	1655	0.000025	131.70	4121.96		
	0.0107	35000	0.000669	2785.21			
	0.0004	1665	0.000025	132.50	4081.10		
	0.0108	35000	0.000675	2785.21			
3	0.0004	1775	0.000025	141.25	4107.12	86425	6877
	0.0107	35000	0.000669	2785.21			
	0.0004	1960	0.000025	155.97	4124.30		
	0.0106	35000	0.000663	2785.21			
	0.0004	1830	0.000025	145.63	4140.53		
	0.0106	35000	0.000663	2785.21			
4	0.0004	1545	0.000025	122.95	3980.96	85195	6780
	0.0111	35000	0.000694	2785.21			
	0.0004	1585	0.000025	126.13	3976.20		
	0.0111	35000	0.000694	2785.21			
	0.0004	1665	0.000025	132.50	3966.68		
	0.0111	35000	0.000694	2785.21			
5	0.0004	1880	0.000025	149.61	4094.15	94275	7502
	0.0107	35000	0.000669	2785.21			
	0.0004	1885	0.000025	150.00	4093.53		
	0.0107	35000	0.000669	2785.21			
	0.0004	1835	0.000025	146.02	4099.71		
	0.0107	35000	0.000669	2785.21			
6	0.0004	2070	0.000025	164.73	4278.34	86740	6903
	0.0102	35000	0.000638	2785.21			
	0.0004	2050	0.000025	163.13	4237.70		
	0.0103	35000	0.000644	2785.21			
	0.0004	2100	0.000025	167.11	4188.96		
	0.0104	35000	0.000650	2785.21			
7						88045	7006
8						94165	7493

Average:	4106.58		7043.90
Stan Dev:	88.82		288.90

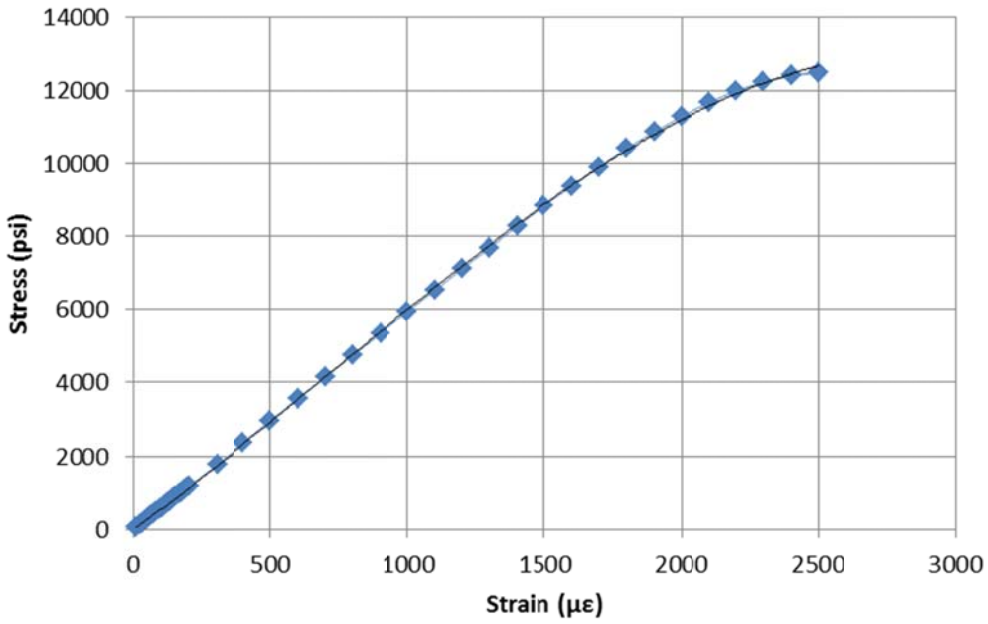

Figure B-0-1 Assumed Concrete Compressive Behavior - 20 ft Span

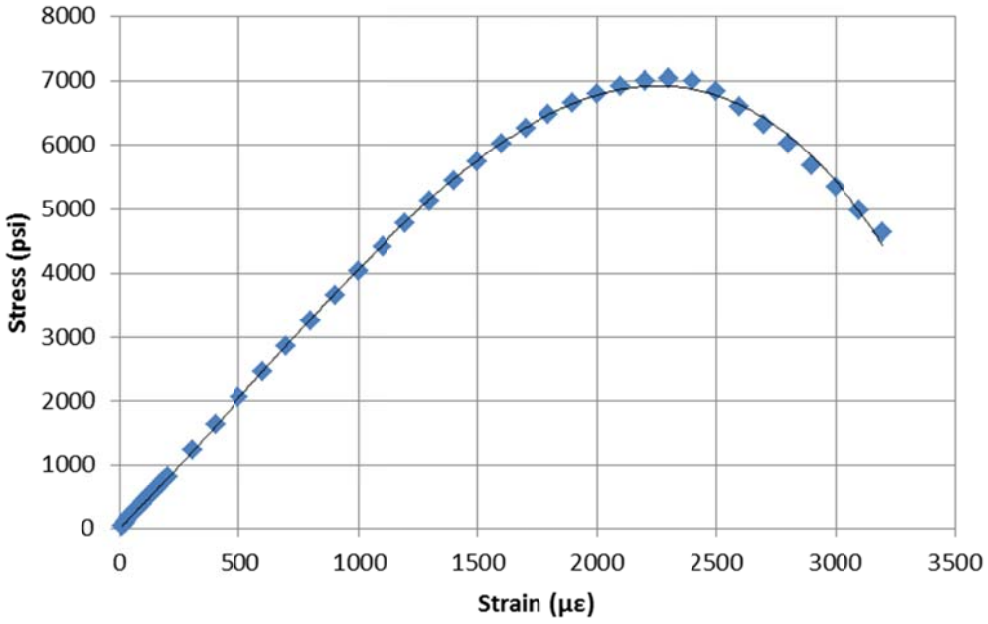

Figure B-0-2 Assumed Concrete Compressive Behavior - 36 ft Span